DEVELOPMENT OF AN AUTONOMOUS NAVIGATION TECHNOLOGY TEST VEHICLE

By

CHAD KARL TOBLER

A THESIS PRESENTED TO THE GRADUATE SCHOOL
OF THE UNIVERSITY OF FLORIDA IN PARTIAL FULFILLMENT
OF THE REQUIREMENTS FOR THE DEGREE OF
MASTER OF SCIENCE

UNIVERSITY OF FLORIDA

2004

This thesis is dedicated to my parents, Karl and Jan Tobler.

ACKNOWLEDGMENTS

I would like thank the many individuals that have contributed to make this project a success, and my educational experience at UF so enjoyable. Specifically, I would like to thank Dr. Carl Crane, III, my academic advisor and committee chair, for his continual support and guidance during my time at the University of Florida. I would also like to thank the other members of my supervisory committee, Dr. John Schueller and Dr. Antonio Arroyo, for their willingness to support the project.

I also need to express my gratitude to the staff of the Air Force Research Laboratory at Tyndall Air Force Base, for their ongoing relationship and financial support of the CIMAR lab. This project would not have been possible without their financial backing.

Special thanks also go to the other students in CIMAR who contributed their time and technical expertise to the project. My time as a student in CIMAR has been a great learning experience and is highlighted by many fond memories, largely due to the outstanding intelligence and friendliness of the other students with whom I associated.

Finally, I would like to thank my parents, who have never wavered in their love and support for me. They laid the foundation for everything I have achieved and become today.

TABLE OF CONTENTS

LIST OF TABLES

LIST OF FIGURES

LIST OF OBJECTS

Object page

Abstract of Thesis Presented to the Graduate School
of the University of Florida in Partial Fulfillment of the
Requirements for the Degree of Master of Science

DEVELOPMENT OF AN AUTONOMOUS NAVIGATION
TECHNOLOGY TEST VEHICLE

By

Chad Karl Tobler

August 2004

Chair: Carl D. Crane III
Major Department: Mechanical and Aerospace Engineering

The Center for Intelligent Machines and Robotics (CIMAR) at the University of Florida has been a leader in the field of autonomous vehicles since 1991. In order to continue these research activities at CIMAR, a new Kawasaki Mule All-Terrain Vehicle was chosen to be automated as a test-bed for the purpose of developing and testing autonomous vehicle technologies. This Mule will be referred to as the Navigational Test Vehicle II (NTV2), because it is the second generation of the Navigational Test Vehicle (NTV) that was first automated at CIMAR in 1991. This thesis describes in detail the design and implementation of the software and hardware systems necessary for converting the stock Kawasaki Mule ATV into an unmanned vehicle capable of remote control or fully autonomous operation.

As part of the automation project, servo actuators were added to the throttle, brake, and steering systems in order to control the mobility functions of the Mule, allowing it to operate as an autonomous vehicle. The operational theory of servo control systems is

discussed, and the throttle, brake, and steering actuator systems are described in detail. In addition, transfer function models have been developed to predict the transient response of each actuator control system.

A description is given of the Joint Architecture for Unmanned Systems (JAUS), which was used as the vehicle control architecture. Because the Mule control software has been designed according to the modular ideology of the JAUS Reference Architecture, new software and hardware components can be readily implemented as part of the autonomous vehicle system, allowing it to be modernized as new technologies develop. Finally, the goals of this project were accomplished, and the Mule was converted into a reliable development vehicle for autonomous systems technology.

CHAPTER 1
INTRODUCTION

1.1 Project Background

Unmanned robotic vehicle systems have evolved rapidly in the past two decades, with new technologies and applications being discovered at an ever increasing pace. Unmanned vehicle systems have been successfully developed and deployed for agricultural, military, nuclear, and other applications that are either hazardous in nature, or require an exacting level of precision or repeatability. Vehicle control and sensor systems have become more advanced and reliable with the increasing availability of smaller, more powerful computers. The modern computing capability and other technological advancements have led to autonomous vehicles equipped with global positioning systems capable of centimeter accuracy, detailed real-time updating terrain maps, and obstacle avoidance systems using three-dimensional vision processing and laser range finding sensors.

The advantages offered by unmanned vehicle systems make them well suited for military applications. In order to develop these technologies, in 1991 the Air Force Research Laboratory (AFRL) at Tyndall Air Force Base initiated an autonomous vehicle program, and contracted the Center for Intelligent Machines and Robotics (CIMAR) at the University of Florida for assistance with the project. That relationship has continued until the present, with a continual transfer of technology between CIMAR and the AFRL robotics research center. Research activities at CIMAR have included all aspects of autonomous vehicle systems, such as vehicle control, path planning, positioning systems,

sensor systems, system architecture, and multiple vehicle coordination. The years of cooperative development between CIMAR and AFRL have yielded many successful joint projects, and produced many practical advancements in the field of autonomous vehicle systems.

1.2 Autonomous Vehicle Development at CIMAR

The first vehicle automated by CIMAR under the direction of the AFRL was the Navigational Test Vehicle (NTV) (see Figure 1-1). The NTV was designed using a Kawasaki Mule 500 as the base platform. The Mule was chosen to be the first test bed for the vehicle automation project based on its compact size, payload capacity, and simple controls. In order to convert the Mule to the vehicle capable of autonomous navigation, servo actuator systems were installed on the vehicle steering, throttle, brake and shifter controls. Initially, a VME computer system was installed to command the actuator systems and perform high-level processing necessary for navigation control and sensory functions. Over its 10 years of service to CIMAR and the AFRL, the NTV evolved through countless design improvements made to the actuator, sensor, and computing systems. After a hardware or software technology was successfully developed and tested on the NTV, it was transferred to other Air Force systems.

One application for the unmanned vehicle technology developed at CIMAR was for the clean up of unexploded buried munitions. The closure of military bases by the Department of Defense created a demand for a safe and thorough way of locating and clearing unexploded ordnance from abandoned test ranges. Unmanned vehicle technology offered a solution that would remove human operators from this dangerous task, and ensure thorough coverage of the ranges by following precisely planned survey

paths. In order to answer that demand, CIMAR automated a John Deere Gator that would become the Autonomous Survey Vehicle (ASV) (shown in Figure 1-2).

Figure 1-1: Navigational Test Vehicle

The ASV was built using similar software and hardware technology that had been developed previously on the NTV. In order to locate buried munitions, the ASV towed a sensor package equipped with an array of magnetometers and ground penetrating radars. The ASV autonomously navigated a carefully planned survey mission covering the intended search field, and recorded time-stamped information from the sensors that was post-processed to determine the exact location of possible buried munitions [Man01]. Once possible buried munitions were located, the next step in clean up effort was to excavate and remove them. A John Deere excavator was automated for this purpose, which could be remotely-operated a safe distance by clean up personnel (see Figure 1-3).

Figure 1-2: The Autonomous Survey Vehicle and Metal Detecting Trailer

Figure 1-3: The Automated John Deere Excavator

The continued technology transfer between CIMAR and the AFRL has led to other successful autonomous vehicles. The All-Purpose Remote Transport Vehicle (ARTS) and Autonomous Mobility Research and Development System (AMRADS) shown in Figure 1-4 were the next-generation of autonomous vehicles that were built at AFRL using technologies developed at CIMAR on the NTV. These vehicles have been used to successfully demonstrate the capabilities of unmanned systems for the military, and

served as prototypes for production models of unmanned systems deployed for service in the field. Since that time, the autonomous vehicle program has continued to expand, and more vehicle platforms have been automated as prototypes for unmanned vehicles suited for a particular military need.

Figure 1-4: The AMRADS

Some smaller more manageable vehicles have been automated in recent years at CIMAR for the purpose of studying cooperative vehicle control, and for demonstrating autonomous systems in more confined environments. Two PowerWheels children's electric cars have been converted for autonomous operation and are known as the "Eliminators" (shown in Figure 1-5). These vehicles are useful for research purposes due to their easy portability and smaller area required for safe operation.

Figure 1-5: One of Two Eliminator Vehicles

One application for multiple vehicle systems being researched with the Eliminators is to have a formation of smaller less-intelligent child vehicles collecting and transmitting data back to a mother vehicle with a greater level of intelligence and functional capability. The mother vehicle would be equipped with more expensive global positioning and guidance systems, while the small child vehicles could rely on a positioning system relative to the mother vehicle. In this manner, the smaller vehicles would function as a sensor array relative to the mother vehicle, and the surrounding environment could be surveyed more efficiently.

Another small scale vehicle automated in CIMAR for technology development and demonstration was a 50cc Suzuki Mini-Quad known as the "TailGator." The rapid development of this autonomous vehicle system was aided by using the Joint Architecture for Unmanned Systems (JAUS) as described in Version 3.0 of the Reference Architecture (RA) document. JAUS is designed to standardize the interface between

elements of autonomous vehicle systems. The standard message sets and component definitions provided a framework for the integration of all systems necessary for autonomous navigation. The TailGator was entered in the 2003 Intelligent Ground Vehicle Competition sponsored by the Association for Unmanned Vehicle Systems International (AUVSI) in Michigan. As a credit to the quality of systems designed in CIMAR, TailGator won 1st place in the navigation challenge competition, which involved following a course of GPS waypoints while simultaneously detecting and avoiding obstacles. It also won 1st place in the vehicle tracking competition, in which it autonomously followed another vehicle through a course using a SICK laser range sensor.

Figure 1-6: The TailGator

Some of the greatest contributions CIMAR has made in the field of unmanned systems technology have been in the area of modular vehicle control architectures. The first control architecture implemented on the NTV was based on a shared memory approach to inter-process communications. Multiple processor boards were mounted on

a VME backplane in order to share data and resources in real-time. The difficulties with this system were due to the fact that a programming error in one process could overwrite shared memory and cause an error in another process using that data, which made debugging of the experimental systems difficult. The shared memory architecture also presented significant difficulties when trying to upgrade hardware or software components, or exchange them between vehicles [Sen98].

This early experience with the NTV established the need for an improved system architecture that would reduce the difficulties encountered with, and disadvantages inherent to the shared memory approach. In order to address this need, four design criteria for a modular, scalable vehicle control architecture were established [Arm99].

1. The architecture should be comprised of a set of well-defined, self-contained sub-modules.
2. Software interfaces for the modules should be well defined and hardware independent.
3. The architecture should be scalable, so system functionality can be varied by adding or removing sub-modules used in the system.
4. The architecture should be a step toward the establishment of a standardized architecture.

The guidelines for the standardized architecture listed above would result in greater interoperability of system components between vehicles, and between alternate versions of the same component due to the standardized interface. Several iterations of the modular control architecture were progressively developed and tested at CIMAR in conjunction with the AFRL. The most successful implementation was known as the Modular Architecture eXperimental (MAX). The MAX architecture became the genesis of a much larger scaled effort to establish a common unmanned system architecture

known as the JAUS working group. Much of CIMAR's current research effort is directed at developing and defining components for the JAUS reference architecture.

1.3 The Joint Architecture for Unmanned Systems (JAUS)

1.3.1 Overview

The Joint Architecture for Unmanned Systems (JAUS) is a collaborative effort between military researchers, research institutions, and private industry to create a standardized architecture for unmanned vehicles. The primary goal of creating a standardized architecture is to reduce unmanned system life-cycle costs, by specifying an interface standard that would allow reuse and compatibility of independently developed system components. If built according to the JAUS standard, a particular component can be inserted into all JAUS compliant systems, and individually upgraded or replaced as technology advances. This is a great benefit as it allows expensive components that have already been developed to be easily used in other vehicle systems, and for outdated or malfunctioning components to be easily replaced. JAUS is defined to be modular and scalable to include all the components necessary for the proposed missions and required complexity of a system. JAUS has been designed to support the entire functional spectrum of unmanned systems, ranging from simple remote-control functionality to fully autonomous intelligent systems. After successful implementation and demonstrations of JAUS controlled test vehicles, the Department of Defense has adopted JAUS as the standard architecture for unmanned ground systems, and included it as part of the Operational Requirements Document for the Future Combat System [Jau04].

1.3.2 Technical Constraints

Four technical constraints have been imposed on the JAUS architecture to ensure that it satisfies the purposes for which it was created. These constraints are:

1. *Platform Independence*

JAUS is designed to be useful for any unmanned system design based on any vehicle platform. In order to be truly interoperable, the components specified by the JAUS reference architecture make no assumptions about the base platform configuration or maneuverability (i.e. Ackerman steered vs. omni-directional).

2. *Mission Isolation*

The set of tasks defined for an unmanned system, which may include gathering information about or altering the state of the environment, or both, are defined as its *missions*. Mission isolation is intended to allow engineers to customize the set of missions for an unmanned system by adding or removing components that support each individual mission.

3. *Computer Hardware Independence*

In order to capitalize on the rapid advancements in computer and sensor technology, JAUS components should not specify a hardware standard. Computing hardware can be selected according to the demands of a particular application. This constraint allows new computer architectures to be used for implementing a component, which can be inserted into an existing system to extend its life cycle.

4. *Technology Independence*

There are usually multiple technical solutions to a given engineering problem, so the architecture must not be bound to any particular technologies. Basically, this means that no assumptions are to be made about the methods used to perform the function of a component. For example, a JAUS position status component delivers position information without specifying how it should be obtained (i.e. GPS, dead reckoning,

inertial measurement, etc.). This ensures that JAUS continues to be a viable architecture as technology advances [Jau04].

1.3.3 System Topology

JAUS is organized into a hierarchy of four levels, namely the system, subsystem, node, and component/instance. The organization of these hierarchal elements is illustrated in Figure 1-7. A system is a logical grouping of all subsystems that typically would function together to gain a cooperative advantage for the complete unmanned system. A subsystem is described as a single localized entity, usually a vehicle or robot, hosting one or more nodes that give it give it communication, command, and control functionality. A node is a distinct processing capability, typically the computing device, and provides a node manager component to manage the flow of the JAUS message traffic to the components hosted on the node. The node also provides the hardware interface needed to support the functionality and communications of each of the software components it hosts. The component is the lowest element of the hierarchy, and each one provides a unique functional capability for the unmanned system. Multiple modules of the same JAUS component can be run on a node, and are distinguished by a distinct instance identification [Jau04].

Each component in JAUS has a strictly defined messaging interface that includes a standard set of messages that are required to be supported by every component, and other messages that relate to its unique functionality. It is important to note that although JAUS defines the function and messaging structure for the component, it does not specify how the function must be carried out. These modular system building blocks allow an engineer to select the components required for a particular application, and add or remove them if the mission of the vehicle system should change. Also, because JAUS

standardizes the communications interface of a component, an engineer can spend more effort developing the functional performance of it, as less time is needed for communications related issues.

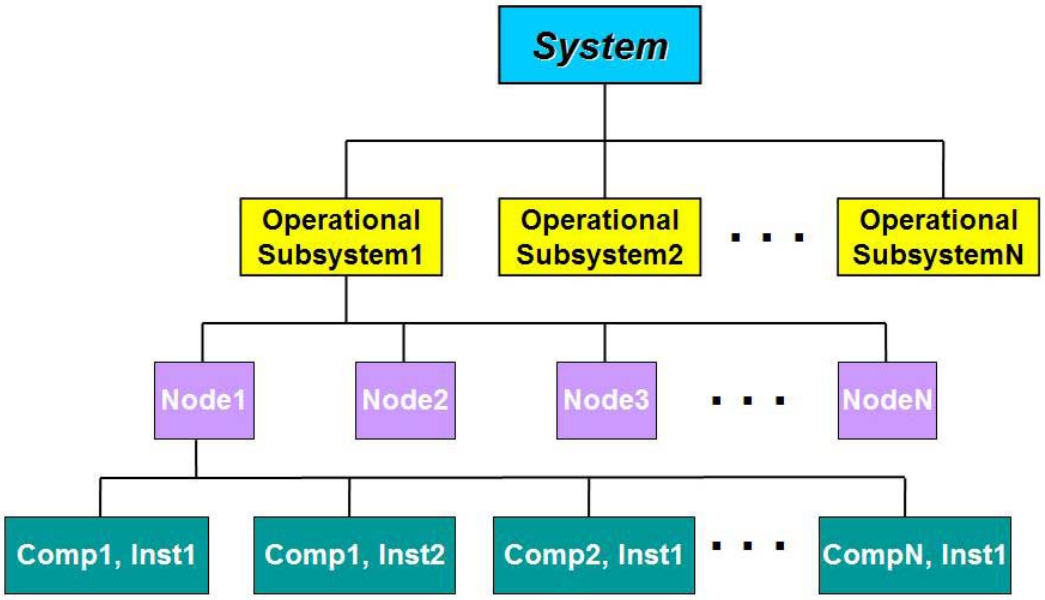

Figure 1-7: Diagram of JAUS Topology [Jau04]

In essence, JAUS is a component based, message passing architecture. JAUS defines a distinct name and identification number for every JAUS component, as well as input and output codes and data formats specific to each component's individual function. Every component must also accept and execute a set of core JAUS command codes.

Components on separate nodes communicate through the combined functions of the Communicator and Node Manager components that are required for each node. When a message is generated by a component, it is sent to the Node Manager, which completes the message by attaching information pertaining to the destination component and node. The completed JAUS message can then be passed to the Communicator, which routes it to the indicated component residing on another node or subsystem. The

Communicator and Node Manager on the node receiving the message will deliver it to the intended component, or queue the message for subsequent delivery if necessary.

1.4 Thesis Focus

After 10 years of faithful service to CIMAR and the AFRL, the decision was made to retire the aging Navigational Test Vehicle, and replace it with a brand new vehicle. Due to the proven reliability and usefulness of the Kawasaki Mule platform used for the NTV, a 2001 4x4 version of Kawasaki's Mule was purchased to be the new CIMAR autonomous technology development vehicle (viewable in Figure 1-8). This new Mule will be referred to as the Navigational Test Vehicle II (NTV2), because it is the second generation of the Navigational Test Vehicle (NTV). The control system of the new Mule was designed based on the JAUS reference architecture, with the implementation of the Primitive Driver (PD) intelligence component being the primary focus of this work. A functional Primitive Driver will allow for remote control operation or autonomous computer control of the basic driving functions of the platform. The PD accomplishes this task by communicating with a Subsystem Commander component, and executing servo control of all actuators that directly affect the motion of the platform.

This thesis will cover the design and development of the vehicle actuation systems necessary to convert the new Mule into an autonomous test vehicle. After introducing the operational theory of servo control systems, the throttle, steering, and brake actuator systems are described in detail. Also, a description is given of the JAUS reference architecture components that have been successfully implemented on the NTV2 to achieve autonomous navigation.

Figure 1-8: Photo of the Mule 3010 4X4

CHAPTER 2
AUTONOMOUS VEHICLE DESIGN: A MODULAR APPROACH

A modular approach was taken when designing the software and hardware systems of the Mule. The advantages of modular control architecture were discussed in Chapter 1 along with the JAUS reference architecture. Hardware modularity allows the systems engineer to take full advantage of the benefits offered by a modular software architecture. For example, if each functional software component was implemented in an individual hardware unit, components could easily be added to or removed from the vehicle system. In this way, a system could be easily reconfigured to include the components needed for different missions. Also, components could be developed, upgraded, or replaced on an individual basis.

There are some disadvantages to the modular approach. One obvious disadvantage is the bulkiness of the infrastructure needed to mount, power, and link the hardware modules. The physical capacity required for this type of set-up may not be available in very small or weight constrained vehicles. Also, the expense of a separate computer for each component greatly increases the cost of the overall system. For these reasons, complete hardware modularity is usually not desirable for production model vehicles where a high priority is placed on minimizing the size and cost of a control system. However, in the case of a developmental platform such as the Mule, the advantages of a modular system justify the added hardware and cost. Not all software components on the Mule have their own hardware module. Multiple components are located in the same hardware module either because those components function best when run

simultaneously on the same computer, or because a dedicated computer was unnecessary or unavailable for a particular component. That flexibility is built into the JAUS reference architecture, which makes it well suited for an "in development" system.

2.1 Hardware Modularization

2.1.1 Hardware Modules

The hardware standard selected as the basis for hardware modularization was the 19" rack frame common in industrial applications. This standard was adopted from the previous NTV, where it had proven useful. Many manufactures support the 19" rack standard, offering products designed to mount directly into the rack, or hardware modules compatible with the standard. A 36" tall standard electronics rack was shock mounted to the rear bed of the Mule as the mounting structure for the hardware modules. Slide-out tray shelves designed for the 19" rack were selected as the basic hardware modules. The shelves are designed to be self-contained hardware modules that can be easily removed or inserted into the Mule system. The electronics rack filled with the tray modules is pictured in Figure 1-1.

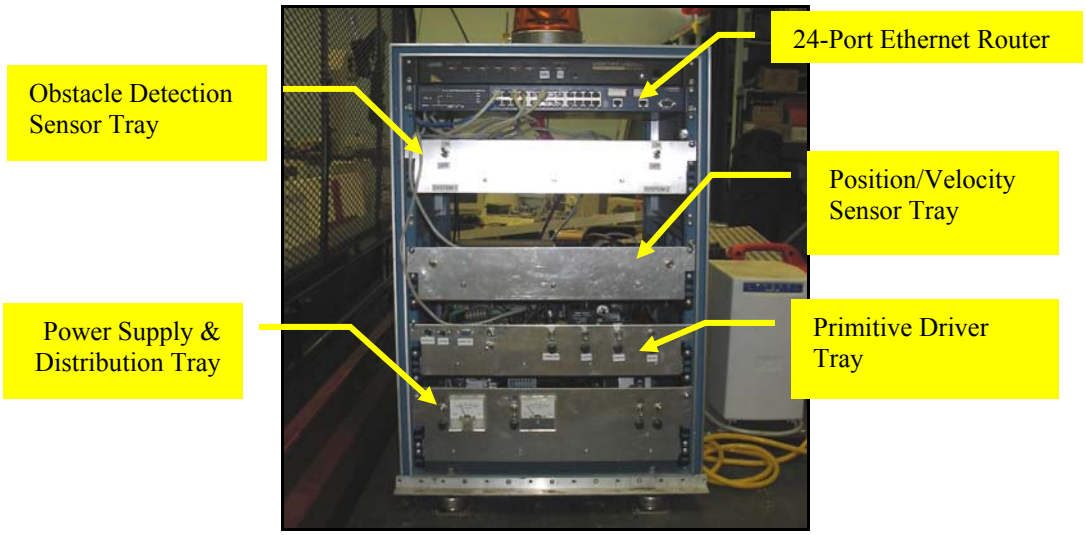

Figure 2-1: Electronics Rack for Tray Modules

In order to simplify the number and type of hardware connections that each unit would require, standards were established for the power and communications hardware interfaces. One 12 VDC power cord would be supplied to power each module. If other voltages were required, the module would have to make its own conversion. Each unit would also be allowed one RJ-45 standard Ethernet connection for the communications system. Other permitted connections were those required to support specific component functionality, such as signal lines from remotely mounted sensors or power lines to drive the actuators. Amphenol military-specification connectors were used for the power lines, and for all other connections to the trays where possible. These rugged connectors lock together and seal out dirt and moisture, making them an excellent choice for the all-terrain Mule. The connections were wired so that the "hot" side had a female connector to reduce the risk of short-circuiting the system.

2.1.2 Power System Design

The power solution designed for the Mule electronics system relies on a 1000 Watt gas powered generator as the primary source of electricity. The generator chosen was a Honda EU1000, because it is equipped with inverter technology that ensures "clean" conditioned power is delivered for use with sensitive electronics. A gas powered generator was selected over a battery based system because it can operate over extended periods of time with an adequate fuel supply, and there is no down-time for recharging. The AC power output from the generator supplies a 940 Watt Uninterruptible Power Supply (UPS) which provides battery back-up when the generator is off. While indoors, the UPS is plugged into an extension cord from a wall outlet.

A power distribution shelf was designed as the lowest level in the electronics rack. This shelf holds the AC to DC power converters, and splits the output to 12 available

power lines. A 500 Watt 12 VDC switching power supply is used to supply power to all other tray modules. A 500 Watt 60 VDC converter supplies power for the steering motor on an auxiliary line to the actuator control module. This exception was made to the 12 VDC supply rule because the steering motor requires a much higher voltage and enough power that it merited a dedicated 60 VDC supply. The AC to DC power converters draw AC power from the UPS, and output to a grid of output lines. Each power output line is fused, and the amperage drawn from each converter is displayed by an ammeter on the front panel of the tray. Input power to each converter is also fused and switched at the front panel of the tray.

At the tray module, the 12 VDC power line connects to an Amphenol connector on the back panel of the tray. The raw 12 volts is then conditioned and converted to 12 and 5 VDC by a custom built power supply board for use by the sensitive electronics. The units are very small and are fused protected on the input and output power stages.

2.1.3 Communications System Design

In order to simplify the communication system between modules, Ethernet was adopted as the standard interface. The communications protocol chosen for transmitting the JAUS messages across the Ethernet lines was User Datagram Protocol (UDP). Each unit is connected by an Ethernet patch cable to a 24 port high-speed industrial switch that is mounted in the rack (Netgear Model FSM726). The switch routes the communication packets to the intended recipient module according to the Internet Protocol (IP) address assigned to each computer. The Ethernet router switch is visible at the top of the electronics rack pictured in Figure 1-1.

In order to provide for wireless connectivity between the onboard Mule computers and remote development systems, commercially available 802.11g Ethernet broadcasting

equipment was used. The IEEE 802.11g standard operates in 2.4 GHz range and transmits data at speeds up to 55 Mbps. A D-Link wireless Ethernet access point (model DWL-2000AP) was installed in the electronics rack and connected to the Ethernet switch. In this manner, a wireless link could be obtained to any of the computers connected on the Mule Ethernet network. This wireless link also allowed tele-op mobility control of the vehicle with an Operator Control Unit laptop equipped with a wireless Ethernet card and joystick.

2.2 JAUS Software Modularization

As specified in Chapter 1, JAUS was designed to fit the criteria of a modular, scalable architecture. The components of JAUS are cohesive software processes that provide some special functionality to the system. Only the functional description and message formats are defined for each component by JAUS. The processor on which the software is implemented, and the methods by which the information is obtained, are left to the engineer to decide.

Hardware independence is one advantage offered by JAUS, due to the well defined messaging interface. The only requirement JAUS places on the microprocessor used to execute component functions is that it supports the JAUS message interface. The JAUS message standards allow modules to exchange information without regard for how that information was obtained or processed. This is an important feature of a modular control architecture, because it allows different processors and different operating systems to function together as part of the complete solution without additional interface considerations. This gives total freedom to the systems engineer to implement each component using any combination of processor, operating system, and programming language deemed appropriate.

2.2 JAUS Components Implemented on the Mule

This section will discuss the JAUS components that have been selected as part of the control system for the Mule. A functional description will be given for each component (as defined by the JAUS reference architecture version 3.0), as well as details regarding the hardware and software used for its implementation.

2.2.1 Communicator and Node Manager

2.2.1.1 Overview

The Communicator and Node Manager technically are separate components as defined by JAUS. These components work closely together to handle all the message routing in a JAUS System. Messages are routed according to the source and destination address information contained within the message header. The sender and receiver component addresses are indicated by a four field identifier for each in the message header. The four fields of the address identifier are: Subsystem ID, Node ID, Component ID, and Instance ID.

Each node in JAUS is required to have a Node Manager that is responsible for managing the flows and controls of JAUS message traffic. The Node Manager contains address information for all components in the system, and attaches this address to outgoing messages generated by the components on that node. The Node Manager is the receiver of messages delivered to that node, and depending on delivery information in the header, delivers the message to an individual component or broadcasts it to all of them on that node. The Node Manager also handles a priority class of messages in an exchange between components known as a Service Connection.

The Communicator component maintains the data communication links to other subsystems within a system. A subsystem may have a single communicator, which

provides a single point of entry for all JAUS messages into that subsystem. Figure 1-2 is a graphic depicting the flow of messages between components, nodes and subsystems.

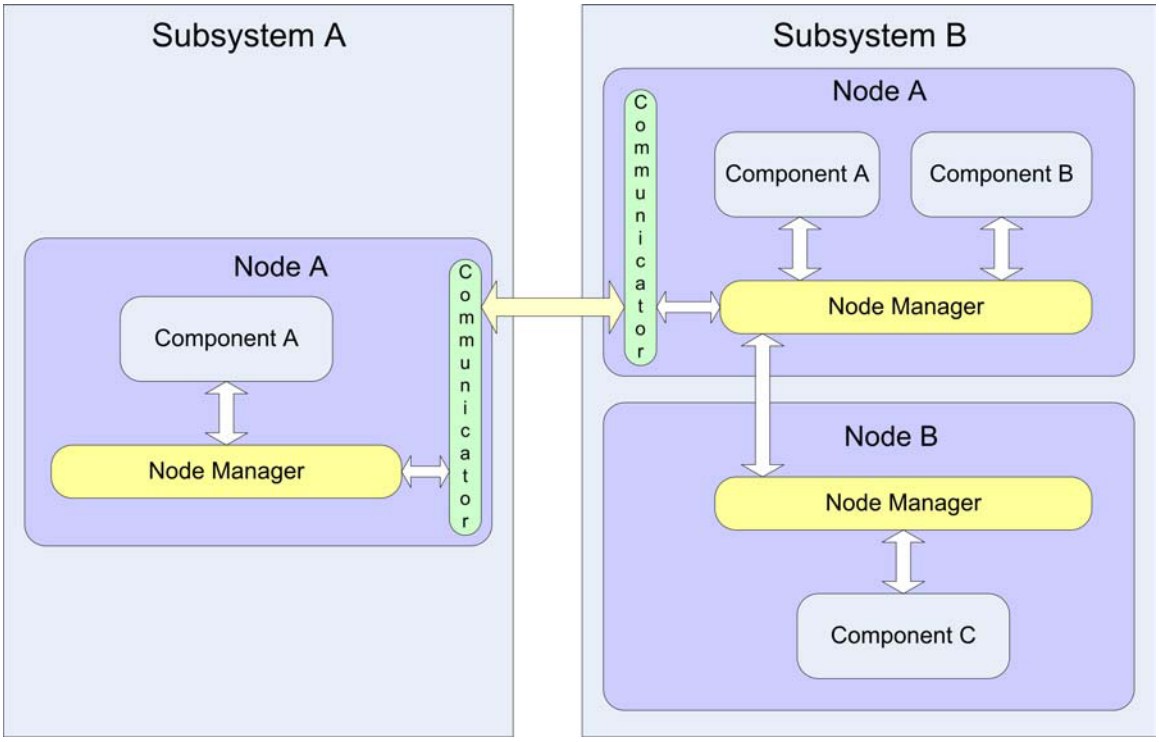

Figure 2-2: JAUS Communicator and Node Manager Interaction

2.2.1.2 Implementation

As currently implemented in the Mule subsystem, the Node Manager and Communicator JAUS components have been combined to form a Message Routing Service (MRS) that is included on every node. The MRS code was written by developers at the Air Force Research Laboratory, and given to CIMAR for use and evaluation. The code was written in C, and runs as an independent thread on processors using the Linux operating system.

The computer hardware selected for the nodes that host the MRS threads were single board computers. These industrial computers were chosen because they offer the functionality of a full size computer in compact, sturdy form designed for embedded

systems. The hardware selected for routing the JAUS messages was discussed previously in Section 2.3.1 on the communications system design.

Linux was chosen as the operating system for all of the single board computers used on the Mule. Linux was specifically designed for real-time, multi-process applications. Real-time refers to the operating systems ability to prioritize and complete tasks within a fixed amount of time. In our implementation of JAUS, multiple software components are run in parallel on the same processor, in addition to other processes used for system analysis and development. The simple realization of multi-thread processing and inter-process communications in Linux made it a logical choice for the Mule computers. Multiple threads running in Linux can communicate via inter-process messaging, or through the very convenient use of global variables in shared memory.

2.2.2 Primitive Driver (PD)

The primary focus of the author's work in CIMAR has been on the implementation of the JAUS Primitive Driver (PD) component on the Mule. The project started with a stock Kawasaki Mule 4x4, and proceeded with the goal of producing a fully automated vehicle, controlled at the lowest level by the JAUS Primitive Driver component.

2.2.2.1 Overview

The Primitive Driver component, as illustrated in Figure 2-3, controls the basic driving functions of the platform, and all common platform devices such as the engine and lights. The PD was designed in JAUS to be capable of controlling the mobility of any class of vehicle utilizing any means of propulsion (i.e. tracked, front-wheel steered, omni-directional). In order to be useful for controlling any vehicle set-up, the PD accepts mobility commands in the form of two wrenches, one propulsive and one resistive, that

define a percentile of effort in any of the three translational or three rotation degrees of freedom for motion.

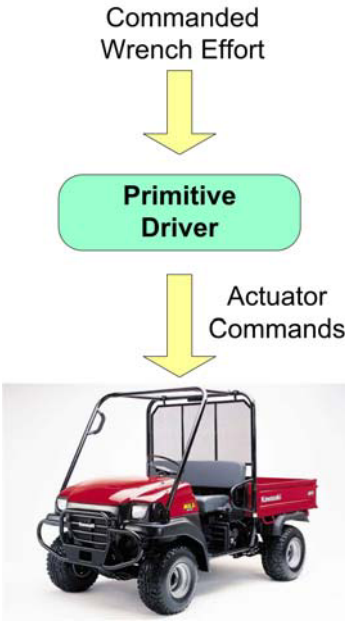

Figure 2-3: Primitive Driver Command Flow

The wrenches can be resolved into three force and three moment components, relating to the orthogonal coordinate system assigned to the assumed vehicle center of mass, as illustrated in Figure 2-4. The convention specified by the JAUS reference architecture is to assign the positive x axis as the forward direction of travel, the z axis pointing downward, and the y axis as defined by a right hand coordinate system. The propulsive wrench can be written in the form

$$\hat{\mathbf{w}}_{\mathbf{p}} = \{f_{px}, f_{py}, f_{pz}; m_{px}, m_{py}, m_{pz},\} \quad (2\text{-}1)$$

in which the net propulsive translational force percentage of effort is decomposed into components in the direction of the three coordinate axes, and the percentage of moment effort about each axis represent the net propulsive rotational moment. The resistive wrench is similarly defined as

$$\hat{\mathbf{w}}_{\mathbf{r}} = \{f_{rx}, f_{ry}, f_{rz}; m_{rx}, m_{ry}, m_{rz},\} \quad (2\text{-}2)$$

which represents force and moment efforts the vehicle must produce to resist translational or rotational movement [Arm00].

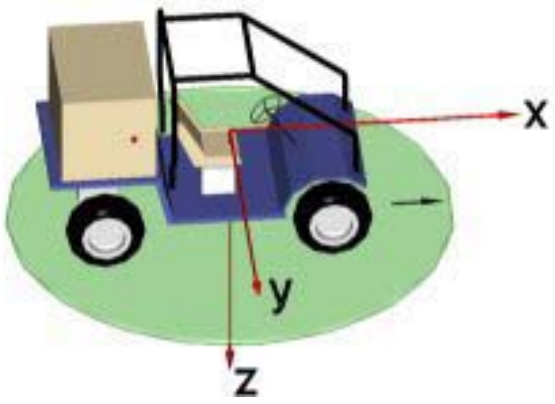

Figure 2-4: Vehicle Coordinate System

The PD translates the wrench commands into control signals for the actuators that directly control the motion of the platform. Most platforms have limited mobility, so only the wrench commands relating to the actuated axes of motion are applicable. For example, a traditional front-wheel steered vehicle like the Mule can execute wrenches commanding propulsive or restive linear effort in the x direction, or a rotational effort about the z axis.

In the JAUS system, the PD functions in a strictly open loop manner, with platform position/velocity control and feedback sensing responsibilities delegated to other components. For example, a propulsive linear effort is commanded instead of a velocity, because velocity control would require a platform velocity sensor.

2.2.2.2 Implementation

Actuator system hardware. The hardware required for the implementation of the Primitive Driver on the Mule included: a computer for running the PD software and communicating JAUS messages with other components, vehicle control actuator systems

with servo motion controllers, hardware for I/O systems, and other supporting electrical and mechanical hardware. The mobility command wrenches for propulsive and resistive effort in the x direction are translated by the PD into a control signal for the throttle and brake actuator systems respectively. At the lowest level, the percentage of commanded linear effort is scaled to the corresponding number of encoder clicks in the 0 to 100 percent position range of the actuators. Then, using position feedback from the encoder, the servo motion controller closes the loop to seek and maintain the commanded actuator position. Similarly, the wrenches for rotational effort about the z axis are mapped to a steering angle controlled by the steering actuator. The design and function of the actuator systems and their associated servo controllers are discussed in detail in Chapter 4.

Computing hardware. A single board computer (SBC) was chosen as the processing hardware for the JAUS node that would host the PD software along with the MRS messaging components. The SBC was ideal for this application for the reasons discussed in Section 2.2.1.2, and because it had the interface ports needed to communicate with the actuator motion controllers. Specifically, it had a PC/104 port and four available serial ports, which served as the data link to the three motion controllers. It also had two Ethernet ports built in for network communication to other nodes, and a compact flash card slot. In order to increase the ruggedness of the computing system, a one gigabyte compact flash memory card was used in place of a traditional hard drive for non-volatile memory storage. This eliminated the potential failure of the rotary disk hard drive due to the shock and vibration inherent in off highway operating conditions.

I/O hardware. In order to monitor the state of certain discrete inputs pertinent to the control logic of the Primitive Driver, a custom digital input board was designed and

fabricated (shown in Figure 2-5). Three eight-bit ports are available on the ESC629 motion control board for use as digital inputs or outputs. However, in order to use this I/O capability, the custom input board was needed in order to set the port bit signal line to a high (+5 VDC) or low (0 VDC) state, based on the input from switch contacts. The input board is designed to uses a supply voltage from the ESC629 board to power a line driver chip, and provide outgoing power to the switches to be monitored. Pull down resistors hold the input signal line for each bit low until the switch is closed, at which point the high voltage is connected to the input channel of the line driver, which outputs the supplied 5 VDC to signal the bit high. LEDs were also built into the circuitry to indicate when a switch has been closed. At this point in the Mule's development, the steering actuator index switch, the throttle relay override switch, and the remote RUN/PAUSE signal have been interfaced this way. It is anticipated that additional digital inputs will be added as needed.

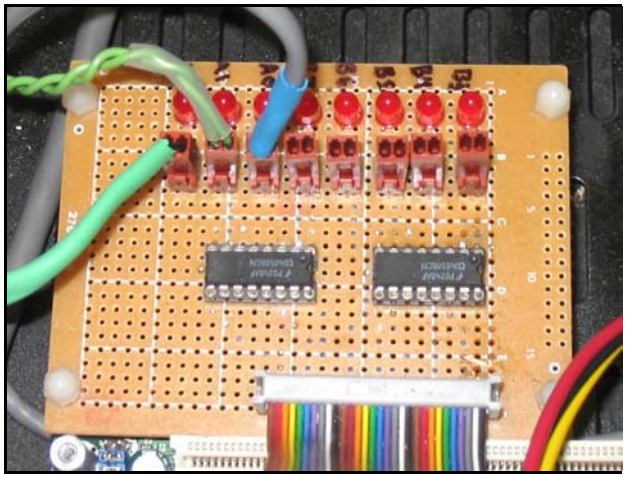

Figure 2-5: Digital Input Board

A similar digital output board for commanding the state of discrete devices on the Mule has been envisioned. This board would use opto-isolator chips to isolate the discrete device circuits from the control logic electronics. This board will provide the

means for starting or stopping the engine, horn, lights, and other platform functional devices.

Figure 2-6 is a photograph of the Primitive Driver tray module that holds the computer and actuator controller hardware. Table 2-1 lists the hardware currently installed in the PD module.

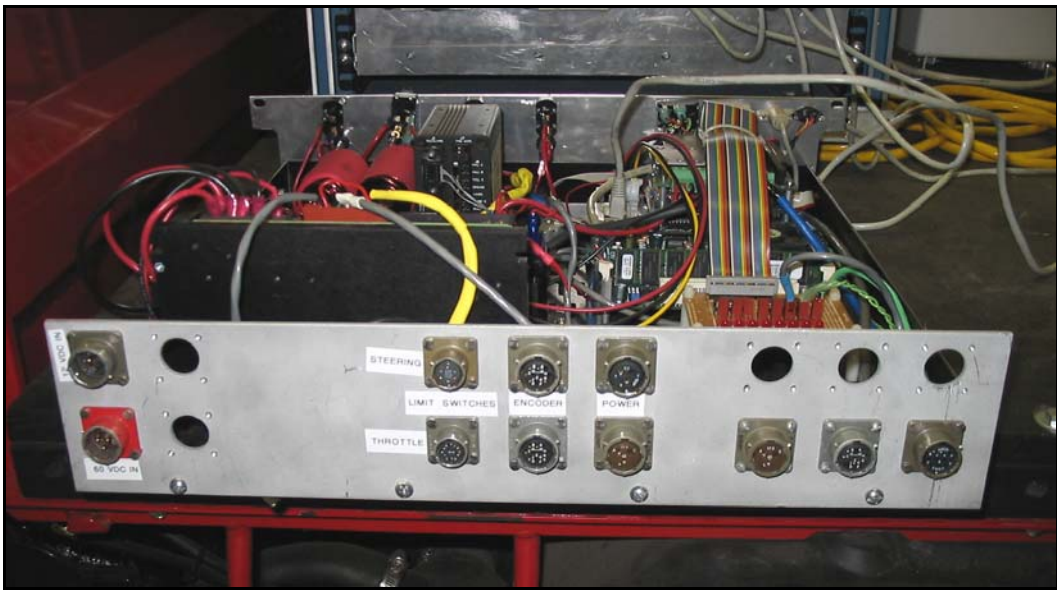

Figure 2-6: Primitive Driver Hardware Tray Module

Emergency stop solution. In the event of an emergency situation, two completely independent methods exist for a human operator to attempt to the halt the Mule. The preferred method is to send an emergency state command to the Primitive Drive via the wireless Ethernet link. Assuming the PD is responding and the wireless connection exists, the PD will respond by engaging the brake at 100 percent effort, and commanding the throttle and steering actuators to zero percent effort. The vehicle will remain stopped in this state unit the emergency clear message is received. This software control way of stopping an errant vehicle is referred to as a "soft-kill." Failure of the wireless link as

detected by a watchdog running in the communications thread of the PD will also trigger an Emergency state soft-kill.

Table 2-1: PD Hardware Components Currently Include in Tray Module

Component	Model Number	Vendor
Single Board Computer	NOVA 7896	ICP Electronics Inc.
Steering Motion Controller	MVP 2001A	Micro Mo Electronics
Throttle Motion Controller	ESC629	Real Time Devices
Steering Motor PWM Amplifier	30A8DD	Advanced Motion Controls
PWM Filter Card	FC15030	Advanced Motion Controls
Digital Input Interface Board	Custom Designed	CIMAR
DC Power Filter and Converter	Custom Designed	CIMAR
Throttle Power Relay	KUHP-11DTT1-12	Potter & Brumfield

The other method used to stop the vehicle is through a hard-kill system that disconnects power to the vehicle's ignition system, which turns off the engine. In order to ensure robust emergency kill functionality, the ignition circuit relay used for the hard-kill was power by circuitry controlled by a separate wireless transmitter. A 900 MHz Freewave radio modem was used to transmit a repeated serial string from a dedicated laptop computer to another Freewave radio mounted on the Mule. The receive modem outputs the serial string to a circuit that powers the ignition relay. If the emergency kill transmitting program is exited, or the wireless link fails, the receiver circuit disconnects power to the relay and the engine dies.

Primitive Driver states. The JAUS reference architecture defines a set of six possible states for components, namely: Initialize, Standby, Ready, Emergency, Failure, and Shutdown. The state of a component is queried and reported through the use of a standard core message set. The general characteristics, transitions, and messaging relating to these states are not discussed here, but can be referenced in Volume II (Reference Architecture) of the JAUS Documentation [Jau04]. Suffice it to say that the control logic of the PD has been programmed to be compliant with the JAUS specification for state operational constraints and transitions. Table 2-2 lists the general JAUS component state transitions. The remainder of this section will discuss specific PD implications of each JAUS defined state.

Table 2-2: General Component State Transition Table from JAUS Document [Jau04]

		Event					
		Shutdown	**Standby**	**Resume**	**Reset**	**Set Emergency**	**Clear Emergency**
State	**Initialize**	Shutdown	Automatic to Standby				
	Standby	Shutdown		Ready	Initialize	Emergency	
	Ready	Shutdown	Standby		Initialize	Emergency	
	Emergency	Shutdown					Standby
	Failure	Shutdown			Initialize		
	Shutdown	Shutdown is non-recoverable					

After a successful Initialization process on start-up, the PD transitions to the Standby state. When the PD is in the Standby state, incoming wrench commands are ignored, the throttle is set to zero percent effort, and the brake is applied at 50 percent effort. When commanded to the Ready state, the brake is released, and the PD begins to respond to wrench commands. An external RF remote controlled switch has been interfaced to the PD digital input in order to signal a RUN/PAUSE command. If the remote switch is opened, the PD puts the Mule in the Standby state until the remote switch is closed again, when the PD resumes the Ready state. When an Emergency state

is signaled, the steering and throttle are sent to the zero effort positions, and the brake is applied at 100 percent effort. This condition remains until the Emergency state is cleared. Table 2-3 summarizes the PD states.

Table 2-3: JAUS State Primitive Driver Implications

JAUS State	Primitive Driver State Implications
Initialization	• All program control threads begin to run • Motion controller filter parameters loaded • Actuator homing sequences executed • Digital input states checked for safety logic • JAUS communications initiated
Standby	• Wrench commands ignored • Throttle set to 0% effort • Brake set to 50% effort
Ready	• Wrench commands executed
Emergency	• Wrench commands ignored • Throttle set to 0% effort • Steering set to 0% effort • Brake set to 100% effort
Failure	• No mobility function control
Shutdown	• All program control threads ended

Primitive Driver software. The SBC used to process the PD software was loaded with the Linux operating system. The code for the PD was written in the C programming language, and structured as multiple threads to take advantage of the parallel processing capabilities of Linux (some actuator manufacturer provided C++ libraries were also included). The throttle, steering, and brake systems' control logic is processed in dedicated threads which maintain communications with the motion controllers, and translate the mobility wrenches into position commands for the actuators. Another thread evaluates the component state logic, and includes a watchdog sequence that signals an

emergency state if communications with the commanding component are lost. Also included as part of the PD program, is a thread that handles all the JAUS message communications. This thread and the JAUS message libraries were adopted from code obtained from researchers at the AFRL to specifically work with their message routing software (MRS).

A window display was created to monitor the PD using the Linux Curses library. This display console provides information about the current state of the PD, commanded wrench efforts, current actuator feedback positions, and identifies the component that currently has command control. Also, if the PD is in an Emergency or Failure state, the terminal window will display the reason why that state was activated. This visual feedback of the PD status has been very useful for trouble-shooting and development.

2.2.3 Velocity State Sensor and Global Pose Sensor

The Velocity State Sensor and Global Pose Sensor are two different components defined according to the JAUS Reference Architecture. In their current implementation as part of the Mule subsystem, they receive input from the same three sensors, so it was practical to develop them on the same node. These components, along with the Global Path Segment Driver Component, have been developed as part of the research of another student at CIMAR. They are briefly explained here to show how they have been integrated into the modular control system in order to augment the Mule's autonomous operating capabilities.

2.2.3.1 Overview

Velocity State Sensor (VSS). The Velocity State Sensor is responsible for determining and reporting the instantaneous velocity state of the vehicle. The velocity state of a point in a rigid body can be described by six parameters defined in terms of a

fixed reference coordinate system that is coincident to that point. The six parameters are: three linear velocity parameters in the direction of the coordinate axes, and three angular velocity terms about each of the coordinate axes. The JAUS RA specifies that the velocity state should be reported in terms of a reference coordinate system that is co-located and aligned with the designated vehicle coordinate system discussed in Section 2.2.2.1.

Global Pose Sensor. The Global Pose Sensor is the component that is responsible for determining the global position and orientation of the platform. The global position is reported in terms of latitude, longitude, and elevation as described by the WGS 84 standard. The platform orientation is defined by the Euler angle parameters Ψ, θ, and ϕ, related to a right-handed reference coordinate system with the x axis facing north, and the z axis in the direction of the gravity vector. A more detailed explanation of these angles can be found in the JAUS RA document [Jau04].

2.2.3.2 Implementation

Optical Encoder. An array of three distinct sensors is used to detect position and velocity information. The first sensor was a two channel Dynapar optical encoder which was installed on the drive shaft of the Mule. The rotation of the drive shaft is coupled to the rotation of the wheels, so as the vehicle moves, the encoder emits a series of quadrature pulses. The quadrature series indicates the direction and relative rotation of the drive shaft, which can then be used to determine the vehicle velocity and relative position. Due to the fact that the gear ratio between the drive shaft and drive axles is not 1:1, a series of tests were performed to determine the relationship between distance traveled, and relative encoder counts.

In order for the output of the encoder to be usable by the SBC, a quadrature decoder produced by US Digital was added. The quadrature decoder utilizes a microprocessor to decode the quadrature signal, and provides an RS-232 serial interface so the encoder position information can be queried by host computer. The encoder measures the actual distance traveled by the vehicle (if it is assumed that there is no wheel slippage), so it can be used as part of a dead reckoning position solution. Dead reckoning is a method of calculating position based on continuously measuring the heading and distance traveled by a vehicle. Also, the vehicle velocity can be calculated based on the time derivative of the relative shaft rotation reported by the encoder.

Inertial measurement unit. The inertial measurement unit selected for the Mule system was the 3DM-G produced by MicroStrain. The 3DM-G combines the sensor output of three angular rate gyros, three orthogonal accelerometers, and three orthogonal magnetometers in its own microprocessor designed to provide orientation information accurate to less than 0.1 degrees. The unit is very small (approximately 3.5x 2.5 x 1 in.), and has an update rate of 100 Hz. The 3DM-G sensor data is input to the SBC via an RS-232 serial connection, where it can be used to calculate position, orientation, velocity, and acceleration in the global reference frame. This sensor can be used to determine the heading information necessary for a dead-reckoning position system. The 3DM-G is an impressive sensor given its comparatively inexpensive cost (approximately $1500), but often needs to be recalibrated due to magnetic field disturbances produced by the Mule's engine during vehicle operation.

GPS receiver. The third sensor implemented as part of the position and velocity sensor suite was a Novatel Global Positioning System (GPS) receiver. The Novatel GPS

sensor receives telemetry data that is transmitted from a constellation of 24 geosynchronous satellites maintained by the Department of Defense. By receiving the telemetry data from multiple satellites simultaneously, a position solution can be realized with centimeter accuracy. The Novatel GPS receiver unit provides global position information in the from of latitude, longitude, and altitude at a update rate of 10 Hz, which is transmitted to the SBC through an RS-232 serial connection. The unit also calculates current heading and velocity based on GPS position information.

Position data fusion. The major disadvantage of a pure dead reckoning approach to a position solution is that slight inaccuracies in the sensor data accumulate over time, causing a decay in position accuracy. The position information reported by the GPS receiver is very accurate, but is susceptible to signal loss if direct line-of-sight with the satellites is not maintained. In order to overcome these inadequacies, the data from all three sensors is combined and filtered using a weighted average calculation. After filtering, the global position, orientation and velocity information is more stable and accurate for use by the Velocity State Sensor and Global Pose Sensor components. Figure 2-6 illustrates the current configuration of the sensors and the sequence of data flow through the JAUS components.

The processing hardware used for the VSS and Global Pose Sensor was identical to the set-up used with the PD. A single board computer equipped with a one gigabyte flash memory card and loaded with the Linux operating system was used for interfacing the sensors, and processing the JAUS component software. Table 2-4 lists the hardware used in the position system module.

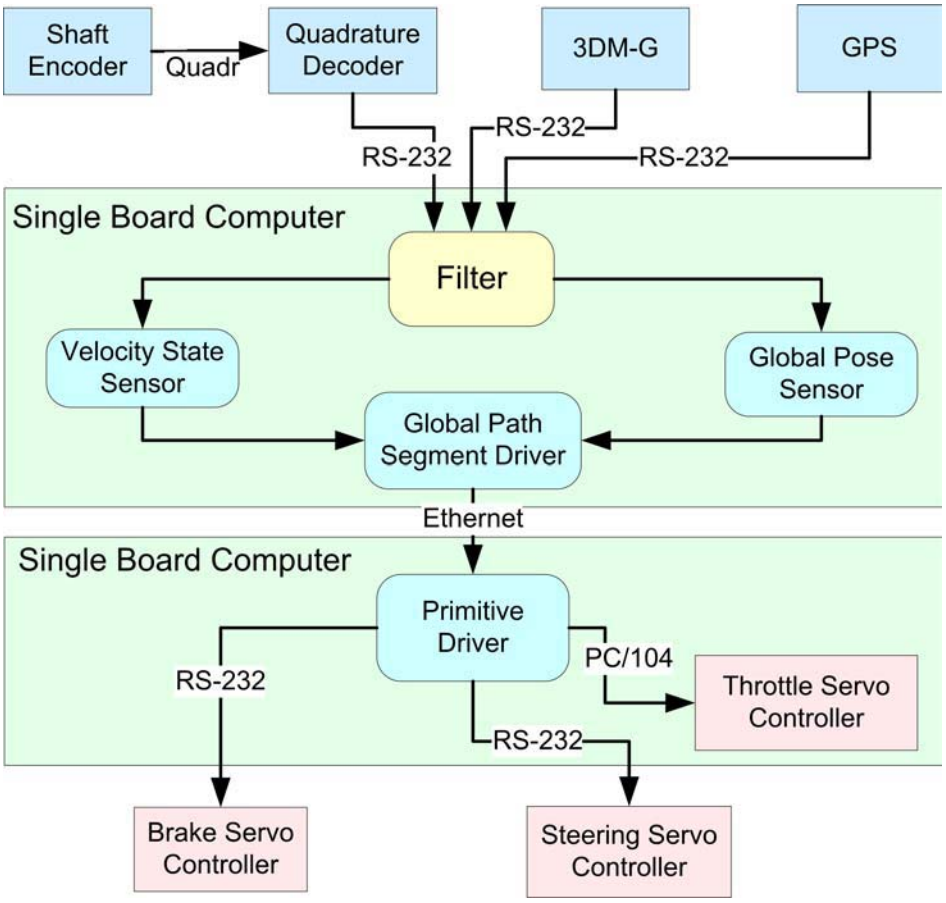

Figure 2-7: Current Mule Component Interface Configuration

Table 2-4: Hardware Included in the Position System Module

Component	Model Number	Vendor
Single Board Computer	NOVA 7896	ICP Electronics Inc.
GPS Receiver	P/N: 01016790	Novatel
Quadrature Serial Adapter	AD4-B	US Digital
Inertial Measurement Unit	3DM-G	MicroStrain
Optical Encoder	HS35	Dyanapar
DC Power Filter and Converter	Custom Designed	CIMAR

2.2.4 Global Path Segment Driver

2.2.4.1 Overview

Fully autonomous operation of the Mule has been achieved by using the JAUS Global Path Segment Driver (GPSD) as the navigational control component. The function of this component is to perform closed loop control of the platform position and velocity as it navigates a preplanned course of path segments defined in the global position reference frame.

The path segments are defined by a second order polynomial that is calculated as a function of three input points and a weighting factor. The path segments lie in the plane formed by the control points (point coordinates given in three dimensions), with the exact shape of the path segment depending on the location of the points and the magnitude of the weighting factor. A more detailed explanation is available in the JAUS RA documentation [Jau04].

The inputs to the GPSD that relate to the desired navigation course are the global point coordinates and weights that correspond to the constituent path segments, and the desired travel velocity. The travel velocity can be changed at any time while the vehicle is navigating the course. In order to accomplish closed loop control of the vehicle heading and velocity, the GPSD queries current position and velocity information from the Global Pose Sensor and the Velocity State Sensor. The feedback data from these sensor components allow the GPSD to stay on course at the desired speed by adjusting the desired wrench efforts output to the Primitive Driver.

2.2.4.2 Implementation

The Global Path Segment Driver has been implemented as a software component on the same node shared by the VSS and Global Pose Sensor. It is important to note that

although these three components share the same computer, in order to be JAUS compliant, they must appear as independent components to other components not located on that node.

2.2.5 Subsystem Commander

2.2.5.1 Overview

The Subsystem Commander component in JAUS is the program that coordinates all the activity within a given subsystem. This component is responsible for all mission planning activities, high-level decision making based on input from other supporting components, and issuing commands in order to accomplish the mission of the subsystem. As per the JAUS RA document, the duties of the Subsystem Commander component may be executed by a human operator, a computer, or a combination of both. The only messaging constraints placed on the Subsystem Commander are that it needs to support the standard core message set that is required of every component.

2.2.5.2 Implementation

At this point in the development cycle of the Mule, the Subsystem Commander has been implemented in the form of an Operator Control Unit (OCU). The OCU is the computer interface that enables a human operator to perform some or all of the duties of the Subsystem Commander. The use of an OCU makes it possible to operate the Mule in tele-op mode, where wrench commands are issued to the Primitive Driver in order to control the mobility functions of the vehicle.

During the initial stages of the Mule PD development, a simple text-based OCU was used to issue wrench commands to the actuator systems. This first OCU was run as a parallel process on the same computer as the PD, and provided a text based terminal interface for issuing JAUS commands to the PD. The OCU and PD are two distinctly

defined components in JAUS, so the MRS Node Manger component also had to be running on the computer in order for the components to exchange JAUS messages. The basic functionality of this OCU proved to be very valuable during testing and debugging of the PD code and actuator systems.

A second, more sophisticated OCU was used later in the development cycle. This OCU provided a graphic user interface, used joystick input to generate wrench commands, and offered many other advanced capabilities such as video feedback display. This OCU, also developed at the AFRL, was installed on a Dell laptop computer running RedHat Linux version 8.0. Using the laptop's built-in wireless Ethernet card, a wireless connection could be established between the laptop OCU and the Mule PD node, which allowed the Mule to operate in the tele-op mode. Testing with the Mule found the maximum range for wireless Ethernet connection between the OCU laptop and the D-Link wireless access point installed on the Mule to be approximately 500 feet with a clear line-of-sight.

At the present time, the Subsystem Commander has only been implemented on the Mule in the form a human operator/OCU combination. However, as more components are added to the Mule subsystem and thereby increase its capabilities, it is anticipated that an intelligent Subsystem Commander will be integrated as the highest level of subsystem command control. The type of tasks that could be handled by this type of intelligent Subsystem Commander are high-level decision making based on input from other components, and path planning and managing operations.

2.2.6 In Progress JAUS Experimental Components

The Mule has already begun to serve its purpose as an autonomous technology test vehicle. CIMAR is working in coordination with researchers at the AFRL to develop

specifications for components that have yet to be defined in the JAUS Reference Architecture. Current student research projects include developing a smart sensor obstacle detection component, a world model component, a dynamic path planning component, and others. As unmanned systems technology advances, so will the demand for new and better performing system components. In conclusion, because the Mule subsystem has been designed according to the modular ideology of JAUS, it will continue to serve for years to come as a test-bed for new and improved autonomous vehicle system components.

CHAPTER 3
ACTUATION SYSTEMS AND HARDWARE

3.1 Description of a Servo System

A servo system can be described as the combination of components functioning together to perform closed loop control of position or velocity of an actuated assembly. A servo control loop controls the position and/or velocity along one axis of freedom of the assembly, so multiple servo loops are need if multi-axis position control is desired. Typically, the desired position or velocity (depending on which control mode is chosen) is output from a host computer, or other external reference source, into a programmable motion controller. The motion controller determines the error between the commanded and actual position, then uses this position error to calculate the output signal based on pre-programmed velocity, acceleration, and PID filter parameters. The control signal generated by the motion controller is then routed to a servo amplifier, which amplifies the control signal to the voltage and amperage levels necessary to drive a DC motor. The motor is usually coupled to some form of gear reduction and then to the assembly that is being position controlled. One or multiple feedback devices connected to the motor or assembly return actual position and velocity feedback to the motion controller, which recalculates the position error and issues new control signal based on the updated position information. Once the desired position is reached, the closed loop servo system will attempt hold that position, even if the load on the actuator changes. Figure 3-1 illustrates a simplified servo control system block diagram.

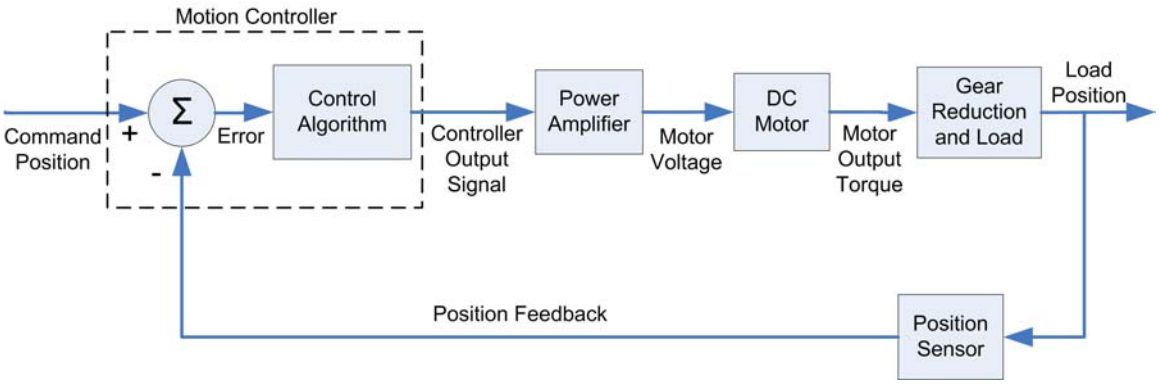

Figure 3-1: Typical Servo Control System

3.2 Design Process for Actuating a Vehicle Control

This section describes the general approach used for designing and implementing servo actuator systems on the vehicle steering, throttle, and brake controls. Sub-system design constraints and decisions specific to the steering, throttle, and brake control actuators are detailed in individual sections of Chapter Four.

The first task in the actuator design process was to outline the general design specifications and functional requirements that would be applicable to all the vehicle actuator systems. These included standards for serviceability, reliability, and aesthetics. Also included in these are universal functional requirements, such as the actuator must be simple to transition between manual and autonomous operational modes.

After the general design criteria for the Mule systems were outlined, the automation process for the Mule continued by defining the design parameters and restrictions for each of the vehicle control sub-systems. This involved measuring the physical requirements for engaging each vehicle control mechanism. Design requirements included the required actuation force or torque, required actuation time, dimensional constraints, and other factors influencing the selection of an actuator. These metrics were

obtained by direct measurement or by approximation if accurate measurement was not possible.

Given the sub-system design objectives and constraints, the next step in the design process was to generate several design alternatives for mechanically linking to and actuating the vehicle control. Different actuation methods and locations were explored by various system design concepts. Each design alternative would then be evaluated to consider its merits and weaknesses by the individuals involved in the project. Cost and the availability of surplus components in the lab were also considered when making the final design selections.

After the mechanical configuration of the actuator was decided upon, the next task in the design process was to select a compatible combination of servomotor, amplifier, servo controller, and feedback device for the complete actuator solution. Options to consider when choosing a method of actuation are whether the system will be driven electromechanically, hydraulically, or pneumatically or by some combination of fluid and electric power.

The next step in the actuation process was to build a physical prototype of the system that had been designed conceptually. Typically, the various components that comprised the actuator solution were first assembled for bench-testing in the laboratory. This involved interfacing a motion controller to a host computer, and connecting any amplifiers, motors, feedback devices, or other components included in the system. The actuator was also load tested with experimental loads comparable to what would be required to actuate on the vehicle. This initial testing was useful for resolving any hardware and/or software integration issues, and made trouble shooting any problems

easier because the actuator was completely isolated from other systems. This initial testing period was also valuable for learning how to operate the actuator components, determining appropriate settings, and developing code that could later be integrated into the Primitive Driver software component.

After each of the actuator systems had been satisfactorily bench-tested, they were integrated into the corresponding vehicle controls on the Mule. Then, once the physical installation was complete, the actuator systems were tested and tuned for optimal performance.

The final step in the process of actuating the vehicle controls was to integrate the control code for each actuator system into the Primitive Driver component used for low-level vehicle control under the JAUS architecture. Then the actuators could be commanded and tested by the same wrench commands the Primitive Driver would be receiving during autonomous operation. This stage also allowed the actuator systems to be operated simultaneously, in order to verify that all systems could function together as intended during autonomous operation.

3.3 Actuator Control Hardware Elements

All the actuation systems added to the Mule use DC powered electric motors. Electromechanical servo systems are typically used in low power applications where high precision, high speed position control is required. The ease of implementation, flexible programmability, and the availability of tools in the lab for working with electromechanical servo systems made them the ideal choice for the Mule actuators.

3.3.1 Servo Motors

A wide variety of electric motors are available for use in servo control systems, with brushed and brushless DC motors being the most commonly implemented. DC

motors come in a wide range of sizes and configurations, and must be selected to match to performance requirements of the system being designed. Things to consider when choosing an electric motor are the torque and speed capabilities, and the voltage and amperage required for operation.

Permanent magnet brushed DC motors were used in the steering and throttle control actuator designs on the Mule due to their availability and ease of implementing in a servo control loop. For permanent magnet DC (PMDC) motors, the relationship between torque and speed is linear, making controller design easier due to simplified system analysis. Also, PMDC motors are very compatible with pulse width modulation (PWM) servo amplifiers, which typically provide the power amplification of the control signal produced by a motion controller. These advantages, along with their cost-effectiveness and reliability, make PMDC motors the popular choice for low power applications where cleanliness is not critical.

The typical disadvantages of a brushed DC motor are maintenance requirements due to the wearing of the graphite brushes used to transmit power to the armature coils. The brushes need to be replaced when they wear to the point that they no longer contact the armature, release dust into the environment as they wear, and have a potential to arch when switching contact points. These disadvantages were not critical in their application to the Mule systems, because the relatively low hours of use mean the brushes will not need replacing for a very long time, and because the small amounts of dust generated by the brushes is insignificant compared to the dust encountered in the Mule's typical outdoor environment. Also, possible arching is not a safety concern because the Mule is not used in explosive environments.

In order to understand the techniques used to perform position control of a brushed DC motor, the basic principles of operation must be understood, including the theory for controlling the torque and speed of the motor. A brushed DC motor consists of a stator, rotor, commentator, and brushes as shown in Figure 3-2. The stator is the stationary external part of the motor that creates a permanent magnetic field using either permanent magnets or electro-magnetic coils. The rotor is the rotating center of the DC motor, and consists of windings that when energized, produce an electrical field to oppose that of the stator. The rotor and its attached windings are also known as the armature. Electricity enters the armature windings through the commutator section of the rotor, which contacts energized graphite brushes that are held fixed with the stator. When the armature coils are supplied with current, the magnetic poles of the armature field attempt to line up with the opposite magnetic poles of the fixed stator field. Just as the armature rotates toward this pole alignment, the brushes jump to a different set of contacts on the commutator, changing the current direction through the armature windings, and thus changing the armature magnetic field orientation. Rotational inertia carries the rotor though the change in commutation, and the new orientation of the magnetic fields continues to drive the rotor toward the new magnetic pole alignment. This commutation cycle of reversing the current flow and hence magnetic poles of the armature windings is repeated to produce continuous unidirectional rotation of the rotor. Most DC motors have several sets of windings in order to produce a smoother rotational motion.

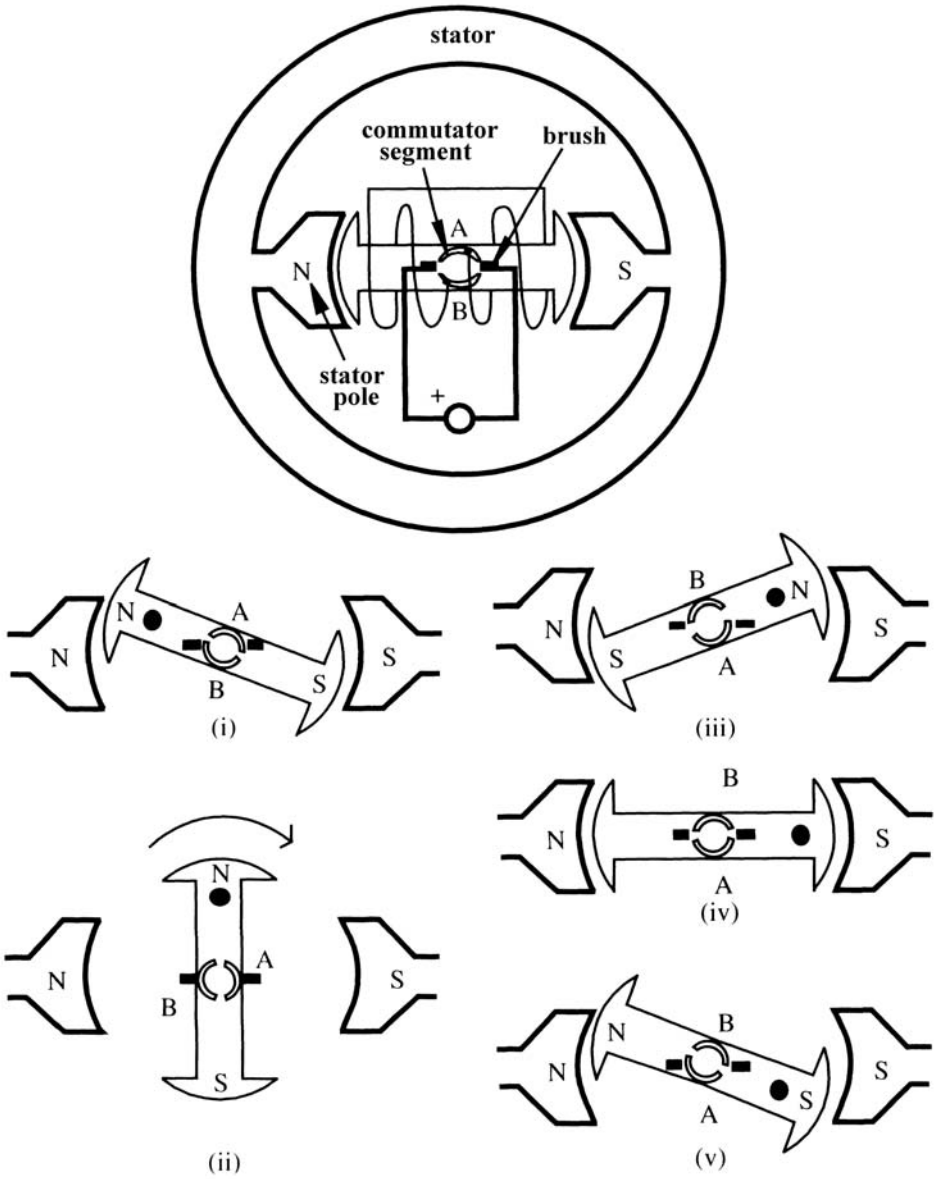

Figure 3-2: DC Motor Operational Theory [His98]

The torque and speed of the DC motor depend on the current and voltage supplied to the electromagnet windings of the armature. The mathematical relationship between the output torque and current is given by the relationship

$$T_m = k_t i_a \tag{3-1}$$

where T_m is the motor torque produced, k_t is the motor torque constant, and i_a is the current in the armature coil. Hence, the torque produced by the motor is directly

proportional to the current passing through the windings of the armature. However, the torque a motor is able to produce is limited by the amperage ratings of the electrical components used in the motor, and by the occurrences of back electro-motive force (emf).

Voltage is induced in a conductor when moved through a magnetic field, so when the conductive windings of the armature spin in the field of the stator, a voltage is induced in the windings. The induced voltage is known as back emf because it opposes the voltage applied to armature. The back emf generated in the armature is directly proportional to its angular velocity ω_a of the rotor as describe by the equation

$$v_b = k_e \omega_a \tag{3-2}$$

where v_b is the back emf and k_e is the back emf or voltage constant.

The electro-magnetic coils of the armature also act as inductors, which produce a voltage as result of changing current, that is described by the relation

$$v_i = L_a \cdot \frac{di}{dt} \tag{3-3}$$

where v_i is the inductive voltage produced, L_a is the inductance of the coil, and $\frac{di}{dt}$ is the rate of change of the current flowing through the coil. This induced voltage is produced by the current direction change in the windings due to commutation, and also opposes the supply voltage applied to drive the motor. This additional inductor produced voltage also reduces the current that can pass through the armature.

The voltage applied to the armature is equal to the sum of the back emf voltage v_b, the inductive drop v_i, and the voltage drop due to the resistance in the armature.

Equation 3-4 is the differential equation for the applied voltage in terms of the armature current

$$v_a = v_b + R_a i_a + L_a \cdot \frac{di}{dt} \tag{3-4}$$

where v_a is the applied armature voltage and R_a is the resistance of the armature. The voltage drop due to the armature inductance v_i is often neglected for steady state operation of brushed PMDC motors, and usually dropped from Equations 3-4, to yield Equation 3-5.

$$v_a = k_e \omega_a + R_a i_a \tag{3-5}$$

Substituting the current-torque relation (Equation 3-1) into Equation 3-5 produces an equation relating the torque, speed and applied voltage.

$$v_a = k_e \omega_a + T_m \cdot \frac{R_a}{k_t} \tag{3-6}$$

Equation 3-6 is fundamental to understanding the torque-speed relation in conjunction with back emf. As the rotational speed of the motor increases, so does the back emf opposing the applied voltage, and thus reduces the portion of the applied voltage available to drive a torque producing current through the armature. That is why maximum torque is achieved at a stalled condition (no rotation means no back emf produced), and maximum angular velocity occurs when the torque is equal to zero (no torque means no voltage drop from current through armature resistance). Rearranging Equation 3-6 to produce Equation 3-7 shows the linear decreasing relationship between torque and speed for a fixed applied voltage.

$$T_m = -\left(\frac{k_e k_t}{R_a}\right)\omega_a + \left(\frac{k_t}{R_a}\right)v_a \tag{3-7}$$

Equation 3-7 can be plotted as a torque-speed curve illustrated in Figure 3-3.

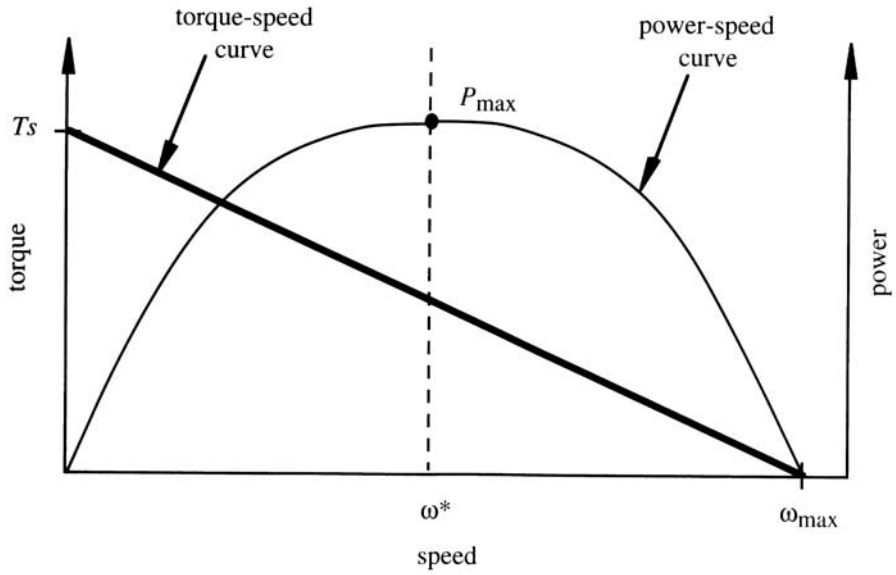

Figure 3-3: Typical Torque-Speed and Power Curves for a PMDC Motor [His98]

In summary, it is useful to remember that in general, the torque produced by a DC motor is proportional to the motor current, and that the motor speed is proportional to motor voltage. The DC motor equations presented in the preceding paragraphs are useful for selecting a motor that will satisfy the design requirements for speed and torque while operating at the voltage and amperage levels of the available power supply. Motor manufacturers will provide all the needed specifications, such as torque and voltage constants (k_t and k_e), and values for motor resistance and inductance (R_a and L_a). The motor manufacturers also generally provide torque-speed curves for various recommended operational voltage levels, that are especially useful for selecting a motor with suitable performance characteristics.

3.3.2 Servo Amplifiers

Another consideration when designing an actuation solution is how to use the low-power output of the motion controller to drive the motor required for actuation. The output of most motion controllers is a control level signal that cannot supply the current or voltage required to drive a DC motor. Therefore, some method of transforming the low-power control signal into a high-power signal capable of driving the motor is necessary. This can be accomplished by using a servo amplifier that is designed to accept either a digital or analog low-voltage control signal and output a higher voltage and amperage supplied from a capable power supply to drive the motor. The control signal produced by the motion controller is commonly an analog signal in the ± 10 VDC range, or a low-power PWM signal, that can represent either a motor torque (current) or velocity (voltage) demand.

Although there are various ways to amplify the control signal, pulse width modulation amplifiers are the most popular for servo control systems due to their cost-effectiveness and superior efficiency. PWM amplifiers work by rapidly switching, or "pulsing", a DC power supply voltage to the motor at a fixed frequency. The supply voltage is held on for variable percentage of the repeating time period *T*, having the effect of producing an average voltage at the motor that is a fraction of the supply voltage. The percentage of the time period *T* that the voltage is held switched on is known as the duty cycle. The duty cycle is defined by Equation 3-8, where t_{on} is the time the voltage is switched on.

$$duty \quad cycle = \frac{t_{on}}{T} \cdot 100\% \tag{3-8}$$

The speed and torque output of the motor can be controlled by changing the duty cycle of the PWM amplifier, as determined by the reference signal from the controller. Varying the duty cycle changes average motor voltage and current, ranging between zero voltage for the zero percent duty cycle, to the full power supply voltage for 100 percent duty cycle. Figure 3-4 displays a simplified PWM amplifier circuit, and plots the corresponding motor and power supply voltage and amperage. It is the inductance of the motor windings that allows the high frequency pulsing of the supply voltage to produce a continuous motor current that fluctuates slightly around an average value.

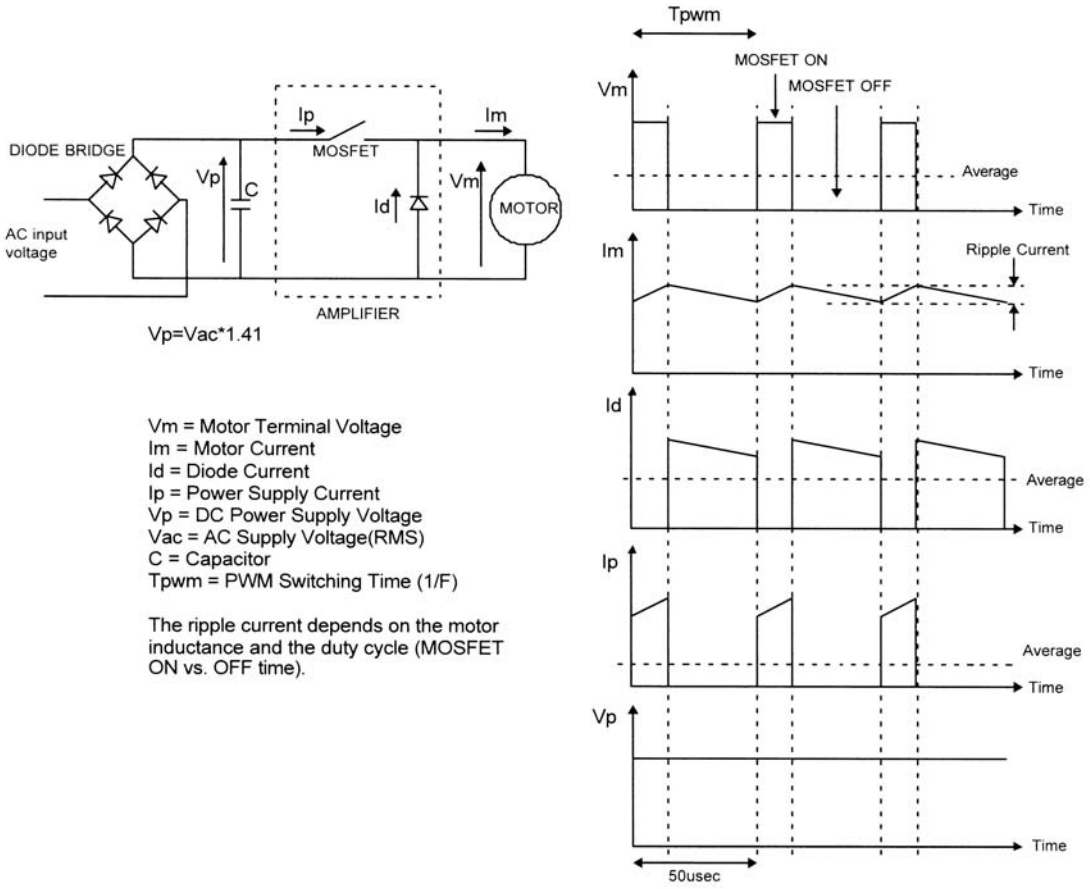

Figure 3-4: Simplified PWM Amplifier Circuit [Adv04a]

PWM amplifiers use Metal-Oxide-Semiconductor Field-Effect Transistors (MOSFETs) for switching the power supply voltage to the motor. The MOSFETs are

switched on by a low-power PWM signal that is output from a digital motion controller, or generated by internal circuitry based on the analog reference signal from an analog controller. MOSFETS are ideal for use as the switches, because they are able to switch large amounts of current at very high frequencies with minimal power dissipation, and are relatively small. In order to operate at maximum efficiency with minimal heat generation, the MOSFETs need to be switched fully on or fully off. An analog voltage signal can be used to control the current through a MOSFET, but a lot of energy is wasted as heat at states between full on and full off. This explains why a PWM control signal is preferred over an analog voltage for driving the MOSFETs [Big03].

In order to drive the motor in both directions, the MOSFETS are arranged in a circuit topology known as an H-bridge. In its simplest form, an H-bridge can be modeled by four switches, a motor, and a power supply as illustrated in Figure 3-5.

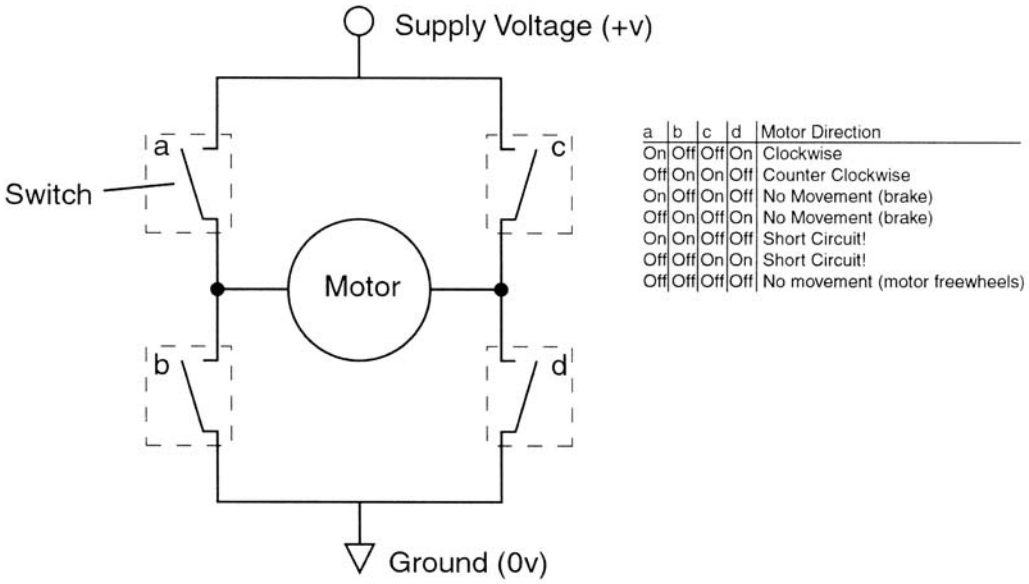

a	b	c	d	Motor Direction
On	Off	Off	On	Clockwise
Off	On	On	Off	Counter Clockwise
On	Off	On	Off	No Movement (brake)
Off	On	Off	On	No Movement (brake)
On	On	Off	Off	Short Circuit!
Off	Off	On	On	Short Circuit!
Off	Off	Off	Off	No movement (motor freewheels)

Figure 3-5: Simple H-bridge Circuit [Big03]

By controlling the state of the four switches in the H-bridge, the motor can be driven in either direction, dynamically braked, or left to freewheel. Closing only

switches a and d connect the supply voltage of one polarity to the motor, causing current to flow through the motor and spin in one direction. Closing only switches b and c place the reverses polarity on the motor, and it will spin in the opposite direction. Figure 3-5 lists possible switch states and how the motor will respond to each state. The H-bridge circuits used in PWM amplifiers includes additional circuitry for controlling the MOSFET switches, but the fundamental principle of operation is the same.

3.3.3 Speed Reduction, Torque Multiplication and Conversion

Generally, DC motors rotate at rates much higher than desirable for most applications. Therefore, the speed is generally reduced to an acceptable rate and output torque increased by some form of torque-speed conversion. Also, by reducing the shaft speed with gears or some other torque-speed converter, a much smaller motor can be used because the output torque has been increased. Additionally, the rotational torque produced by the motor may need to be transformed into a linear force, depending on the method of actuation. Therefore, in vehicle applications, the electric motors will need to be coupled with a torque or force multiplier. A gearbox coupled to the motor is the most common way of converting the high-speed, low-torque output to a low-speed, high-torque output. DC motors are generally available from the manufacturer with an attached gearbox that can be selected with a gear ratio designed to produce a specified range of rotational speed and torque. The output of the gear-head motor can then be coupled to additional combinations of torque or force multipliers to achieve the desired amount of force and speed in the desired direction. Other methods of increasing torque and converting it to a linear force include belt-and-pulley sets, rack-and-pinion gears systems, and lead screws.

3.3.4 Servo Motion Controllers

Another consideration when designing the actuation solutions on the Mule was what type of servo motion controllers would be used to perform closed loop control of each actuator system. A wide variety of motion controllers are commercially available, with many different combinations of computational capability and features. Selection criteria for choosing a motion controller included the hardware and communications interfaces, required feedback signals, type of control signal produced, and additional features offered.

Motion controllers are available in configurations supporting many different hardware and communications standards. Motion controllers can be found in the form of PC/104, PCI, and other card standards that insert into a port on a processor board or bus chassis, and as standalone units that can function with or without communication from a host computer. Communications protocols supported by the standalone type controllers can include RS-232, RS-485, CAN, Ethernet and others. The controllers offer output in the form of an analog voltage or as a PWM control signal. They also can be selected to accept feedback input from most linear and rotational position feedback devices. Often, the motion controllers come equipped with additional features such as multiple axis control channels, programmable memory for independent operation, built in PWM amplifiers, and analog and digital input/output ports.

3.3.5 Servo System Feedback Devices

A wide variety of position and velocity sensors are available to feedback information necessary for the motion controller to perform closed loop motion control. The output of the feedback sensor can be either analog or digital, and should be matched or converted to the input capabilities of the motion controller. Among the most

commonly used sensors for detecting motor shaft orientation are optical encoders, resolvers, potentiometers, and hall-effect sensors. Encoder and resolver feedback can also be used to determine shaft velocity, as well as velocity sensing tachometers.

Optical encoders were used as the feedback sensors for determining the actuator position of the steering, throttle, and brake systems of the Mule. An optical encoder was also mounted on the drive shaft of Mule to provide vehicle velocity information. Encoders are available in absolute or incremental configurations. Absolute encoders produce a unique digital word to identify absolute shaft position, while incremental encoders produce digital pulses as the shaft rotates that indicate relative shaft position displacement. Incremental encoders are more commonly implemented in servo systems, but require that a homing sequence be performed upon initialization in order to determine absolute position. Incremental encoders were used on the Mule systems because adequate position resolution could be obtained at an overall reduced cost than a system implemented with absolute encoders.

Incremental shaft encoders are electro-optical devices that in simplest form are a light source directed toward a photosensor, and separated by a disk with an incremental slot pattern. The slotted disk is coupled to the motor shaft, so as it rotates, an electrical pulse is emitted from the photosensor each time it senses light passing through a slot. The number of pulses generated indicates relative shaft position, while the number of pulses counted per unit-time indicates shaft velocity.

Optical encoders typically use an LED as the photo source and a phototransistor as the photo detecting sensor. The disk is usually made of glass or metal, and is incremented with alternating opaque and transparent segments. The position resolution

obtainable is determined by the number of segments on the encoder disk, with some having more than a thousand alternating segments. In order to increase the position resolution and provide a means of determining the direction of spin, often a second photo emitter-detector pair is added, shifted by one fourth the distance between disk segments. The dual channel encoders are known as quadrature encoders, with channels labeled Channel A and Channel B. The second channel produces a pulse series that is phase shifted 90 degrees from the first. When both channels are considered, a sequence of four different output states are possible with each passing disk segment. As the disk rotates, the state sequence is repeated for each passing segment, and the reverse sequence repeats for the rotation in the opposite direction (see Figure 3-6). Detecting the state changes not only indicates the direction of travel, but also quadruples the effective position resolution. A third index Channel Z is often included with an encoder, which produces a single pulse per shaft revolution, and can be used for homing procedures.

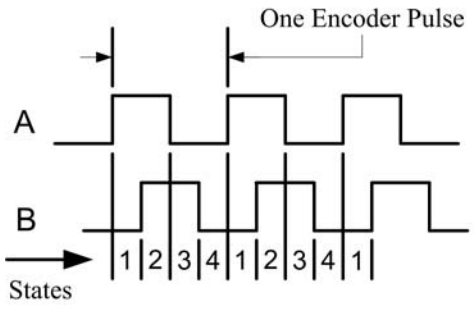

State	Ch A	Ch B
1	1	0
2	1	1
3	0	1
4	0	0
1	1	0
2	1	1
3	0	1
4	0	0

Positive
Direction
Negative

Figure 3-6: Encoder Output Signals and Quadrature States [Fre95]

3.3.6 Limit and Index Switches

If an incremental encoder is used as the position sensor in the servo control loop, a homing routine must be performed on start up in order to be useful as an absolute position sensor. Incremental encoders only sense relative changes in position, so the purpose of the homing sequence is to locate a designated position in the actuator range of

motion as the “home” position. Once the home position is located and set in the controller, absolute position can be identified as the distance relative to the home position.

A typical homing routine begins by commanding the actuator to move in one direction until it triggers an index switch. When the index switch is triggered, the motion controller stops the actuator, and commands it to travel in the reverse direction a pre-set relative distance to the “home” position. Once the actuator has completed its move to the home position, the controller sets the current position to correspond to an absolute index position of zero. The index switch is usually located near one end of the actuator displacement range, so that motion in only one direction will be toward the switch, no matter what position the actuator is in upon start up.

For safety reasons, two other limit switches are also typically added to the actuator system. These switches are located slightly beyond each end of the actuator’s intended range of motion. If tripped, these switches disable power to the motor during a controller failure situation where the actuator attempts to travel beyond its intended range. The purpose of the range limiting switches is to prevent damage to the motor or the vehicle that could occur if an actuator tries to move against the mechanical limits of the system. Figure 3-7 is a diagram of the typical index and limit switch arrangement in a servo system.

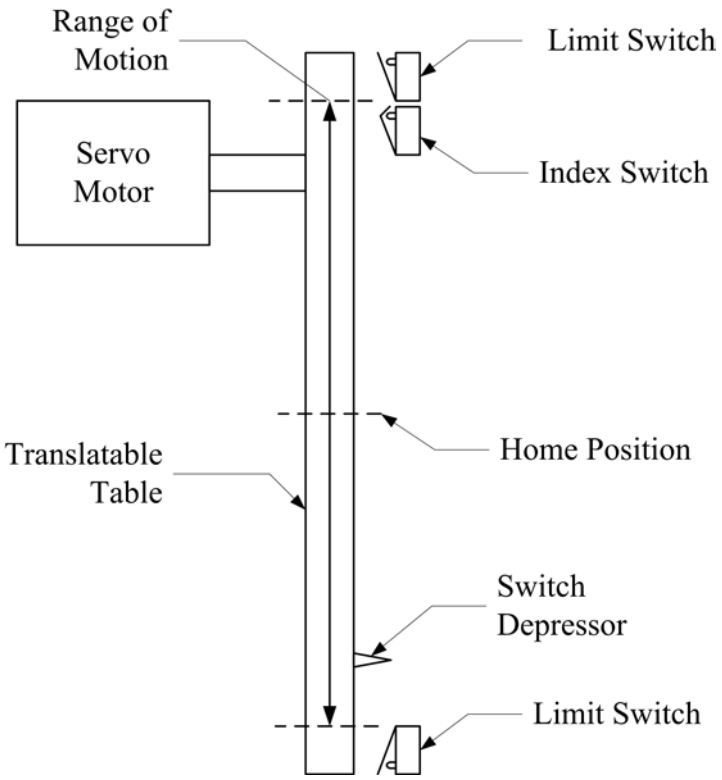

Figure 3-7: Typical Configuration of Index and Limit Switches in a Servo System

CHAPTER 4
ACTUATOR SUB-SYSTEMS

4.1 General Actuator System Requirements

The general design process for the automation of the Navigational Test Vehicle II began by outlining the general design constraints applicable to all of the vehicle control sub-systems. All of the actuator system designs considered for the Mule were required to comply with the following criteria.

1. *Each actuated vehicle control must be able to transition between manual and autonomous control simply and without tools.*

The Mule is a test platform for testing and development of new sensors, controllers, position systems, and other unmanned vehicle system technologies. As such, it was important that the Mule be drivable by both a human operator and by the autonomous navigation control systems. Typically, a sensor, position system, or other component of the unmanned vehicle system is evaluated and developed first on a vehicle driven by a human driver, and later is integrated into the unmanned system. Also, due to the size of the Mule, it was important for it to be drivable by a human operator for positioning at a test site and maneuvering during loading for transport. A simple transition between manual and autonomous control of the vehicle controls would save time and effort during testing.

2. *In the case of system failure, each sub-system should be readily overridable.*

If any of the actuator systems were to fail, it is important that there is a way to override or disengage the failed actuator to allow for manual operation of the Mule.

3. *Actuator systems should be rugged enough to endure projected use without regular maintenance.*

The actuator systems should be designed to operate very reliably and without regular required maintenance. Less time spent maintaining existing systems leaves more time for developing new technologies.

4. *Designs should be simple and easily accessible.*

In the event of an actuator system failure, easy access to the system is critical for troubleshooting and repair operations. Also, simple designs with the necessary functionality are preferred over more complex designs in order to reduce the number of failure points of the system.

5. *All electronic equipment must be sealed to protect against damage from dust and moisture.*

The Mule operates in outdoor environments, so the actuator systems should be designed to protect electronics and other sensitive equipment from damage that could occur from dust and moisture.

6. *The actuator systems should be blend aesthetically with the vehicle.*

The actuator systems should blend with the aesthetics of the vehicle as much as possible. Although the Mule is a test platform, a nice appearance and quality craftsmanship of the actuator systems was desired for showcasing the vehicle capability to our sponsors and the public. It was also desirable that the actuators be designed to integrate into the vehicle system in such a way that they are unobtrusive and do not impede a human operator from comfortably mounting and driving the vehicle.

4.2 Throttle Control System

4.2.1 System Parameters and Design Requirements

Three principle performance metrics characterized the design requirements of the throttle actuator system: actuation force, maximum required displacement of throttle mechanism, and full throttle actuation time. In order to measure the force required to actuate the throttle linkage on the engine, a spring loaded force gage was attached to the linkage near the attachment point of the stock throttle cable. The required pull force to fully engage the throttle control mechanism was determined to be 25 pounds. The maximum displacement of the attachment point at full throttle was measured at one inch. Based on observations of the engine's ability to respond to throttle input, a full throttle actuation time of one second was determined to be sufficient.

Other design constraints for the throttle actuator solution corresponded to the space and locations available for installing the servo-mechanism. Two primary locations were considered; near the throttle linkage in the engine compartment that is located under the cargo bed, and in the front of the vehicle under its plastic hood. Both locations provided adequate space for mounting a capable servo motor and mechanism, and both would be hidden from view and unobtrusive to a human operator.

4.2.2 Design Concepts

In order to generate design concepts for actuating the throttle, the current configuration and function of the vehicle throttle control had to be examined. The fundamental components of the stock Mule throttle control system are illustrated in Figure 4-1.

The Mule throttle is controlled at the engine by pulling on a spring loaded engine throttle lever that actuates the linkages that move the throttle control valve on the

carburetor. In the stock system, the throttle lever is pulled by a cable that is attached to the accelerator pedal. The cable is routed from the engine compartment to the accelerator pedal through a sheath that is held fixed at both ends. When the accelerator pedal is depressed, the throttle cable is pulled through the sheath, pulling the engine throttle lever with it to increase engine speed.

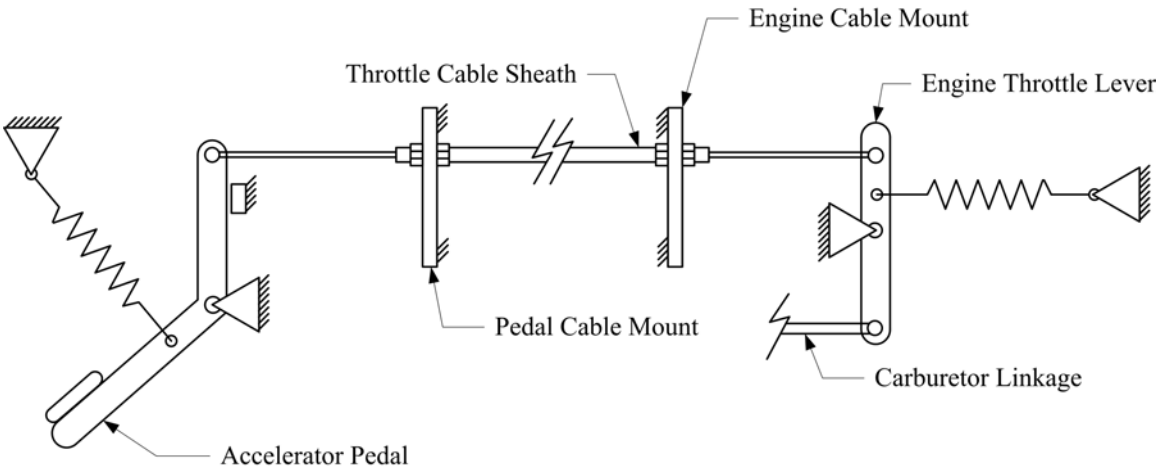

Figure 4-1: Stock Mule Throttle Control System

Three system designs were considered for the throttle actuator. All three designs were similar in that they would exert a linear pull force, but differed in where that force would be applied. The first idea was to mount a servo motor in the engine compartment near the throttle linkage mechanism, and pull directly on the engine throttle lever with a servo controlled cable added to the linkage. The second idea was to mount the servo unit in the front of the vehicle near the accelerator pedal, and pull on the pedal mechanism. The third idea was to mount the throttle servo in an uncluttered space under the hood of the vehicle, and run a second throttle cable back to the throttle lever in the engine compartment.

4.2.3 System Design and Hardware Selection

After some deliberation, the third design was selected, placing the throttle actuator under the hood in an available space that would allow unobstructed access to the actuator system. This mounting location provided greater isolation from the heat, vibration and dust that would be encountered by an actuator mounted in the engine compartment. Also, access to the engine compartment for troubleshooting the actuator would have been much more difficult due to the equipment mounted on the cargo bed that must be raised for access. The parallel cable design was chosen over interfacing to the accelerator pedal or the existing throttle cable because the area surrounding them is very cluttered, and the second cable provides a more direct link to the throttle control on the engine.

4.2.3.1 Servo mechanism

After the parallel cable design idea had been selected, the exact implementation had to be determined. A servo mechanism was designed taking into consideration all of the general design criteria listed in Section 4.1., and the throttle actuator design specifications as outlined in Section 4.2.1.

The servo mechanism design for the controlling the throttle required that the stock engine throttle lever be modified to accept the addition of the second throttle cable, which would act in parallel to the original cable. The second throttle cable, which was purchased from Kawasaki, was routed with the original cable from the rear engine compartment to the front of the vehicle. The front end of the cable sheath was mounted under the hood in the location chosen for the servo motor. The front end of the second cable is pulled by a controller cable attached to a boss on the servomotor shaft. When the rotational position of the servomotor is changed, the controller cable wraps around the boss and pulls on the attached throttle cable. The controller cable is connected to the

second throttle cable with a coupling that will allow a quick disconnect without tools should it be necessary. The parallel cable design allows the engine throttle to be controlled by the actuator system, or by a human driver, with no physical configuration changes required to operate in either mode. This arrangement is illustrated in Figure 4-2.

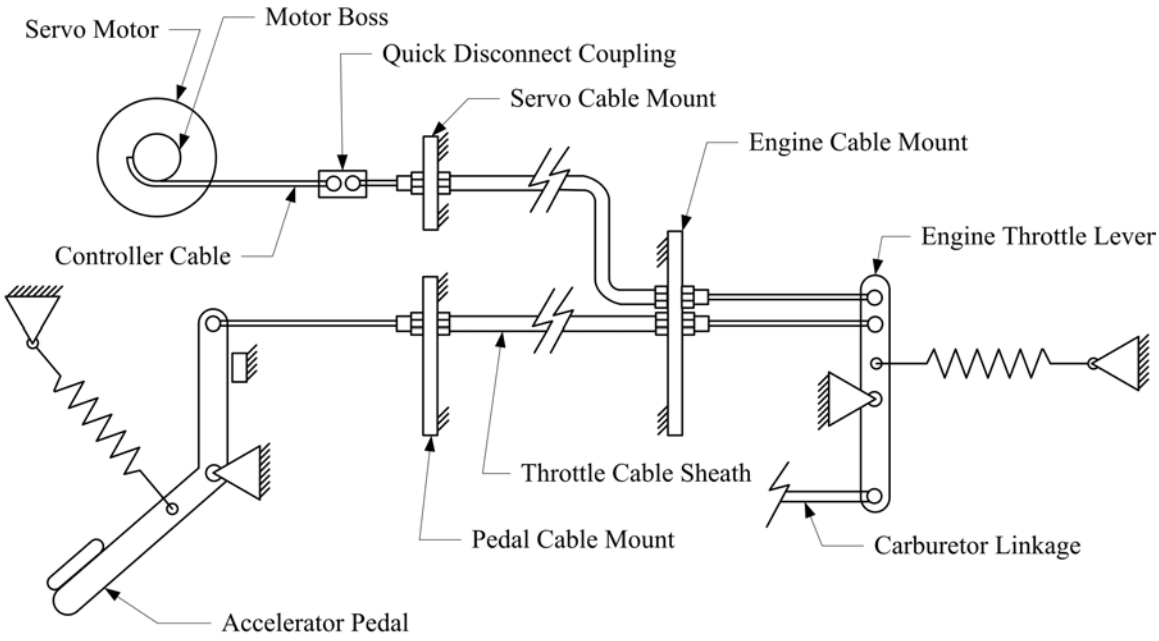

Figure 4-2: Actuated Mule Throttle Control System

4.2.3.2 Servo motor

The servo motor and optical encoder combination used for the throttle actuation solution was available as a surplus component from the retired Navigational Test Vehicle (NTV). Although the design metrics for the throttle system of new Mule were slightly different than those for the previous NTV, the motor and encoder were still well suited for the throttle actuation.

The servo motor is a Pittman brush-type DC gearhead motor, model GM9434 with a 65.5:1 gearhead. The motor has a 24 volt rated windings, capable of delivering 41.3 oz-in. of max. torque, and a top speed of 6151 RPM at the rated voltage (these torque and

speed values are for the motor only and do not include the mechanical advantage of the gearhead) [Pit02]. Using Equation 3.7 and values of the motor constants supplied by the manufacturer, the torque-speed curves for the motor were generated as displayed in Figure 4-3.

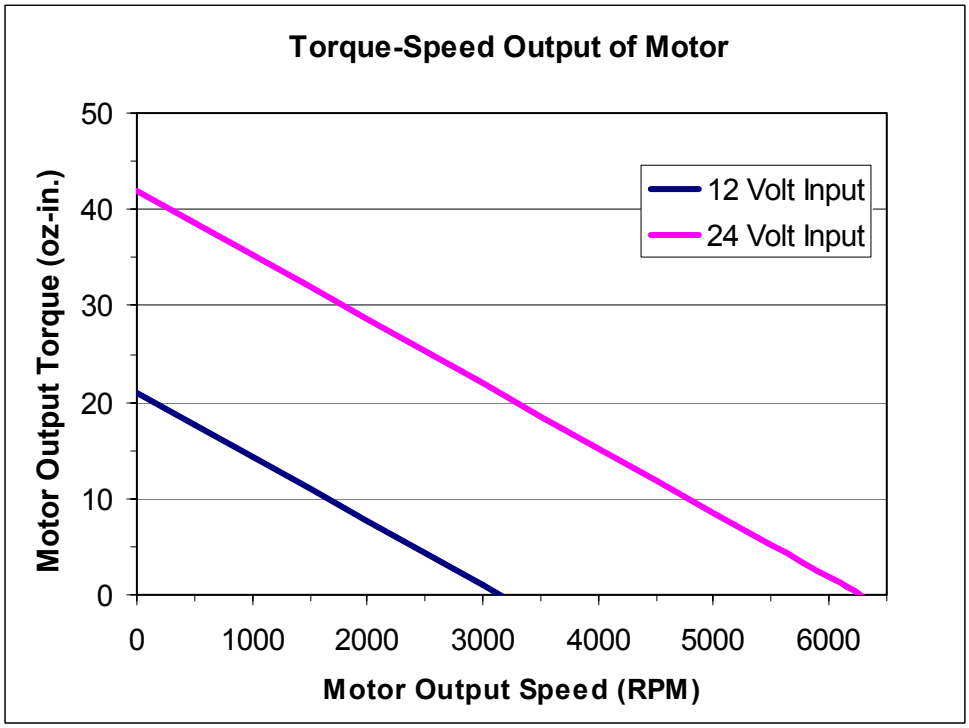

Figure 4-3: Torque-Speed Curve for Throttle Servo Motor

The 12 volt DC power supply was already installed on the Mule and available for use, so the motor's performance at 12 volts was evaluated. The torque-speed curve for the output of the 65.5:1 gearhead was generated next, and included the 66% gearbox efficiency rating supplied by the manufacturer. The results are plotted in Figure 4-4 below.

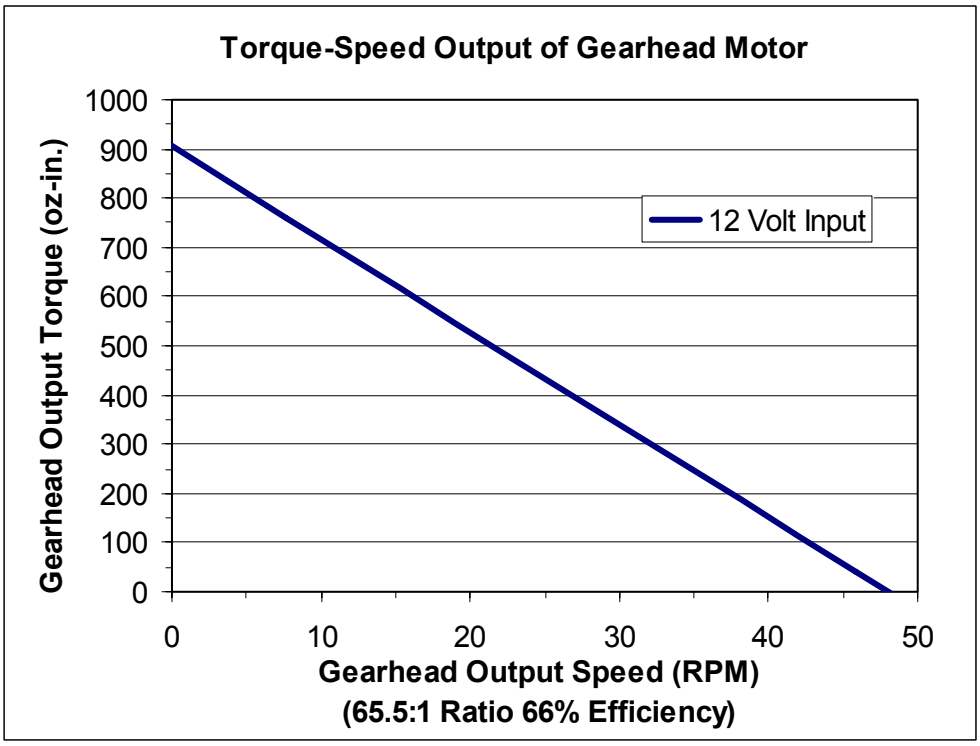

Figure 4-4: Torque-Speed Curve for the Gearhead Output

In order to fully actuate the throttle cable, a pull force of 25 lbs was required. A 0.75 in. diameter boss was connected to the output of the gearhead, and would require 150 oz-in. of torque in order to exert a the necessary 25 lbs of tension on the controller cable. The required 150 oz-in. is well within the 900 oz-in. torque capability gearhead motor at 12 volts, and corresponds to a speed of 40 RPM (see Figure 4-4). At 40 RPM, the one inch of cable displacement required for full throttle position can be wrapped around the 2.36 in. circumference boss in 0.64 seconds. This actuation time is within the one second design specification. In reality, the actuation time will be even faster, because the spring loaded cable system only reaches the maximum 25 lbs of pull force at the end of the one inch displacement. Also, the maximum current draw for the motor in a stalled condition was calculated to be 4.05 amps. However, because the motor will only

be required to hold a torque load of 150 in-lbs at the full on position, a current draw of 0.67 amps should be the maximum required.

4.2.3.3 Servo motion controller and amplifier

The motion controller selected for the task of controlling the throttle servo system was the ESC629 2-Channel DC Servo Motor Interface Board produced by Real Time Devices of Finland. The ESC629 was selected in the PC/104 form factor due the compactness and ruggedness of the PC/104 standard, and the availability of the interface port on the host single board computer. The ESC629 has two independent channels available for simultaneously performing motion control of two servo systems. Two onboard full H-bridges are built into ESC629, which function as PWM amplifiers capable of handling 10 amps peak current sourced from an external power supply of up to 60 VDC. Additional features include three programmable eight bit ports for use as digital input or output, PWM control signal output for interfacing to an external power stage, and two incremental quadrature encoder input ports [Rea01].

Real-time motion control computations are accomplished by the ESC629 using two National Semiconductor LM629 integrated circuit (IC) chips. The LM629 is a dedicated motion control processor designed for use with DC servo motors that can perform complex positioning tasks with minimal intervention from the host computer. Built into the LM629 are: a trajectory control unit, a tunable PID filter, and a position counter. The LM629 is designed to accept a quadrature feedback signal, and output sign (direction) and PWM (magnitude) control signals. The LM629 receives commands from the host computer via the PC/104 bus interface, and then generates the motion trajectory profile and performs closed loop position control of the system. A block diagram of a typical implementation of the LM629 in a servo system is illustrated in Figure 4-5 [Nat99].

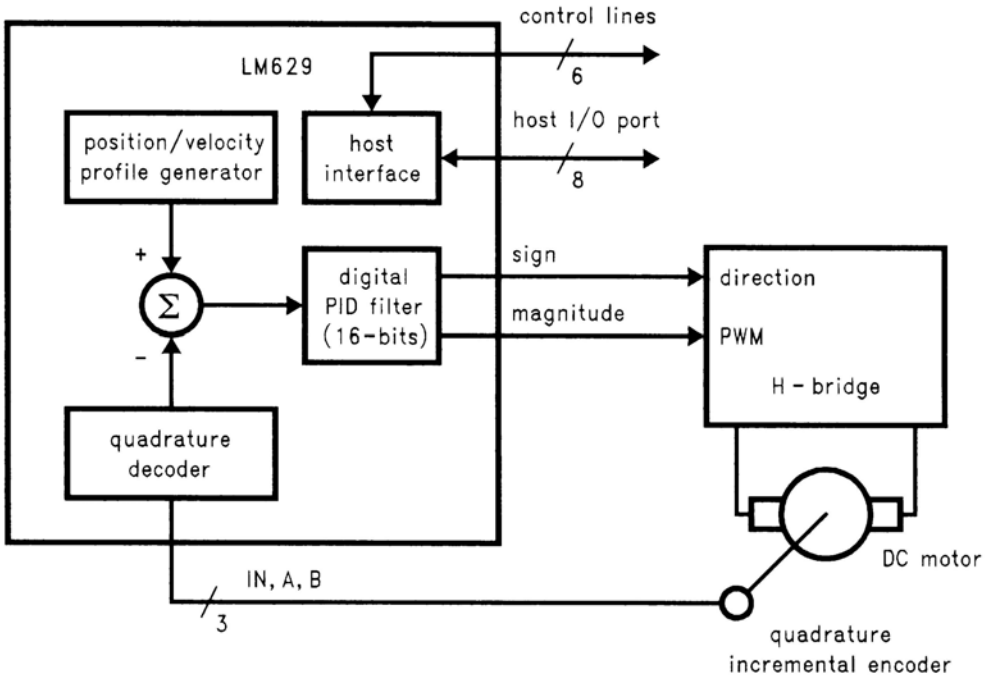

Figure 4-5: Typical LM629 Based Servo Motor Control System [Nat99]

The onboard H-bridge of the ESC629 was all that was required as a PWM amplifier for the throttle servo motor. With a maximum current rating of 10 A and maximum voltage rating of 60 VDC, the H-bridge was easily able to handle the 4.05 A maximum current draw from the 12 volt supply. The ESC629 is equipped with screw terminal blocks for interfacing the 12 VDC external power supply, and motor power output lines to the H-bridge.

The ESC629 software drivers for the Linux operating system were supplied by Real Time Devices, and allowed for a relatively smooth set up with the host single board computer. After successfully bench testing the controller with the all the components of the complete servo system, it was integrated into the Primitive Driver control component. Then the installed throttle actuator system was tested and tuned as a functional element of the vehicle control system.

4.2.3.4 Optical encoder

The optical encoder used to monitor the position and velocity of the throttle servo is a Dynapar Model H23102411423D. This is an incremental quadrature encoder with a single channel resolution of 1024 pulses-per-revolution (PPR), resulting in an effective quadrature resolution of 4096 increments. The encoder is package in a rugged housing that is NEMA-4 rated and has an operational temperature rating up to seventy degrees Celsius. The ¼ in. drive shaft of the encoder is connected to a ¼ in. output shaft on the servo boss with a flexible coupling that allows for slight shaft misalignment.

The amount of rotation of the 0.75 in. servo boss necessary to engage the throttle to the full on position was found to be 0.425 of a revolution. Given the effective resolution of the indicated encoder, that percentage of a revolution corresponds to 1740 quadrature increments over the entire throttle cable displacement range. That level of resolution is more than sufficient for accurately controlling the throttle servo system.

4.2.3.5 Limit and index switches

An index switch was required as part of the servo system in order to perform the initial homing procedure. Also, upper and lower range limit switches were installed that would prevent damage to the system in the case of a system failure overshoot. In order to integrate the switches into the throttle servo system, the servo boss was designed as a cam shaft actuating the switches at certain angles of rotation. Upper and lower tracks were designed for rollers of the switch actuators, with flat spots machined in the tracks where the switches engage. The index switch and lower range limit switch share one track, and the upper range limit switch has its own track. The flats are designed to allow approximately ½ of the boss revolution between the lower and upper range limit switches. The photo of the servo boss is displayed in Figure 4-4.

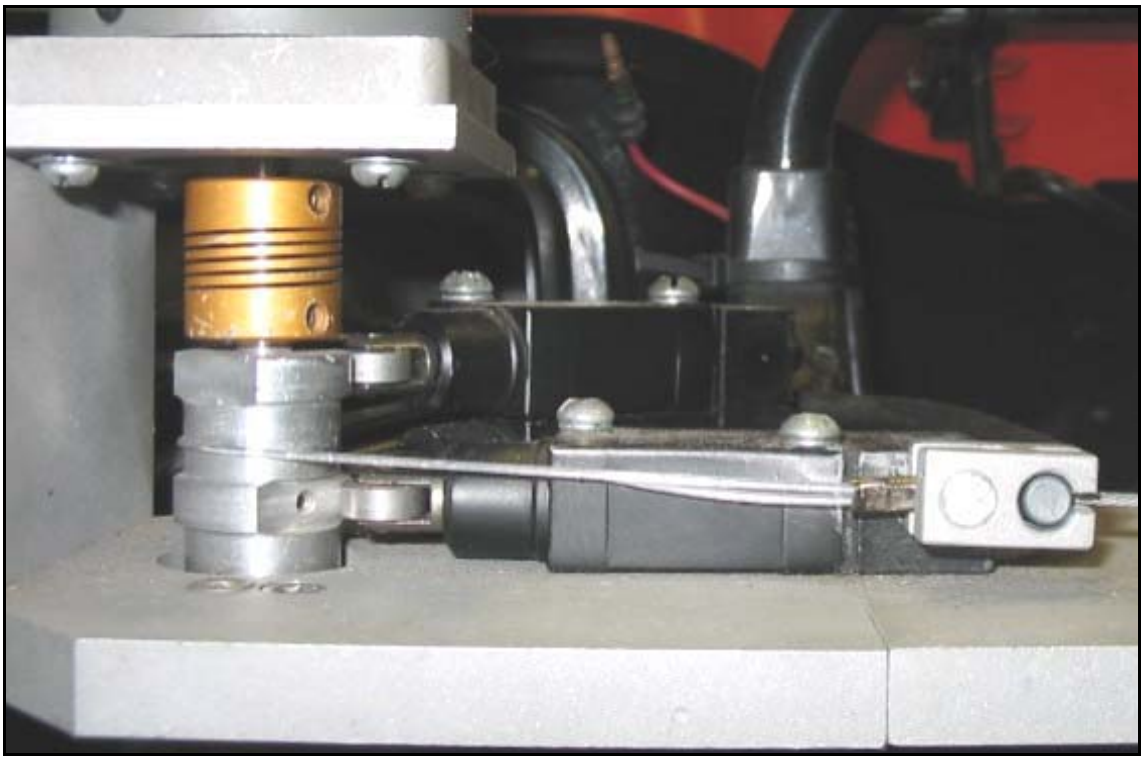

Figure 4-6: Servo Boss with Cam Tracks

The range limit switches were wired normally closed in series with the ground circuit of a relay that supplied power to the H-bridge amplifier. That way, in the event of an error situation, power to the motor would be disconnected. A range limit switch override switch was also installed to power the relay, and a program written to reset the servo boss position after an error situation had occurred. This throttle limit override switch was also monitored by the Primitive Driver via digital I/O, which included code to prevent autonomous operation if the override switch was engaged. As an additional safety measure, 100 lb-test nylon fishing line was used as the controller cable. The fishing line provided and easily replaceable failure point in an error situation where the limit switches were overridden before the controller was reset.

4.2.4 Satisfaction of Design Criteria

Figure 4-5 is a photograph of the finished throttle actuator solution. One advantage of the parallel cable design was the flexibility it allowed for the servo motor mount location. The servomotor, encoder, and limit switches were assembled in a custom aluminum bracket and mounted under the hood on an exposed section of a vehicle frame crossmember. This location provided maximum accessibility and adequate protection from the weather conditions. The servo motor, encoder, and limit switches do not require regular maintenance, and will easily endure the limited dust, moisture and heat encountered under the plastic hood. Another design criteria satisfied by this actuator design was that either the manually controlled cable or the servo controlled cable could actuate the engine throttle lever with no hardware changes necessary to switch between control modes. Also, in the event of an actuator error, the controller cable could be easily disconnected from the cable coupling with no tools required. Finally, because the complete actuator system is entirely hidden from view when the hood is down, it is very discrete and does not detract from the aesthetics of the vehicle.

4.3 Steering Control System

4.3.1 System Parameters and Design Requirements

The primary performance metrics for the steering actuator system design were the amount of torque needed to turn the wheels, and the desired rate of rotation of the steering shaft. A torque wrench with a socket fitted on the steering nut was used to measure the amount of torque needed to turn the steering shaft. This measurement was performed on concrete and grass, and the maximum required torque measured on any surface was 225 in-lbs. In order to ensure that the steering actuator would be able to provide enough steering torque even when the vehicle was heavily loaded or on very

rough terrain, a design factor of two was chosen, to set the maximum required torque metric at 450 in-lbs. The required rotation rate was determined to be at least one revolution per second (60 RMP), based on the estimate of a human driver's ability to rotate the wheel.

Figure 4-7: Photograph of the Throttle Actuator Servo Unit

Other design constraints were the locations and amount of space available for an actuator system capable of driving the steering system. The steering shaft consists of three shaft segments connected by U-joints. The final segment drives a pinion in a typical rack-and-pinion steering gear box, which changes the steering angle with standard tie-rods. Due to the density of other vehicle systems in near proximity to the final two segments of the steering column, the first segment (the one connected to the steering wheel at one end) was the most logical segment that could be interfaced for driving the

system. The area below and to the side of this segment could most easily accommodate a servo system.

An acceptable servo system design would also need to entail some method for disengaging the servo drive system when manual steering mode is desired. This was necessary for two reasons. First, because back-driving the motor would produce a current in the motor leads that could damage the motor drive electronics. Secondly, the friction in the large gearbox used with the servo motor would make turning the steering wheel very difficult for a human driver.

4.3.2 Design Concepts

The most practical design concepts considered for position controlling the steering angle all involved a servo motor and encoder combination coupled to the steering drive shaft. It was decided that the steering wheel should remain as a part of the system for manual operation, so direct drive of the shaft was eliminated as a possibility. Thus, the most practical solution was some form of a parallel shaft drive system, in which the servo motor could drive that steering shaft using matched spur gears or a belt and pulley system.

4.3.3 System Design and Hardware Selection

The final decision was to use a belt and pulley system, with the servo motor positioned parallel to the steering shaft. This configuration offered more flexibility in motor positioning that meshed gear teeth, because the length of the belt could be varied accordingly. It would also be easier to implement, because a belt system would be more tolerant of slight misalignments.

4.3.3.1 Servo mechanism

The servo mechanism designed was similar to the steering actuator systems successfully implemented on other automated vehicles at CIMAR. A CAD rendering of the steering actuator design is displayed in Figure 4-8.

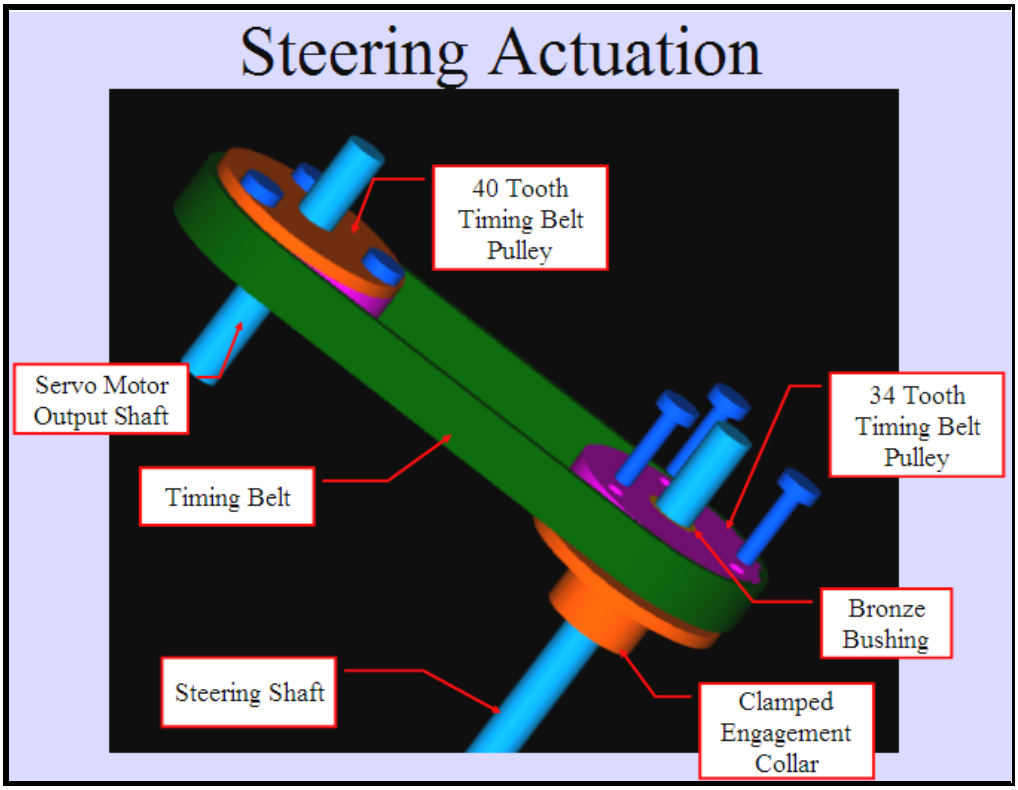

Figure 4-8: CAD Rendering of Steering Actuator Configuration

The servo motor was mounted parallel and on the left side of the upper segment of the steering shaft. A custom aluminum case and mounting hardware were designed and fabricated to hold the servo motor in this position. A plastic glove compartment was removed, and several vehicle controls were relocated in order to mount the servo motor in the front panel area of the Mule, so it would be as unobtrusive and discrete as possible. A 40 tooth timing pulley was fixed to the gearhead output shaft of the motor, and using a timing belt, drives a 34 tooth timing pulley installed on the steering shaft. In order to provide a provision for transitioning the steering system between automatic and manual

control, an engagement collar was fixed to the steering shaft just above the free-spinning steering shaft timing pulley. In order to engage the steering pulley, three steel pins must be inserted through coaxial holes in the engagement collar and steering pulley. This effectively locks the steering pulley to the steering shaft in order to allow servo control of the steering. Hence, all that is need to convert the system between manual and automatic control is to insert or remove the pins.

4.3.3.2 Servo motor

The servo motor selected for the driving the steering system was a model U12M4H/GH12-60 of the Servodisk line offered by the Kollmorgen Corporation. This motor was selected because it offered high standards for quality and performance, and satisfied the design specifications for speed and torque. It was also chosen because it had been previously purchased by the lab, making it a cost-effective option as well.

The U12M4H is a PMDC motor with a printed disk armature, commonly known as a “pancake” style motor. Conventional PMDC motors have armature that consists of electromagnetic coils of wire wound around a heavy iron core used to increase the continuity and intensity of the magnetic fields. In contrast, the armature of a pancake motor is a flat disk with copper conductors arranged as radial lines on the surface of disk. When current is directed outward in the radial conductors, it interacts with the perpendicular magnetic field of permanent magnets, producing a tangential force or torque about the motor axis. Figure 4-9 shows an exploded view of a Servodisk motor in order to make visible the disk armature, radially mounted permanent magnets, and carbon brush functional elements.

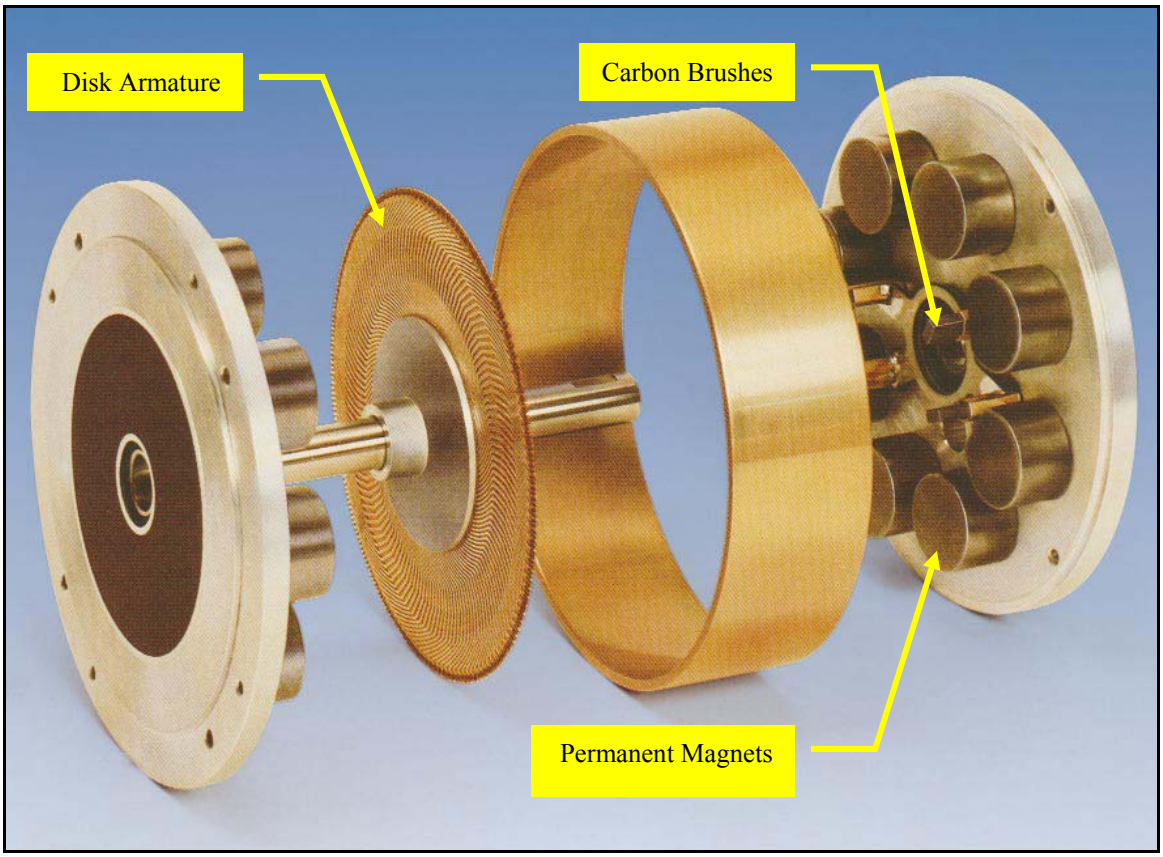

Figure 4-9: Exploded View of a Kollmorgen Servodisk Motor [Kol04]

The unique armature design of the pancake motor can produce some significant performance advantages of over the conventional iron-core PMDC motor. The disk armature of the pancake motor has no heavy iron element and therefore a much lower mass moment of inertia, resulting in faster acceleration times. Also, because there are no coils of wire and no iron core in the disk armature, the inductance is much lower than for the conventional wire wound armature. The significantly reduced inductance means current can flow more readily to produce torque sooner, and less inductive torque losses due to rotor speed. Another advantage resulting from the reduced inductance of the disk armature is less arching at the brushes, which means they will last longer and higher speeds (higher commutation rates) are possible. All these advantages, combined with its

torque and speed capabilities, made the Kollmorgen Servodisk motor an ideal choice for the steering servo system.

The U12M4H/GH12-60 Servodisk is fitted with a 60:1 gearhead capable of delivering up to 1548 in-lb of torque, and rated for a speed of 50 RPM when operated at the rated 62.7 VDC. A pulley gear ratio of 34:40 was selected for the timing belt drive system to bring the torque/speed capabilities of the servo motor closer to the design goals. Also, when operating at its continuous torque rating of 602 in-lb, the motor will draw 7.9 amps of current. Under stalled conditions, the motor could draw a peak amount of 88 amps [Kol04].

Using motor specifications and a modified version of Equation 3-7 as suggest by the manufacturer, the torque-speed curve was plotted for the U12M4H motor operated at 60 VDC (modified equation includes effects of static friction torque and viscous damping). This curve is plotted in Figure 4-10. Note that this is the theoretically predicted torque-speed curve, and is for the motor operated without the gearhead.

Given the 60:1 ratio in the gearhead, and the 34:40 ratio between the timing pulleys, the desired 60 RPM steering shaft rotation rate translates to 3060 motor RPMs. The corresponding torque value of 107.4 oz-in., or 6.7 in-lb, can be obtained from the torque-speed equations or the plot viewed in Figure 4-10. Considering the mechanical advantage of the gearhead and pulley ratios, 6.7 in-lb will produce approximately 342 in-lb at the steering shaft. Note that this torque value does not account for the gearbox mechanical efficiency, as it was not provided by the manufacturer. If the typical gearbox efficiency of 90% is assumed, any steering torque load of 308 in-lb or less will theoretically permit the desired rotation rate of 60 RPM.

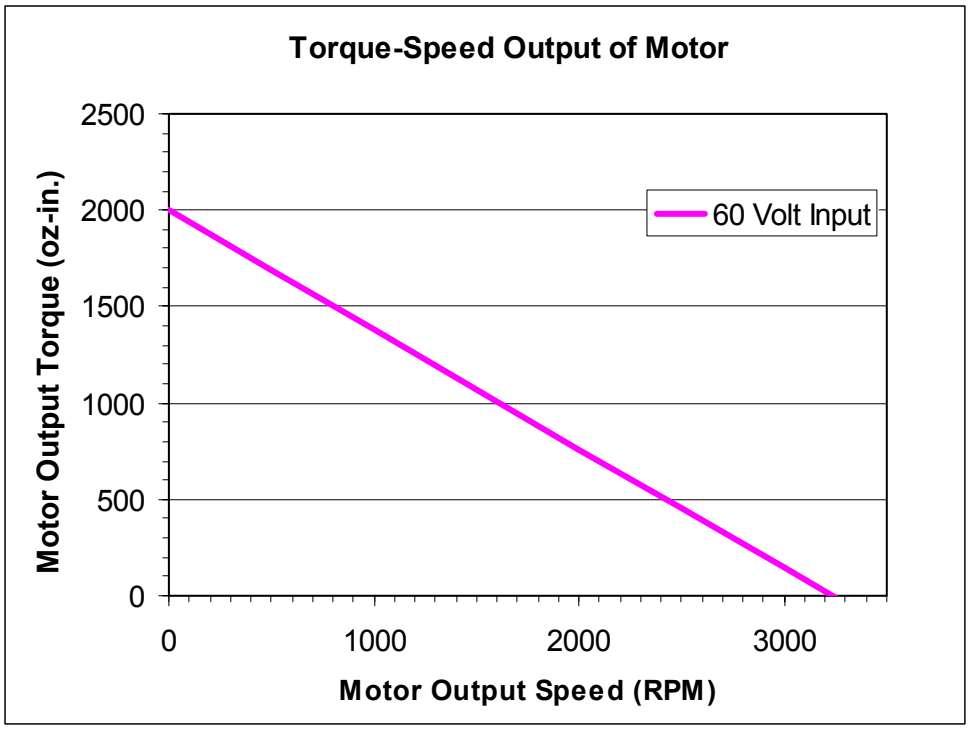

Figure 4-10: Torque-Speed Curve for U12M4H Servodisk Motor

4.3.3.3 Servo motion controller

The steering servo system was initially implemented using the second servo control channel that was available on the ESC629 motion controller used for the throttle system. This controller worked fine when tested in the lab, but behaved erratically when tested in the field. After various trouble-shooting sessions, it was determined that when the vehicle was heavily loaded (i.e. three people and equipment), causing an increased steering torque demand, the controller would sometimes quit functioning. After this discovery, the ESC629 was deemed unreliable and inadequate for use with the steering actuator system.

After abandoning the ESC629, it was decided to use an MVP 2001A motion controller available as a surplus component from the retired NTV. The MVP 2001A is produced by MicroMo Electronics, Inc. It is a full-featured stand-alone motion controller that can be programmed to operate completely independently, or operate under the

control of a host computer as an element of a distributed control system. Features of the MVP 2001A include both analog +/- 10 VDC linear and PWM control outputs, an integrated 50 Watt PWM drive amplifier, and analog and digital I/O capabilities. Communications with the unit are accomplished via RS-232, RS-485, or DeviceNet (CAN) serial interface standards. The MVP 2001A accepts two channel incremental encoder feedback in order to perform closed loop position/velocity control.

The MVP 2001A was implemented as a slave unit to the to the single board computer running the Primitive Driver control code. Desired position commands are sent from the PD and queried feedback information is returned using an RS-232 serial line connected to an available serial port of the SBC. In order to generate a control signal from the feedback system, the MVP 2001A uses PID filters, which are programmed by the PD during an initialization sequence. The PWM control signal generated by the MVP 2001A had to be sent to an external power amplifier because the onboard 50 W amplifier is not sufficient to drive the steering servo motor.

4.3.3.4 Servo amplifier

The servo amplifier selected for the system was PWM brush type amplifier model 30A8DD produced by Advanced Motion Controls (displayed in Figure 4-11). This model is designed to receive a digital PWM control signal from a digital controller, but has some stand-alone functionality for testing and tuning the amplifier settings. The PWM input signal determines the output PWM duty cycle, while the “Direction In” input determines which side of the H-bridge output is switched to control motor direction. The 30A8DD is rated for 20 to 80 VDC, and is capable of handling a continuous current of 15 amps and a peak current of 30 amps. The steering amplifier is powered by a 60 VDC, 500 Watt power supply capable of delivering approximately eight amps of continuous

current. The servo gearhead motor will produce approximately 602 in-lb of torque with eight amps, which is more than maximum design requirement. Therefore, the 30A8DD is well suited for handling the maximum deliverable power from the 60 VDC supply. The amplifier also has current limit adjustment settings, an amplifier disable input, and fault indicating outputs [Adv04a].

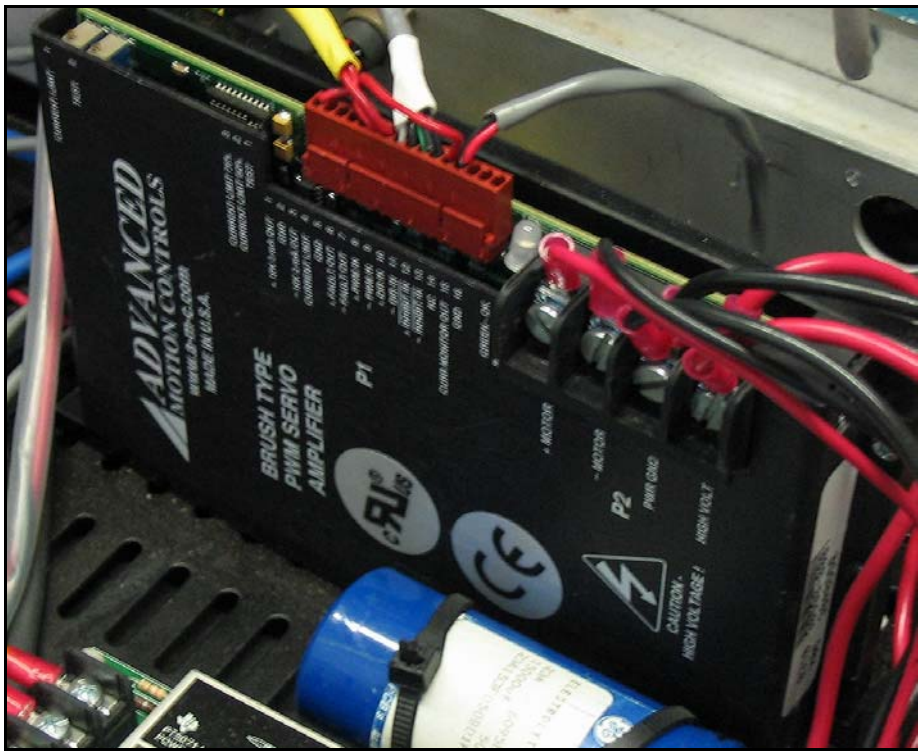

Figure 4-11: AMC PWM Amplifier

The output of a PWM amplifier is a pulsed supply voltage, so a minimum amount of motor inductance is required in order to deliver an adequately filtered current to the motor. The 30A8DD requires a minimum load inductance of 150 µH, but the Servodisk motor selected has an inductance of less than 100 µH due to its lack of iron-cored windings. In order to add inductance to the system, a 300 µH external filter card (model FC15030) was also purchased from Advanced Motion Controls. The filter is essentially two large iron cored inductors that are wired in series with the motor leads. The added

inductance also reduces the potential for signal interfering noise emitted from the amplifier due to the high dV/dT of the output power stage [Adv04b].

When the steering actuator system was first assembled and tested on the vehicle, it was observed that when the motor reversed directions rapidly, the servo amplifier would indicate a fault condition. This phenomenon was determined to be a power supply over-voltage fault caused by the deceleration of the motor load required when changing the direction of rotation. During deceleration or braking of the motor, the mechanical energy of the load is converted into electrical energy that charges the power supply output capacitor to a voltage higher than the over-voltage shutdown point of the amplifier. In order to correct this situation, a large 15000 μF capacitor was wired in parallel to the power supply to absorb the energy generated during direction changes. This successfully prevented the over-voltage error from reoccurring. Adding capacitance also helps to reduce noise in the power supply circuit caused by the rapid switching of the PWM amplifier. The capacitor charges during the part of the PWM cycle when the H-bridge switches are open, and discharges when they close.

4.3.3.5 Optical encoder

The incremental optical encoder used to monitor the position and velocity of the steering servo system was a Dynapar Model H23102411423D, identical to the encoder chosen for the throttle actuator. The encoder drive shaft was connected to the rear end of the motor shaft with a flexible shaft coupling. The effective position resolution of the encoder is 4096 quadrature position increments per revolution of the motor shaft. However, with the addition of the 60:1 gearhead and 40:34 timing gear ratios, the resultant resolution of the system is 208896 positions per revolution of the steering shaft.

This equals a resolution of 1/580th of a degree for steering position system. This high level of resolution was not required, but presented no difficulties for the system.

4.3.3.6 Limit and index switches

As with the throttle servo system, an index switch and range limit switches were added to the steering actuator system. The range limit switches disable the servo amplifier in the event of an overshoot error than could stall the motor or damage the mechanical steering components. These switches were attached on the outside of the vehicle frame below each of the steering tie-rods. Aluminum levers were clamped to the tie-rods to actuate the switches at the end of the maximum possible steering angle. The index switch used for homing was positioned just before the left side range limit switch, so that starting the homing sequence from any position in the range is successful. The adjacently mounted left-side homing and limit switches are pictured in Figure 4-12.

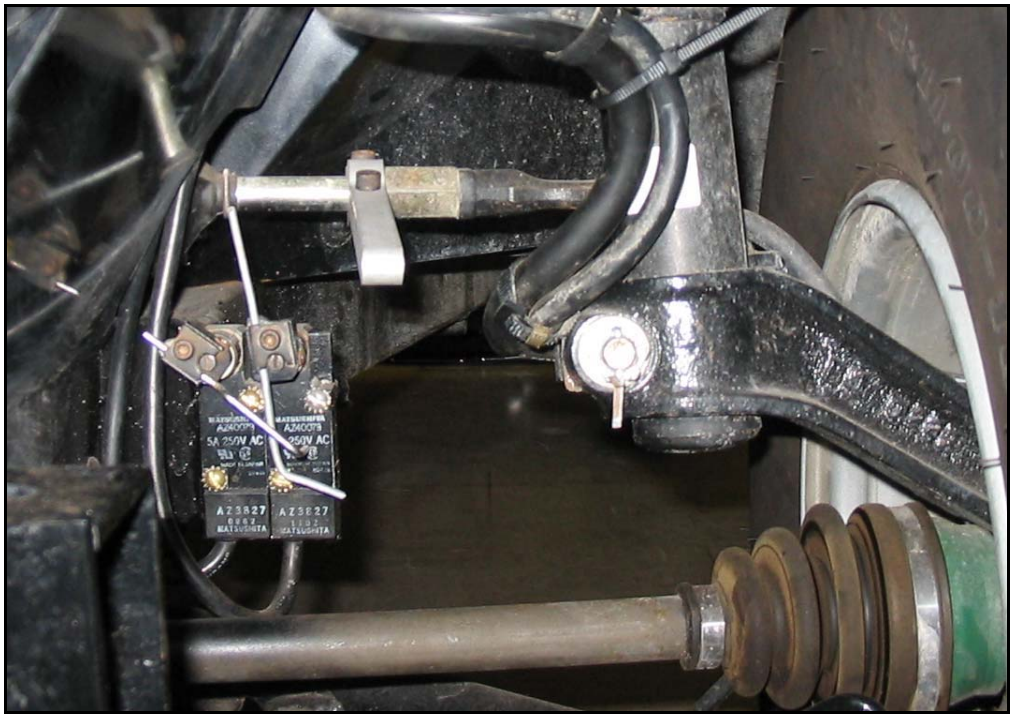

Figure 4-12: Steering Limit and Index Switches

4.3.4 Satisfaction of Design Criteria

In summary, the Servodisk gearhead motor will easily handle the max design torque of 450 in-lb, and in theory will operate at the desired speed of 60 RPM at torque loads less than 308 in-lb. In reality, when operating on typical surfaces (grass, asphalt, dirt) the steering has been observed to respond faster than 60 RPM, and much faster than a human operator could physically turn the wheel. The system is easily converted between manual and autonomous operation modes by simply removing the pins from the engagement collar. This procedure also allows the system to be manually overridden in the event of a controller failure. The system components are sealed against dust and moisture, and the only suggested maintenance is occasional lubrication of the driven pulley bearing. The actuator system is very accessible, and was positioned in the dash area of the Mule to be as unobtrusive and discrete as possible. Figures 4-13 and 4-14 show the Mule dashboard before and after the steering system was installed.

Figure 4-13: Stock Mule Steering

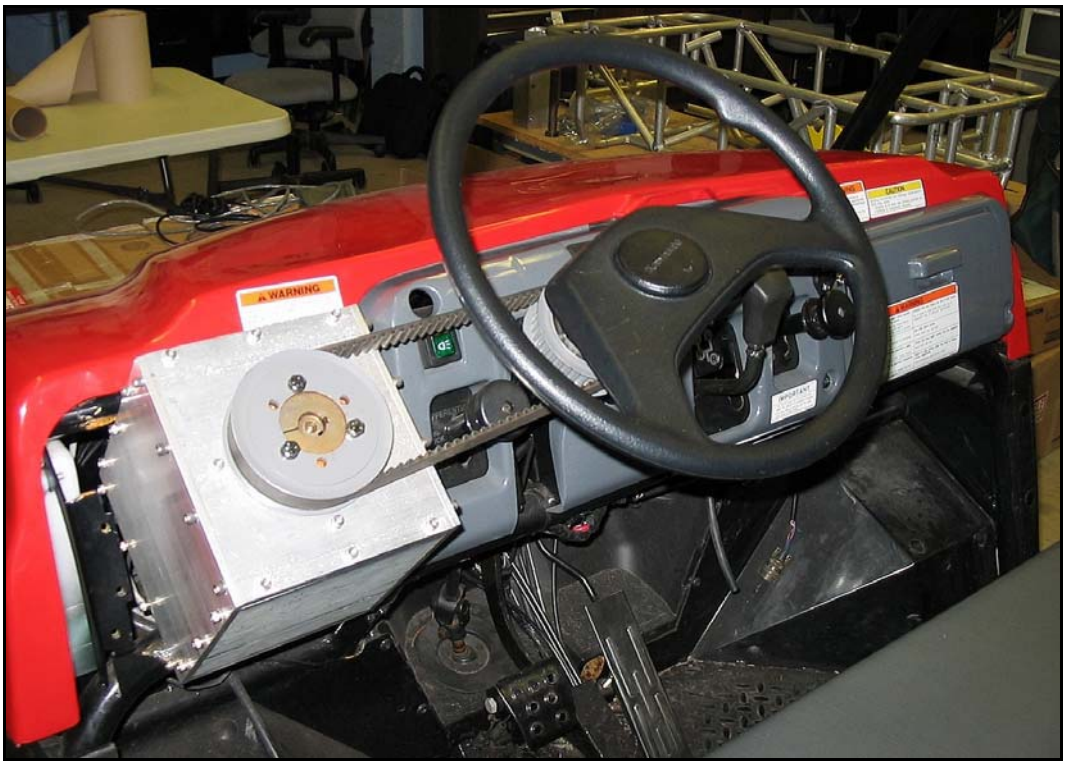

Figure 4-14: Modified Mule Steering

4.4 Brake Control System

4.4.1 System Parameters and Design Requirements

A reliable brake actuator solution was critical for the proper functioning of the automated Mule. Automated vehicle brakes are necessary for bringing the vehicle to a halt at the end of an autonomous mission, for controlling vehicle speed, and for preventing movement during an emergency or standby situation. Braking capability is an essential safety feature, and as such the system designed would have to be very reliable. When fully actuated, the brake system should bring the vehicle to a halt in the shortest stopping distance possible. In order to obtain the minimal stopping distance, the braking force applied to the wheels should be slightly below the force threshold that would lock the wheels and cause less effective stopping. Although the Mule operates in both on and off-road conditions, the brake system was designed to provide the amount of braking

force required to bring the vehicle to a short stop on a pavement surface. The coefficient of friction of paved surfaces is greater than that of grass, sand, or other soft surfaces, so more braking force can be applied before locking the wheels. The exact amount of force the brake actuator would need to produce was dependent on where the force would be applied, which would be decided by the servomechanism design. The time required to reach 100 percent braking force should be the minimum possible, with a half second or less being the quantified benchmark.

4.4.2 Design Concepts

Two fundamentally different approaches were considered for actuating the brake system of the Mule. The stock brake system consists of a standard brake pedal lever, that when depressed pushes the piston in a master cylinder to pressurize the brake fluid distribution system. Steel tubing routes the pressurized fluid to the brake caliper pistons on the front wheel rotors, and the brake shoe pistons of the rear wheel brake drums.

One idea considered for the brake solution was to mount a second parallel functioning brake master cylinder that would be pressurized by a computer controlled linear actuator. The brake lines from the second master cylinder would tee into the existing steel brake lines, so that either master cylinder could pressurize the system to halt the vehicle. In order to function properly, the tubing tee connectors would have to be electrically actuated valves, in order to ensure that only one master cylinder at time would be connected to the system. In order to switch between manual and autonomous control, the Primate Driver would have to command the tee valves to switch between the first and second master cylinders. The advantages of this solution would be great flexibility in mounting locations, because the steel tubing could be routed from anywhere, and a direct connection between the actuator and the master cylinder. The disadvantages

would be the added complexity of control electronics for the tee valves, and difficulty overriding the systems in the event of a computer or electric failure.

The second approach considered was to interface with the existing brake lever mechanism, and push or pull it with enough force to simulate a human driver's input to the brake pedal. The advantages of this idea were that the stock braking system would not be breeched, and the installation could be simpler than the other approach. The disadvantages were that depending on placement, the actuator could interfere with manual operation of the brake pedal.

4.4.3 Hardware Selection

Due to the added electronic and control complexity required by the parallel master cylinder design idea, and the potential for no manual brake control in the event of a system failure, this idea was not pursued. It was decided to design an actuator system that would engage the same pedal lever used by the human operator.

4.4.3.1 Servo mechanism

Various methods of pushing or pulling on the brake pedal lever were possible at several different locations. The brake pedal lever pivots about a point along its length, so a linear actuator could be directly attached to the lever at either the pedal end or the master cylinder end. Unfortunately, on the pedal side of the lever pivot, the actuator would have to be placed around the driver's leg area, which would be obtrusive to a human operator. If attached at the master cylinder side of the lever, the actuator would be hidden from view, but that area is very densely packed with other vehicle systems. In order to avoid these difficulties, a cable and pulley system was designed that would allow the actuator to be mounted in a more convenient and discrete location.

Figure 4-15 is a functional diagram of the brake actuator system. The actuator system was designed with a cable attached to a pivoting axle mounted in a bracket welded to the underside of the brake pedal (see Figure 4-16). The cable is then routed from the pedal through a sheath with one end fixed to the floor, and at the other end terminating at a fixture welded to the frame of the vehicle under the hood. From that point, the cable is attached to a heavy-duty tension spring, which is pulled by the linear actuator. Two sheathed cables were routed in parallel from the brake pedal for added strength. The cables were available in the lab as surplus brake parts from a Suzuki ATV.

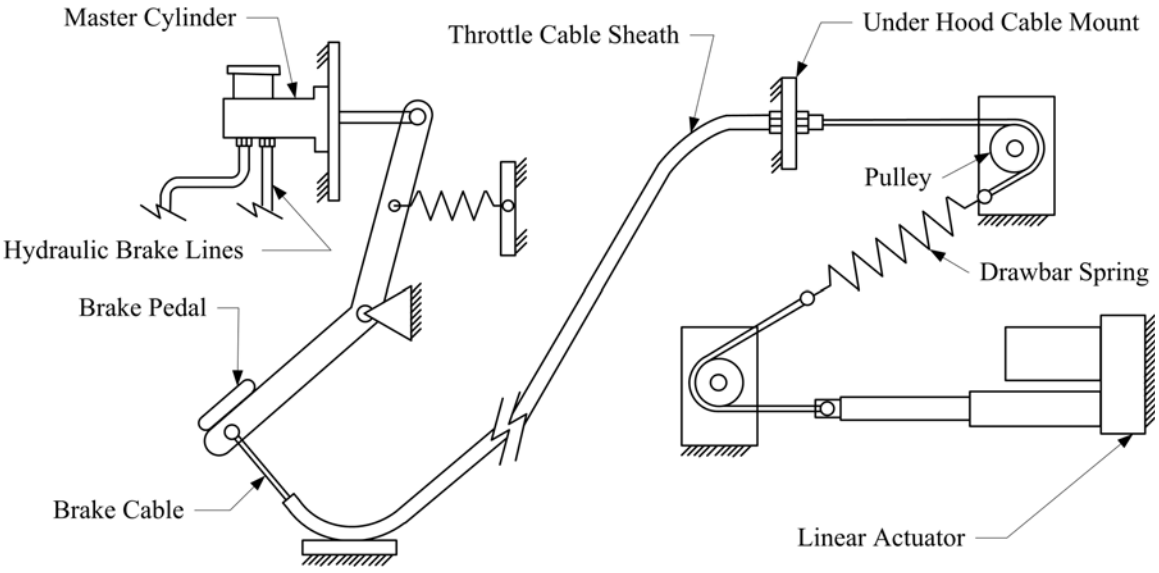

Figure 4-15: Functional Diagram of the Brake Actuator System

The spring was added in series with the cable system in order to create a linear relationship between the actuator position and the tension force the cable applied to the brake pedal. This was necessary due to the extremely non-linear relationship between the brake pedal displacement and the resulting pressure rise in the brake fluid system. During normal operation, most of the brake pedal displacement serves only to remove slack from the mechanism and pressurize the system to a baseline level (pressure when

effective braking force begins). Once the pedal is at the bottom of its displacement range, increasing the force applied to the pedal will increase the brake fluid pressure and braking force, but with very little additional displacement of the pedal. Adding the spring makes force control more feasible with a position controlled actuator. This is because the spring creates a displacement range for the actuator that is linearly related to the resulting applied force.

Figure 4-16: Photo of the Brake Pedal Cable Attachment Bracket

In order properly size the linear actuator, drive motor and spring, the amount of cable tension force required to stop the vehicle needed to be measured. To accomplish this, the cable and sheath system were installed on the vehicle as they would be in the final system. Then, using a spring loaded force gage attached to the end of the cable, the amount of pull force required to bring the vehicle to a halt was measured.

To begin the braking tests, the Mule was accelerated to its maximum velocity on a paved road, and then the brakes were applied by the driver's foot with the intent of bringing the vehicle to a halt as rapidly as possible (without locking the brakes). The distance traveled between the point where the brakes were first applied, and the stopping point was marked on the ground. Then, the procedure was repeated, only this time the brakes were applied using the installed cable system and the spring force gauge. After multiple trials on the pavement surface, it was estimated that nearly 100 lbs of tension pull force were required to bring the vehicle to a halt in approximately the same distance attained by the human operator.

The minimum required length of stroke of the linear actuator also had to be determined. It was noted that the actuator end of the cable had to be displaced approximately 2 in. in order to remove all of the slack from the brake pedal mechanism and pressurize the system to the baseline level. Any additional displacement beyond this point would be due to the stretching of the spring. A safety drawbar spring with a spring constant of 110 lb/in. and maximum displacement of 2 in. was selected. With this spring connected in series with the brake cable, approximately one more inch of displacement would be required to achieve the minimum required force of 100 lbs. Hence, the linear actuator would need a minimum stroke length of at least 3 inches to apply the minimum required force to the system.

The best location available for the linear actuator and spring components of the automated brake system was determined to be under the hood of the vehicle. In this location, they would be protected from weather conditions and easily accessible. With some slight modifications, the system was installed under the hood above the right wheel

well. In order to group the linear actuator, spring and cable components closer together, two pulleys were added to configure them in the shape of a Z. Figure 4-17 is a photo of the brake actuator system under the hood of the vehicle.

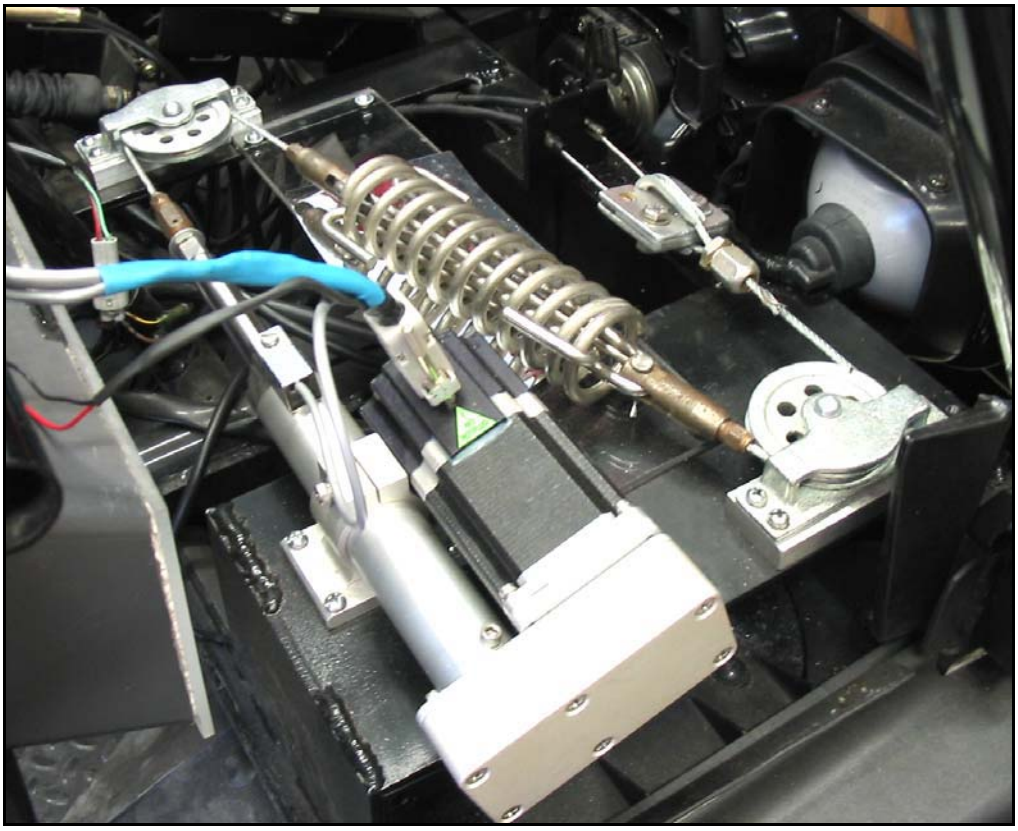

Figure 4-17: Brake Actuator System

4.4.3.2 Smart motor

Once the servo mechanism had been designed, and the exact actuator performance metrics were known, the linear actuator and servo motor combination could be selected. The search for a suitable linear actuator concluded with the Smart Bug actuator available from Ultra Motion. The Smart Bug is a lead screw linear actuator that is driven by a parallel mounted servo motor. The motor drives the lead screw with a geared pulleys connected by a Kevlar reinforced cog belt. Figure 4-18 is a cut-away view of the Smart Bug actuator.

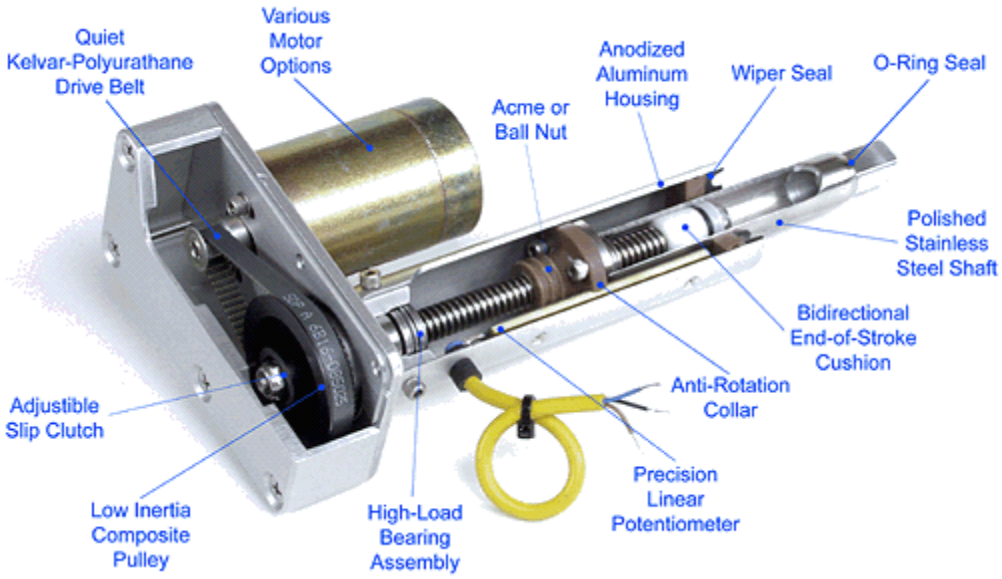

Figure 4-18: The Bug Actuator [Ult04]

The model of Smart Bug Actuator selected for the brake system was the 1-B.125-QS23-4-1NO-B/EC4, which incorporates a ball screw and motor combination capable of 500 lb of thrust and speeds of over four in/sec. The 1-B.125-QS23-4-1NO-B/EC4 uses a 1:1 gear ratio between the servo motor and screw drive pulley. This model also includes built in limit switch provisions and has a stroke length of four inches. The thrust-speed curve for this model is displayed in Figure 4-19. Given the thrust and speed information provided by the manufacturer, a pull force of 100 lb can be moved at a rate of approximately 3.25 in/sec. The home position of the actuator was set such that the actuator pulled the 2 inches of slack out of the system. This was done so that an effective braking force could be applied immediately with any commanded displacement of the actuator. Hence, to obtain an applied brake force of 100 lb, the actuator would only have to move approximately one more inch, which could be accomplished in approximately 0.3 seconds.

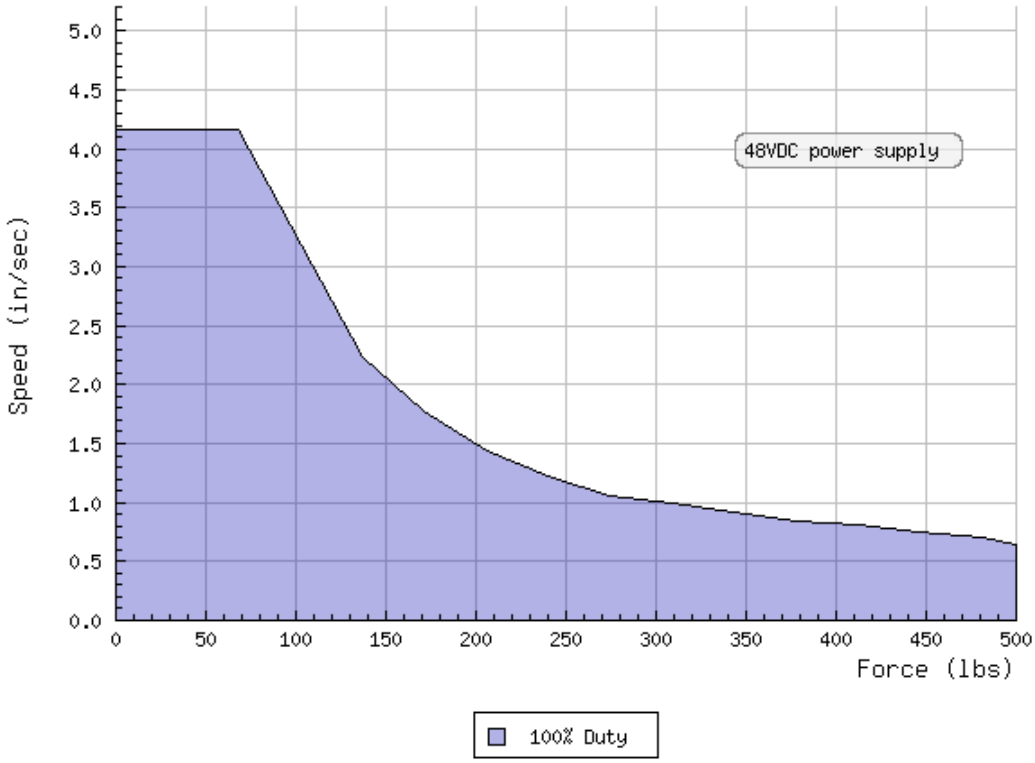

Figure 4-19: Thrust-Speed Curve for Smart Bug operated at 48 VDC

The servo motor that drives the ball screw is a SilverMax S-23H-5 "smart" motor manufactured by Quick Silver Controls Inc. The motor is considered "smart" because it has a motion controller, encoder and power amplifier built together as a single unit. The built-in controller has programmable memory, so the unit can function as a completely independent motion control solution. Alternatively, the unit can be controlled entirely by commands sent from a host computer, or function in a hybrid configuration executing onboard programs and responding to host communications.

Some features of the SilverMax include three digital inputs with pull-up resistors, and four ports that can be set as digital I/O or analog inputs. The communications interface standards of the SilverMax are RS-232 and RS-485, with both "9-Bit Binary" and "8-Bit ASCII" protocols being supported. The power supply voltage can range from

12 to 48 VDC, and it can operate at up to 80º C. The built in encoder resolution is 4000 counts per revolution. When operated at 48 VDC, the S-23H-5 can supply 190 oz-in of continuous stall torque, and will draw a maximum current of four amps [Qui03].

The SilverMax is not a traditional PMDC servo motor. Instead, the drive motor is a 50-pole synchronous permanent magnet motor, commonly identified as a stepper motor. Advanced commutation control systems implemented on the high pole count motor effectively transform it into an AC brushless servo motor. Its integrated motion controller uses feedback from the built-in encoder to determine the position error, and varies the motor torque to achieve the desired position. The primary advantage of using the high pole count motor is the large torque available over a range of low speeds. In many applications, the need for a gearhead is eliminated, because low-speed high-torque characteristics of the motor match desired speed-torque curve directly. This eliminates the weight, backlash, and inefficiency introduced by a gearhead. Another advantage available with the SilverMax is an "anti-hunt" function that can be activated in the control software. This mode eliminates the position hunting (dithering) that is common in servo systems, by switching the motor to open-loop mode at the end of a move to hold a position like a stepper motor.

In order to take advantage of the stand-alone functionality of the SilverMax, it was implemented in the brake actuator system according to a hybrid distributed control configuration. A program was written and stored in the non-volatile memory of the SilverMax that would initialize the controller parameters and perform a homing routing. Once the home position had been located, it would wait to receive brake commands from the Primitive Driver host computer. The SilverMax also monitored a digital input,

connected to a toggle switch on the dash, which would switch the actuator between automatic and manual modes. If the switch was toggled to manual mode, the SilverMax would quit responding to brake commands from the PD and extend its position to release the slack in the brake pedal. When the switch is toggled to automatic mode, the actuator returns to the home position, and again starts listening for brake commands from the host computer. The state of the manual/auto brake switch is monitored by the PD, which will not allow autonomous operation if the brake is in the manual mode.

4.4.3.3 Limit and index switches

The Smart Bug linear actuator has custom external tube mount limit switches available. These are magnetic switches activated by a magnet on the ball screw nut. The external mounting of the magnetic switches provides a clean, simple way to implement the switches in the actuators range of motion.

Two switches were installed for the brake servo system. One switch was located so that it would close when the actuator was fully extended. This switch was used as the index switch for the homing routine and a range limiting switch during autonomous operations. Another range limiting switch was located on the actuator tube just beyond the 100 percent brake position.

4.4.4 Satisfaction of Design Criteria

The complete brake actuator system functioned exactly as designed. Actual operation of the system has shown that a 100 lb braking force can be applied in less than half a second. The system transitions seamlessly between manual and autonomous operation with the simple flip of a switch on the dash. In the event of a system failure, a pin can be removed to disconnect the actuator from the cable-spring system to allow manual operation. The entire system is transparent to the drive because it is under the

hood, which also provides easy access and protection from the elements. The system components are rugged and virtually maintenance free, with occasional oiling of the cable being the only service recommendation. Field testing has proven the effectiveness of the brake system.

CHAPTER 5
ACTUATOR SERVO SYSTEM ANALYSIS

5.1 Servo Controller Operational Theory

The elements of the throttle, steering, and brake servo systems implemented on the Mule are displayed in block diagram form in Figure 5-1. The motion controller is the independent processor responsible for performing the calculations necessary to accomplish closed loop control of the actuator position. During autonomous operation, the Primitive Driver receives platform mobility commands from higher level navigation control components, and translates them into an absolute position commands for the corresponding throttle, steering, or brake actuators. The Primitive Driver communicates the desired actuator position to the motion controller via RS-232 serial or PC/104 bus interfaces. The Primitive Driver also initializes the actuator motion controllers by setting desired acceleration, velocity, and PID filter parameters, and performs homing routines to ascertain the absolute position reference frame for each actuator.

The motion controllers used to control the actuators on the Mule utilize trajectory generators, which calculate transient incremental command positions based on input parameters specified by the host computer. In order to compute the desired position of the actuator as a function of time, the trajectory generator creates a trapezoidal velocity profile using the specified acceleration, maximum velocity, and desired final position. The motion controller then uses this information to control a move by continuously accelerating the actuator at the specified rate (if physically possible) until the maximum velocity is reached, or until deceleration must begin to stop at the desired final position.

The maximum velocity and target position control parameters can be changed while the actuator is in motion, allowing a composite trajectory profile to be created. Figure 5-2(a) shows a simple trapezoidal velocity profile, while Figure 5-2(b) displays a velocity profile generated by changing the velocity and final position during the move. Note that the final stopping position is the integral of the trapezoidal velocity profile.

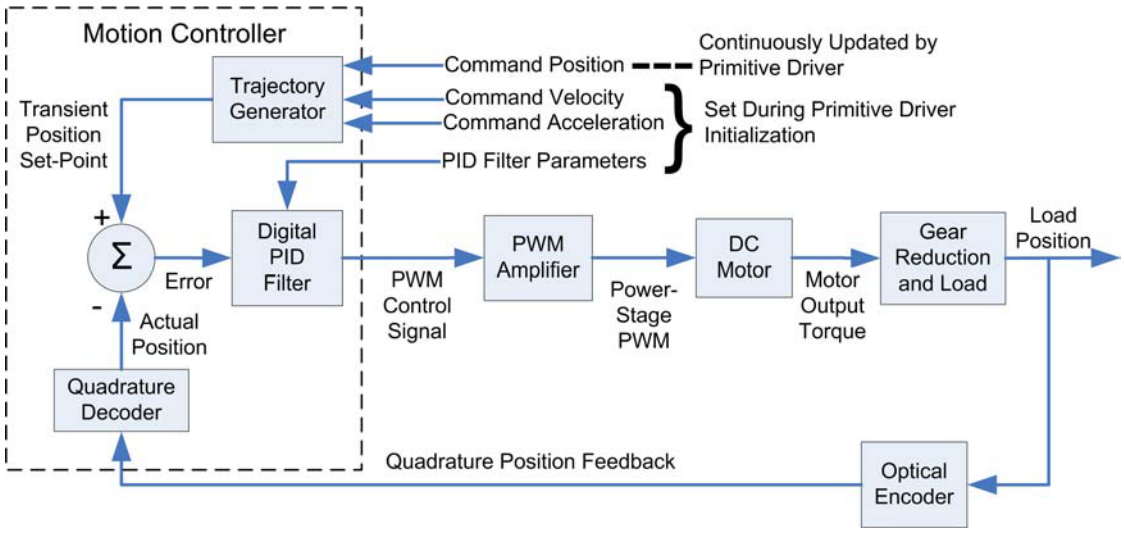

Figure 5-1: Block Diagram of Servo Systems Implemented on the Mule Actuators

Also shown in Figure 5-1 is the digital PID filter designed to create the control signal that is used with a power amplifier to effectively drive the servo motor to the desired position. In order to calculate the position error term used by the filter, the actual position (feedback position from quadrature decoder) is subtracted from desired position supplied by the trajectory generator. The current position error is then passed to the digital PID filter, which performs various operations on the error signal in order to calculate the command signal. The command signal is then converted to a current by the power amplifier, which produces a torque in the motor intended to minimize the position error.

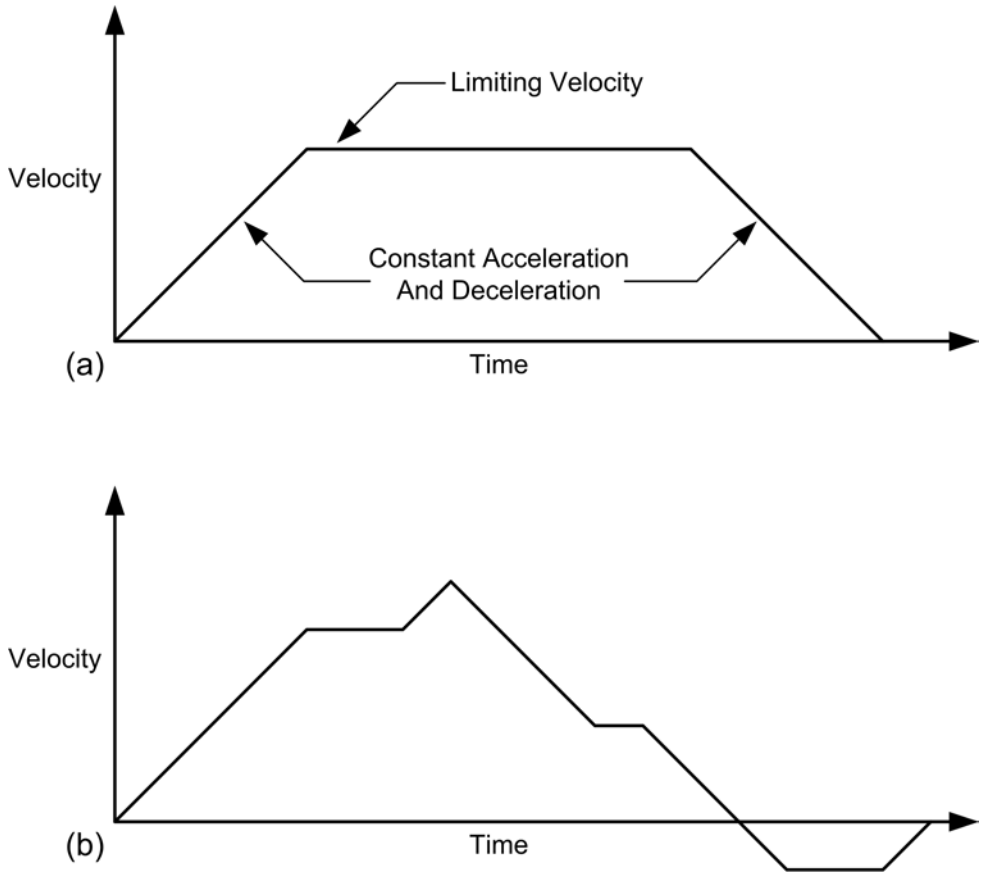

Figure 5-2: Trapezoidal Velocity Profile Graphs (a) Standard Profile (b) Modified Profile

The performance of a servo control system, or its ability to seek and maintain the commanded position in a timely and stable manner, strongly depends on the PID filter parameter settings. A typical proportional, integral, and derivative (PID) filter consists of three parallel acting sub-filters, each of which performs a different operation on the error signal. The results of the proportional, integral, and derivative sub-filters are then summed to calculate the servo control signal as illustrated in Figure 5-3.

The performance of a control system is usually indicated by the transient response characteristics to a change in reference input. A simple step input is easy to generate, and is valuable for examining the transient response of a servo control system. The system step response is characterized by three attributes illustrated in Figure 5-4(a): the rise time,

the maximum overshoot, and the settling time. The rise time, t_r, is the time it takes the system to rise from 10 to 90 percent of the final value. The maximum overshoot, M_p, is the maximum peak value of the response curve measured above the step input, reported as a percentage of the step size. The settling time, t_s, is the time required for the response curve to reach and stay within two percent of the final value [Oga97].

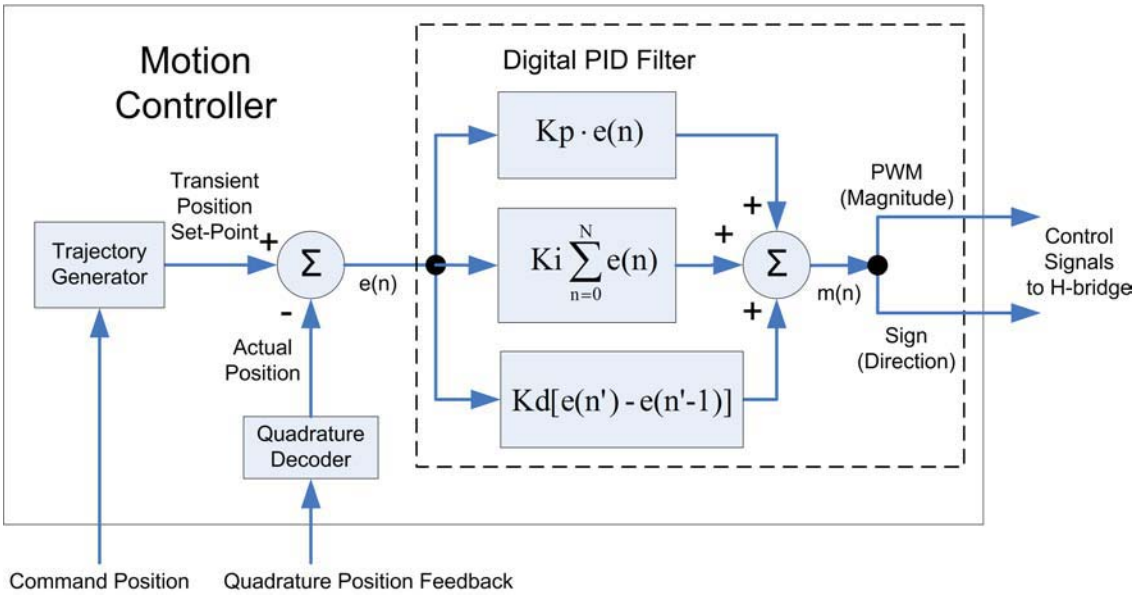

Figure 5-3: PID Filter Block Diagram

Figure 5-4(b) shows the step response of a critically damped control system. The transient response characteristics of a critically damped system are optimal because it exhibits the minimal rise time, without overshooting or oscillating about the input value. The ultimate goal of tuning a control system is to produce a critically damped response to any change in the reference input value.

The parameters that must by selected to produce optimal controller performance are the Kp, Ki, and Kd coefficients of the respective proportional, integral, and derivative filter elements. Other parameters that can typically be set to improve PID controller performance are an integration limit term and derivative sampling rate term. The

following discrete-time equation is an example of the a typical digital PID control signal calculation

$$m(n) = Kp \cdot e(n) + Ki \sum_{n=0}^{N} e(n) + Kd[e(n') - e(n'-1)] \qquad (5\text{-}1)$$

where m(n) is the control signal output at sample time n, e(n) is the position error at sample time n, and n' is the derivative sampling interval which is an integer multiple of the control loop sampling period [Nat03].

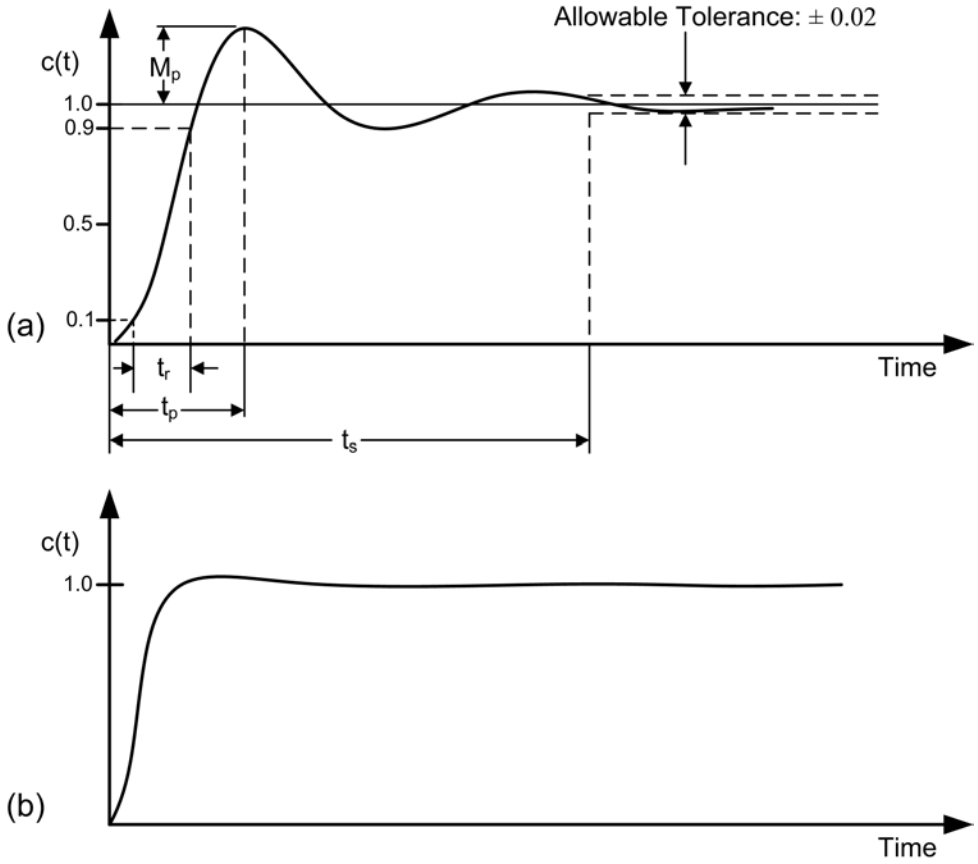

Figure 5-4: Unit Step Response Plots (a) Response Showing Transient Response Attributes (b) Response of a Critically Damped System

The proportional filter element produces a command signal proportional to the position error, where the gain coefficient Kp is the constant of proportionality. The proportional controller can be compared to a spring obeying Hooke's law, because the controller responds with a restoring force proportional to the displacement from the

desired position. If Kp is too small, the system will respond slowly, but if Kp is too large, the system responds with too much force, causing excessive overshoot and oscillations about the desired position. For an optimal system response, Kp is typically set at a value that yields a minimal rise time, but does not cause oscillations or unacceptable overshoot [Nat99].

The integral operator of the PID filter produces a control signal intended to eliminate the deflection effects of a static torque load while the controller is holding a position (steady-state error), and eliminate flowing error while the shaft is spinning. The corrective force provided by the integral term is proportional to the integral of the position error with respect time, where Ki is the constant of proportionality. One possible difficulty associated with the integral term is controller "wind up", a backlash effect observed when the integral term contribution to the control signal has summed to a high value and the load is suddenly removed. This causes the system to violently overshoot the desired position, like a stretched spring that is suddenly released. To prevent this from occurring, most motion controllers offer an integration limit term that can be set as a maximum contribution from the integral portion of the filter. A high value of Ki provides quick compensation for steady-state error, but increases overshoot and ringing (damped oscillations). In general, Ki is set at the smallest value that effectively cancels the effects of a static torque load, without producing undesirable overshoot of ringing [Nat99].

The derivative filter term provides a controller output proportional to the rate of change of the position error, which compensates for rapid changes in load or controller set point. This term has an effect similar to a viscous damper in a spring-mass-damper mechanical system. The derivate control element is included to minimize oscillations

and overshoot, which has a stabilizing effect on the system. Most motion controllers allow the user to specify the derivative sampling interval as an integer multiple of the control loop sampling period, which can be useful for a better approximation of the continuous time derivate. Longer sampling intervals are typically used with low-velocity, high inertia loads [Nat99].

5.2 PID Filter Tuning

PID filter parameters are usually selected, or "tuned" experimentally, especially if the exact system dynamics are not known, or not well defined. Because accurate models of the throttle, steering, and brake actuator systems were not readily available, the values for the control variables of the respective PID filters were determined experimentally. In cases such as these, where many approximations would have to be made for unknown parameters of the dynamic system model, tuning methods are often more effective for selecting suitable PID parameters than a model based approach. This is due to the fact that the cumulative error introduced by the approximations for unknown model constants usually results in a dynamic model of limited accuracy and usefulness.

The widely published Ziegler-Nichols ultimate cycle PID controller tuning method was used as a first attempt at selecting the PID filter gains for the actuator systems. However, the gains calculated using this method produced instability in the actuator systems, so an iterative approach was used for tuning the controllers.

The general approach used for tuning the PID filter gains began by setting the velocity and acceleration parameters of the trajectory generator sufficiently high, so as to generate the best possible approximation of a step input to the system. Figure 5-5 shows the actual step input produced by the throttle system trajectory generator when the velocity and acceleration parameters were set high enough during the initialization of the

motion controller. Then, with the Ki and Kd coefficients set to zero, Kp was successively increased until the point where an increase in the magnitude of Kp produced no improvement in the system rise time. Next, the derivate coefficient Kd was increased, and the derivative sampling period adjusted, to the minimum amount required to dampen any noticeable overshoot. Then, the integration term multiplier Ki was increased to eliminate any steady state error observed after the actuator had completed the move. These initial adjustments were made by visually observing the response of each actuator. The next step in the tuning process was to plot the actuator step response curves on an actuator position versus time graph, and compare the performance attributes of each iteration. In this manner, final adjustments were made to the PID filter gains in order to produce the best possible system response.

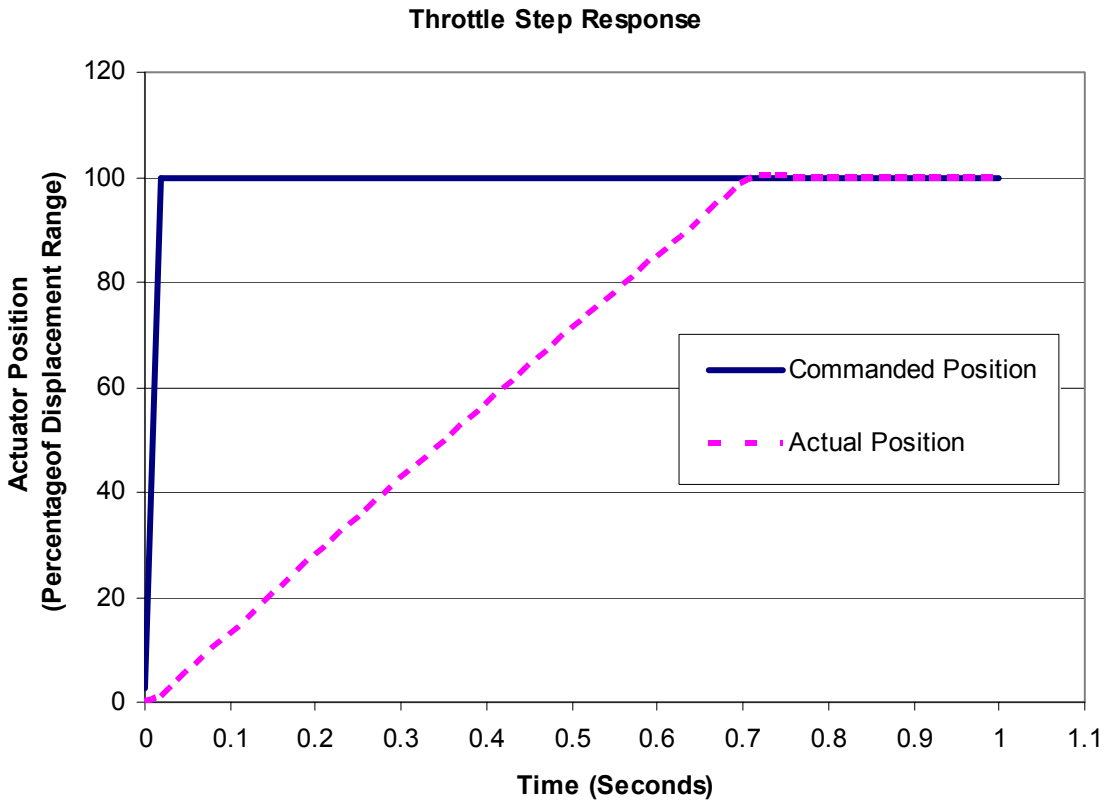

Figure 5-5: Step Input Produced by Throttle System Trajectory Generator

5.3 Actuator System Mathematical Modeling

When designing and implementing a servo control system, mathematical modeling of the system dynamics is generally attempted in order to obtain a useful model for predicting system behavior. Mathematical models, usually in the form of transfer functions, can be determined for individual elements of a servo control loop, or for the entire closed-loop system.

One technique used for obtaining a system model from experimental data is step-response based modeling. This method of determining a dynamic model of the system is useful because only the time-domain response data generated from a step input to the system is required. To formulate a system model, the attributes of the step-response curve are analyzed in order to match it to an appropriate mathematical model (i.e. fist-order, second-order, etc.). The step-response tests can be carried out in quick succession, and are relatively easy to analyze compared to more complex physical models. The results predicted from a step response model can be compared to the output of the actual system in order to access the accuracy of the model. Based on the comparison of the model predictions and the actual system response, the model coefficients can be adjusted if necessary to achieve a more accurate fit.

In order to model the transient response of the "plant" elements of the servo control loop (servo motor, gear box, and servo mechanism), an open loop step response test can be performed on that part of the system. Based on the step response curve, an appropriate mathematical model can be chosen, and model constants selected to yield the plant transfer function. This allows the engineer to design a controller for the system (or select the control parameters for a prefabricated motion controller) that will achieve the required levels of closed loop performance based on analysis of the dynamic model. In

the case of a servo actuator system, the input to the plant model is a voltage, and the output is the actuator velocity.

No attempt was made to determine the plant model for the Mule actuator systems, because additional set up would be required for performing the open loop tests, and because satisfactory selection of the PID control gains was accomplished using tuning methods. Instead, the closed loop systems were modeled, because they would predict the behavior of the current actuator system implementations, and as such, would be more useful for others working on higher level vehicle velocity and heading control systems. The closed loop system transfer functions would represent the combined effects of the motion controller, plant, and feedback sensor servo loop elements, with the model input being the reference position, and the output being the actual (predicted) position. Determining the closed loop model was also more practical, because the system was already installed on the vehicle in the configuration needed for testing, so no additional set up was required. Also, the reference position step input would in the same form as the actuator wrench commands issued to the Primitive Driver, so the model would be formulated from actuator response data similar to what would be produced during autonomous operation.

Before the details of the individual actuator system models are presented, one important system constraint needs to be discussed. As an amateur designer of servo control systems, the author selected power supply voltages that were equal to the rated voltage of the servo motors. Obtaining the desired velocities from the actuator systems required them to be operated at their rated voltages, which meant that the servo amplifiers must emit a 100 percent duty-cycle PWM signal to drive the servomotor at the desired

actuation speed. This can be described as voltage limiting or torque saturation, because no amount of tuning the controller will increase the maximum torque and speed available from the motor already operating at the maximum supply voltage. This situation has resulted in transient response characteristics of the closed loop actuator systems that closely resemble the response of a pure integrator system, because the motor responds very linearly to the application of the 100 percent duty cycle supply voltage. Also, because the actuator systems are voltage limited, true models of the unconstrained system response would only be obtainable for very small step sizes, making them less useful because they would not be representative of large changes in reference input that would be common during autonomous operation of the systems. Therefore, the velocity limited throttle and steering actuator systems were modeled at integrators, which very accurately predicted system response to reference input commands over the entire actuator displacement ranges.

Another consideration regarding the voltage limiting constraint imposed by the power supply voltages is the possibility for integrator wind-up if the integration term of the PID filter is used. If the system is voltage limited, and cannot instantaneously follow the commanded step input, the controller output can integrate to a very high value as the actual position lags behind the commanded input. This accumulated integrator error can cause overshoot and instability in the system. To prevent this situation from occurring, the integration term can be omitted from the control algorithm, an integration limit can be implemented, or the controller can be designed such that a command input will never be generated that exceeds the physical limits of the system. An example of the last strategy

is initializing the maximum velocity parameter of the trajectory generator to the maximum velocity capability of the actuator.

Although the Mule actuator systems satisfy the design specifications originally outlined for them, future system designers would be advised to select power supply voltages 10 to 50 percent higher than the maximum required voltage for the application [Adv04a]. Although this is the recommendation, the supply voltage should not exceed the maximum voltage limitations of the motor, or be so high that a mechanical over-speed could result from an amplifier failure or runaway controller condition.

5.3.1 Integrator Mathematical Model

The integrator transfer function is developed from the continuous time defining relation

$$\frac{dc(t)}{dt} = km(t) \tag{5-2}$$

where c is the system output variable, m is the manipulated system input variable, and k is a constant that depends on the physical system characterizes. Cross multiplying and integrating both sides of the Equation 5-2 yields

$$c(t) = k\int_0^t m(t)dt \tag{5-3}$$

which can be transformed to the frequency domain using the Laplace transform

$$\mathcal{L}\{c(t)\} = \mathcal{L}\{k\int_0^t m(t)dt\}$$

to become

$$c(s) = k\frac{m(s)}{s} \tag{5-4}$$

The transfer function for the integrating system is then defined by

$$TF = \frac{c(s)}{m(s)} = \frac{k}{s} \tag{5-5}$$

A discrete time model of an integrating system is particularly useful for the Mule actuator applications which use digital controllers. The motion controllers use sampled data and the digital control signal is generated once for each sampling period, so the system is more accurately viewed in terms of discrete time rather than continuous time signals. The discrete time model for an integrating system is defined by Bollinger and Duffie [Bol88] as

$$c_n = c_{n-1} + kTm_{n-1} \tag{5-6}$$

where T represents the sampling period, and k can be found from the steady-state slope of the response $\frac{dc}{dt}$ and the step size M by the relationship

$$k = \frac{\left(\frac{dc}{dt}\right)}{M} \tag{5-7}$$

Using the backward shift operator B, Equation 5-6 can be transformed into a discrete time transfer function of the form

$$TF = \frac{c_n}{m_n} = \frac{kTB}{(1-B)} \tag{5-8}$$

This discrete time transfer function is valid during the integrating section of the response, until the actual position is equal to the commanded position, where the system transfer function becomes a simple constant multiplier of one. This time index n where the actual position becomes equal to the commanded position is defined by

$$n = \frac{1}{kT} \tag{5-9}$$

The closed loop transfer function used for modeling the throttle and steering actuator systems is illustrated in Figure 5-6 as a block diagram.

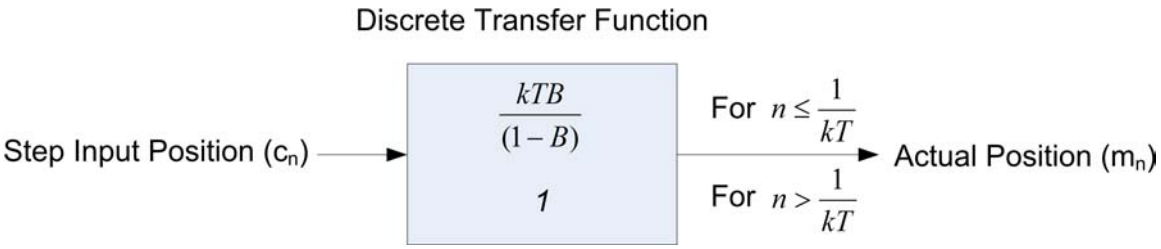

Figure 5-6: Discrete Transfer Function for Modeling Mule Actuator Systems

5.3.2 Throttle System Model

The values of the motion controller parameters that yielded the best closed loop system performance for the throttle actuator are displayed in Table 5-1. These include the PID filter gains, the integration limit term (IL) and the derivative sampling interval (DS). Also displayed in Table 5-1 are the trajectory generator acceleration and velocity values used to create the step input. The step input used was the entire displacement range, or 100 percent displacement. Trials were also performed using other values for the step input, but system responses were very comparable, because they all closely followed the velocity limited position trajectory. This is visible in Figure 5-7, which shows the transient response to step inputs of 10, 50, and 100 percent displacement. The transient response attributes, including any steady-state error (SSE), which were obtained from a 100 percent step input are listed in the Table 5-2. The integrator model constant *k* and sampling period *T* were also calculated from the response data and displayed in Table 5-2.

Table 5-1: Throttle Actuator Motion Controller Parameter Values

Kp	Ki	Kd	IL	DS	Acc	Vel
7000	50	30000	100	4	1000000	5000000

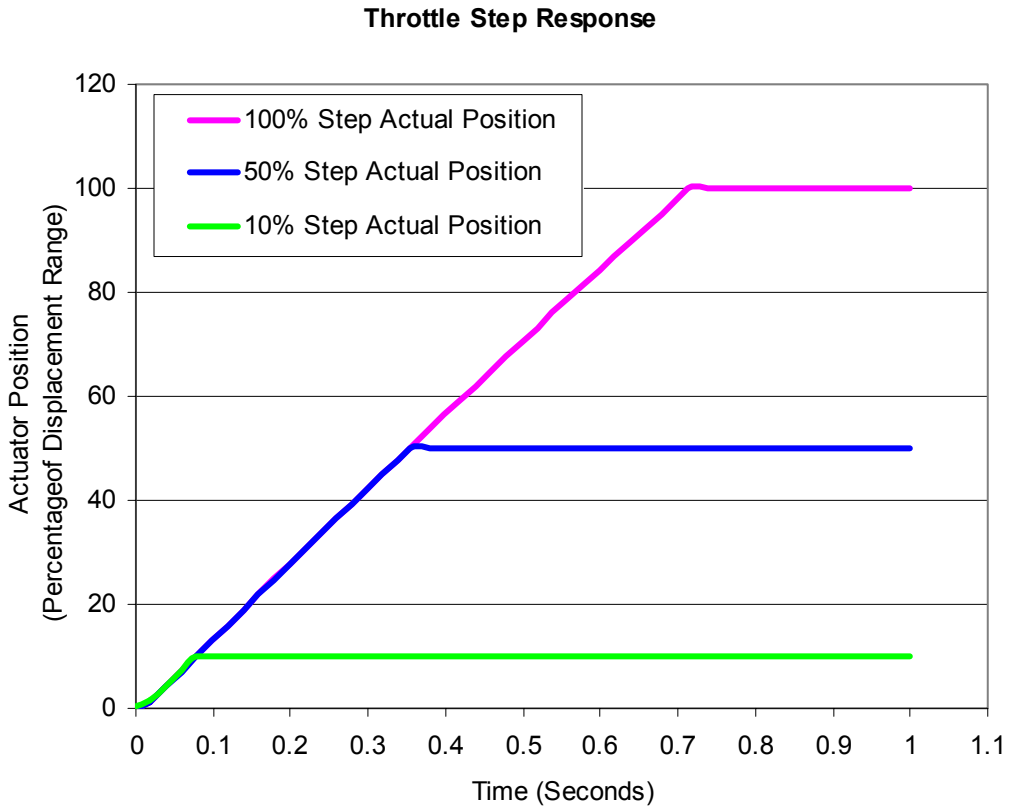

Figure 5-7: Throttle Step Response to 10, 50, and 100 Percent Step Inputs

Table 5-2: Throttle Actuator 100 Percent Step Response Attributes and Model Constants

Step (%)	**t_r (sec)**	**M_p (%)**	**t_s (sec)**	**SSE (%)**	***K* (%/sec)**	***T* (sec)**
100	0.56	0.22	0.70	0	1.4256	0.02

Figure 5-8 displays the discrete transfer function model predictions plotted with the actual throttle system response for step inputs of 50 and 100 percent displacement. The plot shows that the discrete model almost exactly predicts the behavior of the actual system.

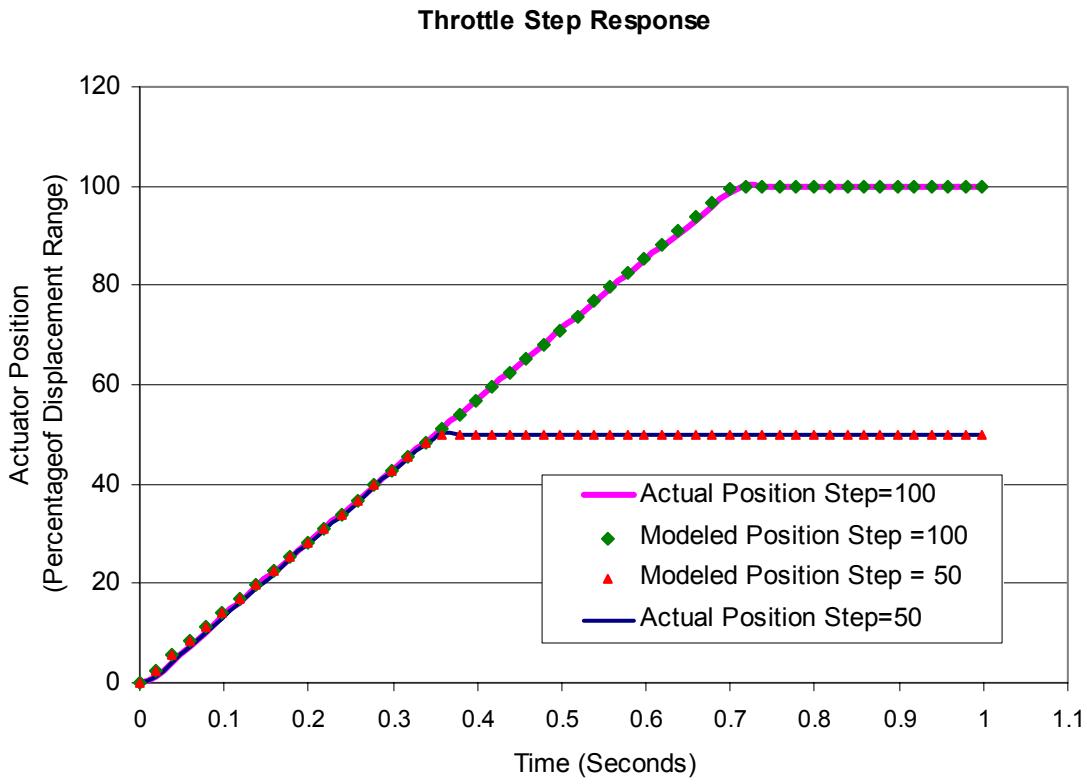

Figure 5-8: Discrete Transfer Function Model Plotted with Actual Throttle Actuator Response of for Step Inputs of 50 and 100 Percent Displacement

5.3.3 Steering System Model

The values of the motion controller parameters that yielded the best closed loop system performance for the steering actuator are displayed in Table 5-3. The motion controller used for the steering system has a fixed derivative sampling interval of two times the loop sampling period. Also, this motion controller does not offer a user selectable integration limit term. As with the throttle system, multiple trials were performed with various values of the step input to ensure that all the system responses followed the same velocity limited position trajectory, as illustrated in Figure 5-9. The transient response attributes obtained from a 100 percent step input are listed in Table 5-4. The integrator model constant k and sampling period T are also calculated from the response data and displayed in Table 5-4.

Table 5-3: Steering Actuator Motion Controller Parameter Values

Kp	Ki	Kd	DS	Acc	Vel
10000	200	5000	2	100000	200000

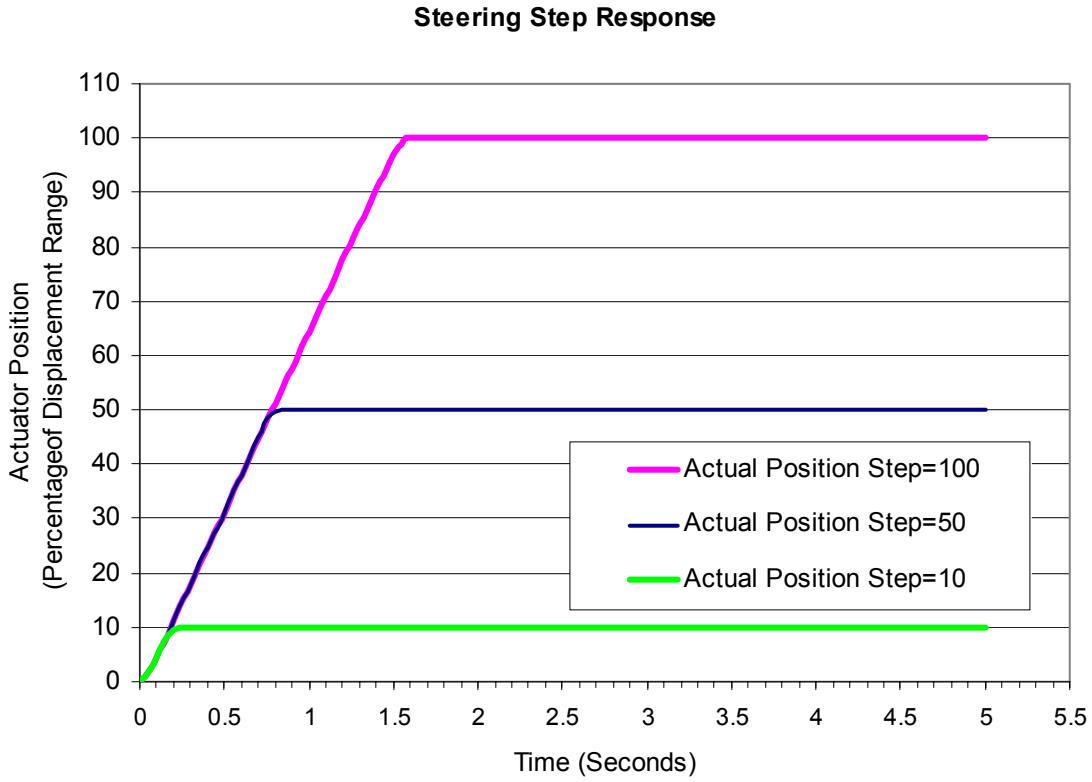

Figure 5-9: Steering Step Response to 10, 50, and 100 Percent Step Inputs

Table 5-4: Steering System 100 Percent Step Response Attributes and Model Constants

Step (%)	t_r (sec)	M_p (%)	t_s (sec)	SSE (%)	*K* (%/sec)	*T* (sec)
100	1.20	0	1.52	0	0.6622	0.04

Figure 5-10 displays the discrete transfer function model predictions for the steering system. The actual steering response curves are plotted with the model predictions for step inputs of 50 and 100 percent displacement. The plot shows that the discrete model is a very good approximation of the actual system behavior.

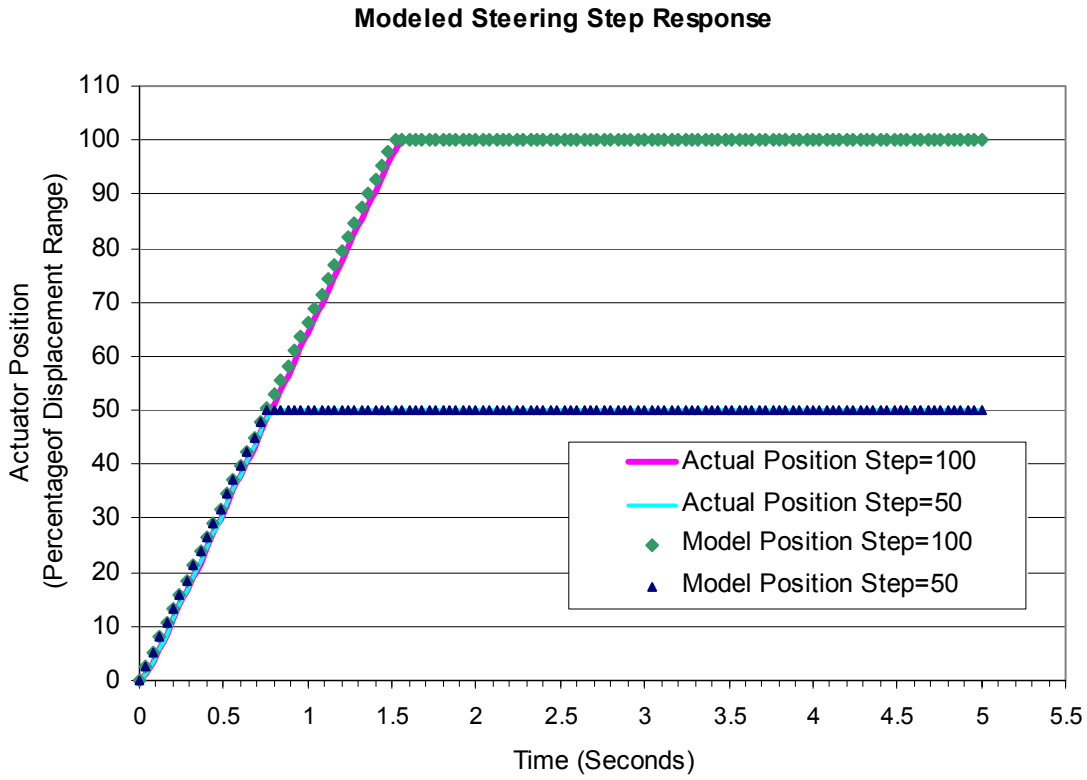

Figure 5-10: Discrete Transfer Function Model Plotted with Actual Steering Actuator Responses to Step Inputs of 50 and 100 Percent Displacement

5.3.4 Brake System Model

The motion controller integrated into the Smart Bug Actuator used for the braking system utilizes an enhanced digital PID filter. Additional sampling rate filters and feedforward terms have been added to the control algorithm with the intent of creating a more robust and better performing closed loop position controller. In place of the single derivative filter element of the traditional PID controller, this enhanced version uses two cascading velocity feedback gain terms that use velocity feedback information that has been passed through one or both of two user configurable low pass filters. Also, a velocity feedforward term is added to the algorithm in order to compensate for the position lag introduced by the negative velocity feedback gain terms. An acceleration feedback gain term and an acceleration feedforward term are also included in the control

filter. The acceleration feedback term counteracts rapid changes in shaft velocity like a virtual flywheel, which contributes to overall system smoothness. Similar to the velocity feedforward term, the acceleration feedforward term is added to compensate for any position lag that could be caused by the negative acceleration feedback filter action. A more detailed explanation of the control algorithm designed for this motion controller can be found in the SilverMax User Manual [Qui03].

The control filter values for the brake motion controller that produced an acceptable closed loop step response for the brake actuator system are listed in Table 5-5. Figure 5-11 displays the brake actuator transient response to step inputs of 100, 50, and 10 percent of the total actuator displacement range. The transient response attributes obtained from a 100 percent step input are listed in Table 5-6.

Table 5-5: Brake Motion Controller Parameter Values

Filter Parameter	Parameter Variable	Value
Proportional Gain	Kp	300
Velocity #1 Feedback Gain	Kv1	0
Velocity #2 Feedback Gain	Kv2	6
Velocity Feedforward Gain	Kvff	6
Acceleration Feedback Gain	Ka	20
Acceleration Feedforward Gain	Kaff	20
Integrator Gain	Ki	1000
Velocity #1 Feedback Filter	Fv1	150 Hz
Velocity #1 Feedback Filter	Fv2	250 Hz
Acceleration Feedback Filter	Fa	400 Hz

Although torque saturation and velocity limiting did occur when the brake actuator responded to a 100 percent step input, the closed loop step response appears have the characteristics of a critically damped second-order system. As a result, the integrator model used to approximate the throttle and steering systems' closed loop response would not be adequate, and a second-order mathematical model was chosen to describe the brake system transient response behavior.

Equation 5-10 is presented by Bollinger and Duffie [Bol88] as a discrete model of a second-order system

$$c_n = a_1 c_{n-1} + a_2 c_{n-2} + b_1 m_{n-1} + b_2 m_{n-2} \tag{5-10}$$

where a_1, a_2 , b_1, and b_2 are defined for a critically damped system using the sampling period T, natural frequency ω_n, and time constant τ by

$$a_1 = 2e^{-\omega_n T} \tag{5-11}$$

$$a_2 = -e^{-2\omega_n T} \tag{5-12}$$

$$b_1 = 1 - e^{-\omega_n T} - \omega_n T e^{-\omega_n T} \tag{5-13}$$

$$b_2 = e^{-\omega_n T}(e^{-\omega_n T} + \omega_n T - 1) \tag{5-14}$$

The natural frequency, ω_n, and time constant, τ, for a critically damped second-order system are determined based on information from the step response data according to the following relations

$$\tau = \frac{1}{2} t_{0.594} \tag{5-15}$$

where $t_{0.594}$ is the time it takes the response to reach 59.4 percent of the steady-state value, and

$$\omega_n = \frac{2}{t_{0.594}} \tag{5-16}$$

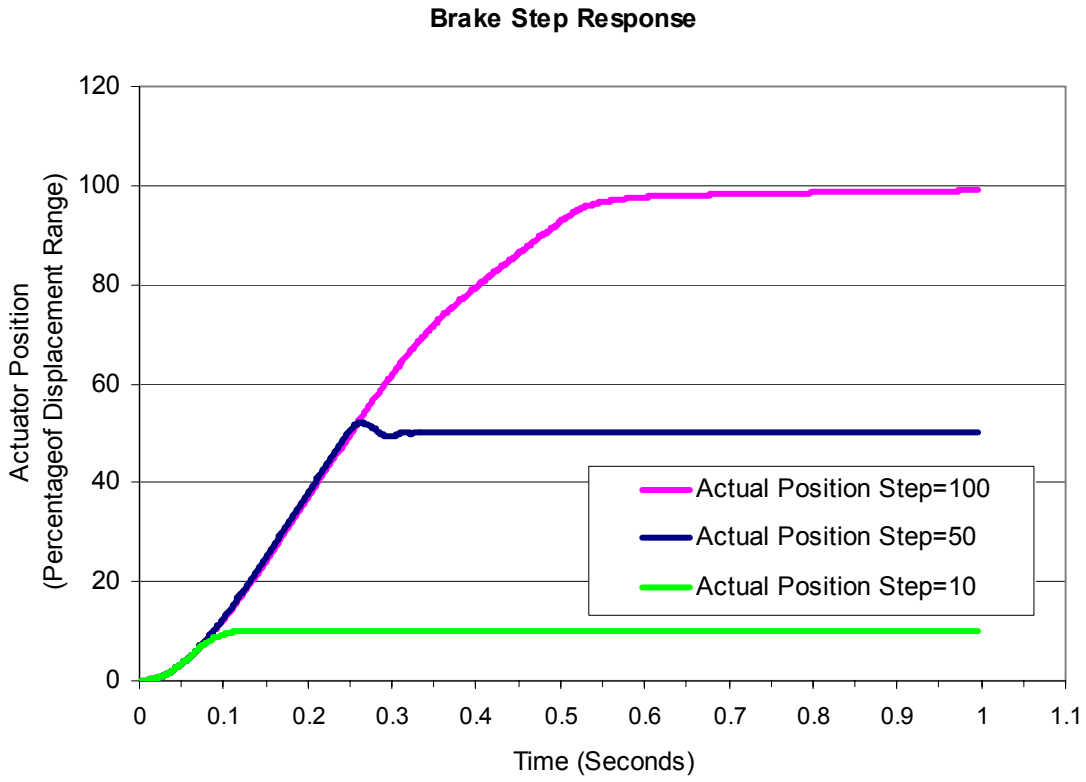

Figure 5-11: Brake Step Response to 10, 50, and 100 Percent Step Inputs

Table 5-6: Brake Actuator 100 Percent Step Response Attributes

Step (%)	t_r (sec)	M_p (%)	t_s (sec)	SSE (%)	$T_{0.594}$ (sec)
100	.39	0	0.65	1.02	0.289

Table 5-7: Brake Actuator Best-Fit Second-Order Critically Damped Model Constants

τ (sec)	ω_n (Hz)	ζ	a_1	a_2	b_1	b_2	T (sec)
100	.39	1	1.92	-1	0.00006	0.00005	0.001548

Using the backward shift operator *B*, Equation 5-10 can be transformed into a discrete time transfer function for a second-order system of the form

$$TF = \frac{c_n}{m_n} = \frac{k(b_1 B + b_2 B^2)}{1 - a_1 B - a_2 B^2} \tag{5-17}$$

where the gain constant k is found from the steady-state response c_{ss} and the step size M by the relationship

$$k = \frac{c_{ss}}{M} \tag{5-18}$$

Figure 5-12 is a plot of the discrete transfer function model predictions for the braking system. The actual steering responses are plotted with the model output for step inputs of 50 and 100 percent displacement. The first model output was generated using values for the transfer function parameters that were calculated using Equations 5-11 to 5-16. After comparing the first model prediction to the actual system output, the transfer function constants were slightly adjusted to achieve a best-fit model of the system (values listed in Table 5-7). The response curves generated for step inputs for 50 and 100 percent illustrate that the best-fit discrete model is an extremely good predictor of the actual system behavior.

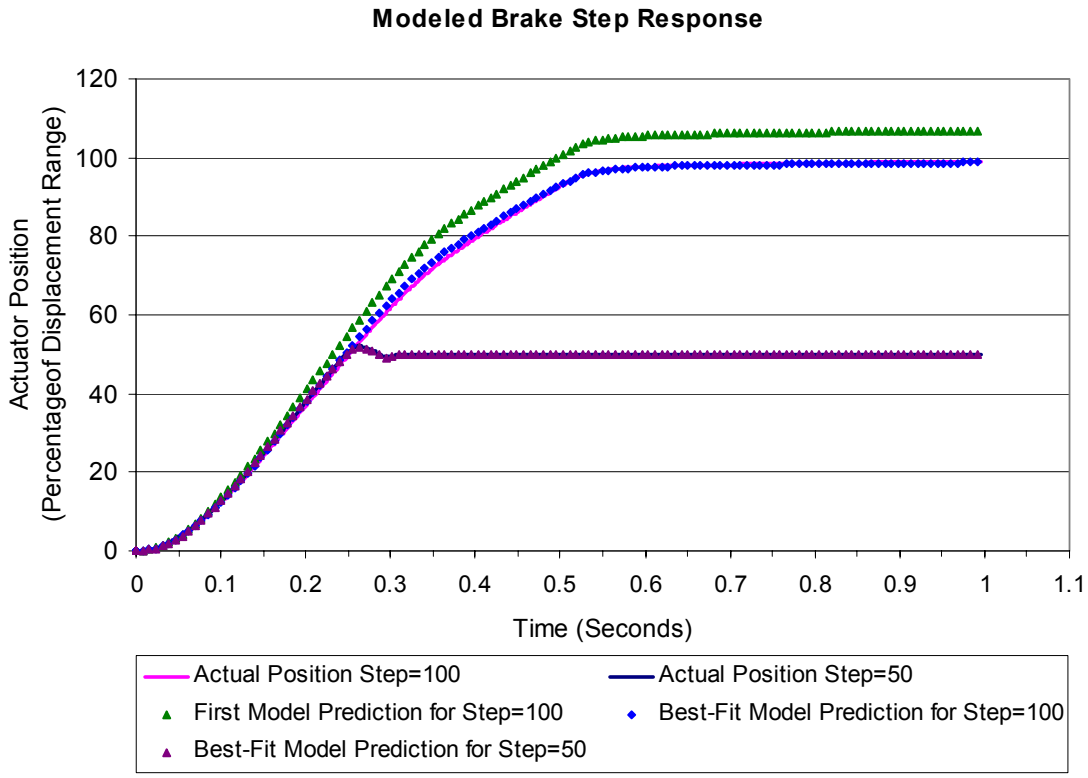

Figure 5-12: Discrete Transfer Function Models Plotted with Actual Brake Actuator Responses to Step Inputs of 50 and 100 Percent Displacement

CHAPTER 6
CONCLUSIONS AND FUTURE WORK

6.1 Conclusions

The first time the Navigational Test Vehicle II operated under wireless tele-op control was June 17, 2003, in preparation for JAUS controlled autonomous vehicle demonstration at Tyndall Air Force Base (see Object 1). The only change that had to be made in order for the Air Force Research Laboratory system to assume command control of the NTV2 Primitive Driver was to enter the designated component IP addresses. The standard messaging interface outlined by the JAUS reference architecture made this nearly immediate interoperability of systems developed at different laboratories possible.

Object 1: NTV2 Tele-Operation Demonstration at Tyndall Air Force Base (8.1 MB, mule1stTeleOp.mpeg. 45 seconds)

Over the course of a year since that time, additional intelligence components have been added to the Mule, and during testing and demonstrations in November 2003, it successfully demonstrated GPS waypoint navigation at speeds of approximately 12 mph (see Object 2). The modular design of JAUS components and their hardware implementation on the Mule has proven very functional, as the PD and other components have evolved through multiple hardware and software redesigns.

Object 2: NTV2 Autonomous GPS Waypoint Navigation (13.2 MB, AutonomousMule.wmv. 62 seconds)

The throttle, brake, and steering actuator systems designed to control the mobility functions of the Mule meet or exceed the outlined design criteria. The systems have been field tested repeatedly, allowing system "bugs" to be identified and corrected. At the

present time, the actuator systems are very reliable. In conclusion, the goals of this project have been accomplished, and the Mule has been converted into a reliable development vehicle for autonomous systems technology (see Figure 6-1).

6.2 Future Work

As with any development project in a research laboratory, the work is never finished. Immediate projects pending for the NTV2 include designing an electronics enclosure and integrating control of the shifting and other vehicle discrete devices. The electronics enclosure is needed to protect the hardware rack modules from the environment, and should support the modularity incorporated thus far into the NTV2 systems. The project to automate the shifters was started by the author, but at this time has not been fully integrated. Two Addco linear actuators were installed to position control the forward-neutral-reverse and high-low gear selectors. The actuator controllers however remain to be integrated into the PD functionality. At the subsystem level, many JAUS components remain to be implemented on the NTV2, which will give it added autonomous capabilities.

The previous Navigational Test Vehicle served CIMAR and the AFRL for ten years, experiencing continual hardware and control software upgrades, and serving as the test platform for countless unmanned systems experiments. Only the creativity and imagination of future students in CIMAR will determine what future modifications and missions are in store for the NTV2. It is the hope of the author that his work on the Mule will continue to serve and support the research efforts of other students for many years to come.

Figure 6-1: Navigational Test Vehicle II

LIST OF REFERENCES

Adv04a Advanced Motion Controls, "PWM Servo Amplifier Engineering Reference," *Technical Manual*, Advanced Motion Controls Camarillo, CA, http://www.a-m-c.com/download/instnotes.pdf, May 2004.

Adv04b Advanced Motion Controls, "Inductive Filter Cards Engineering Reference," *Technical Manual*, Advanced Motion Controls Camarillo, CA, http://www.a-m-c.com/download/inductivefiltercards.pdf, May 2004.

Arm99 Armstron, D.G., Crane, C.D., Waltz, W. "Air Force Research Laboratory Modular Architecture Development for Unmanned Vehicles," Center for Intelligent Machines and Robotics, University of Florida, 1999.

Arm00 Armstrong, D., Crane, C., Novick, D., Wit, J., English, R., Adsit, P., Shahady, D. "A Modular, Scalable, Architecture For Unmanned Vehicles," Proceedings of the Association for Unmanned Vehicle Systems International (AUVSI) Unmanned Systems 2000 Conference, Orlando, Florida, July 2000, pp. 1-14.

Big03 Bigge, B., "The Evolution of Motor Control," Master's Thesis, University of Sussex, UK, 2003.

Bol88 Bollinger, J.G., and Duffie, N.A., *Computer Control of Machines and Processes*, Addison-Wesley, Reading, MA, 1988.

Fre95 French, P.W., "Automation of an All-Terrain Tow Vehicle," Master's Thesis, University of Florida, 1995.

His98 Histand, M.B., and Alciatore, D.G., *Introduction to Mechatronics and Measurements Systems*, McGraw-Hill, Boston, MA, 1998.

Jau04 JAUS Working Group, "Joint Architecture for Unmanned Systems (JAUS)," *Version 3.1, Volume 2*, The Joint Architecture for Unmanned Systems, http://www.jaugs.org, April 2004.

Kol04 Kollmorgen, "SERVODISK Catalog," *Technical Manual*, Kollmoregen Motion Technologies Group, Commack, NY, http://www.motionvillage.com/products/product_literature/product_brochure/pdfs/KOL1037.pdf, June 2004.

Man01 Mandapat, R.E., "Development and Evaluation of Positioning Systems for Autonomous Vehicle Navigation," Master's Thesis, University of Florida, 2001.

Nat99 National Semiconductor, "LM628/629 Programming Guide," *Technical Manual AN693U*, National Semiconductor Corporation, Santa Clara, CA, 1999.

Nat03 National Semiconductor, "LM628/629 Precision Motion Controller," *Technical Manual DS009219*, National Semiconductor Corporation, Santa Clara, CA, 2003.

Oga97 Ogata, K., *Modern Control Engineering*, Prentice Hall, Upper Saddle River, NJ, 1997.

Pit02 Pittman, "LO-COG DC Gearmotors," *Bulletin LCG*, Pittman Corporation, Harleysville, PA, 2002.

Qui03 QuickSilver Controls, "SilverMax User Manual," *Technical Manual Rev. 4.01*, QuickSilver Controls Corporation, San Dimas, CA, 2003, http://qcontrol.com/SilverMax%20Servos/silvermax_23.htm, June 2004.

Rea01 Real Time Devices, "ESC629 2-Channel DC Servo Motor Interface Board User's Manual," *Technical Manual*, Real Time Devices Finland Oy, Helsinki, Finland, 2001.

Sen98 Senior, A.J., "Design of a Vehicle Control System for Autonomous or Teleoperated Vehicles," Master's Thesis, University of Florida, 1998.

Ult04 Ultra Motion, "Bug Actuator Linear Actuator," *Product Data Sheet*, Ultra Motion , Mattituck, NY, http://www.ultramotion.com/products/bug.php, May 2004.

BIOGRAPHICAL SKETCH

Chad Karl Tobler was born August 3, 1976, in St. George, Utah, to Karl and Jan Tobler. In 1994 he graduated from Pasco High School in Pasco, Washington, and then attended Brigham Young University in Provo, Utah. After completing his freshman year at BYU, Chad put his academic pursuits on hold and served a two year mission in Puerto Rico for the Church of Jesus Christ of Latter-Day Saints. After returning from the mission, he completed his studies at BYU, receiving a bachelor's degree in manufacturing engineering in May 2001. In order to pursue his interest in automation and robotics, Chad began a master's degree program in the Mechanical Engineering Department at the University of Florida in August 2001. After completing his studies at UF, Chad will begin working for Harris Corporation in Palm Bay, Florida.